PEOPLE TO PARASITES: GLOBAL AND MOLECULAR APPROACHES TO COMBAT HUMAN MALARIA

by

HEATHER MICHELLE KUDYBA

(Under the Direction of Vasant Muralidharan)

ABSTRACT

Malaria is a debilitating and often fatal disease caused by infection with *Plasmodium* parasites. In addition to parasites infecting billions of people annually, malaria poses a significant social and economic burden on some of the most impoverished regions of the world. There are currently no effective vaccines and drug resistance has emerged to all clinically available drugs for malaria treatment. The World Health Organization's (WHO) objective is to eliminate malaria as a global health burden by 2030. There are two distinctive, but vital areas of research needed to achieve the WHO's goal: discovery of new diagnostics and identification of drug targets. This dissertation covers three areas of research that touch on each of those needs. The first manuscript is the field assessment of a malaria molecular diagnostic compared to standard microscopy in Roraima, Brazil. The second is a methods paper on the development of molecular tools to study the parasite. The third manuscript covers my main thesis work in which I utilized molecular tools to investigate an ER chaperone, PfGRP170, during *P. falciparum* asexual development. Overall, this thesis provides research that will assist the malaria community in our fight against this disease.

INDEX WORDS: *Plasmodium falciparum*, Malaria, Malaria Diagnostics, CRISPR/Cas9, Endoplasmic reticulum, ER stress

PEOPLE TO PARASITES: GLOBAL AND MOLECULAR APPROACHES TO COMBAT HUMAN MALARIA

by

HEATHER MICHELLE KUDYBA

BS, Southern Polytechnic State University, 2013

A Dissertation Submitted to the Graduate Faculty of The University of Georgia in Partial Fulfillment of the Requirements for the Degree

DOCTOR OF PHILOSOPHY

ATHENS, GEORGIA

2019

PEOPLE TO PARASITES: GLOBAL AND MOLECULAR APPROACHES TO COMBAT HUMAN MALARIA

by

HEATHER MICHELLE KUDYBA

Major Professor:	Vasant Muralidharan
Committee:	Silvia Moreno
	Drew Etheridge
	Karl Lechtreck

Electronic Version Approved:

Suzanne Barbour

Dean of the Graduate School

The University of Georgia

May 2019

DEDICATION

This thesis is dedicated to my husband Karl Kudyba, my three cats (Aslan, Apollo, and Azula), and my sweet puppy (Ava).

ACKNOWLEDGEMENTS

I would like to start my acknowledgements by thanking numerous teachers at McEachern High School whose compassion and kindness gave me the strength and motivation to further my education: Linda Savage, Andrea Norred, Commander Eugene Sudol, Lynlee Doar, Barbara Beyke, Todd McMath, Kristy Royer, and Gretchen Davis. These teachers made a strong impression on a young mind from a troubled home. They spent endless hours before, during, and after school teaching me how to make a CV, apply to college, soothing my anxieties, prepare for the SAT, and so much more. When I graduated many of these teachers contributed to a gift card to help me get supplies for college. I am beyond thankful.

I would also like to thank many of my undergraduate professors who helped to prepare me for graduate school: Jack Duff, Dr. Stephanie McCartney, Dr. Jennifer Louten, Dr. Michael Beach, Dr. Peter Sakaris, Dr. Rajnish Singh, Alda Wood, and Nancy Reicher. These professors went above and beyond to help me learn how to read scientific literature, design experiments, and find several undergraduate research opportunities. In addition, I would like to acknowledge Dr. Judith Fridovich-Keil, Dr. Patty Jumbo-Lucioni, and Marquise Hopson for hosting me for Emory's Summer Undergraduate Research Program.

I would like to thank Traci Thomas who hired me at Lost Mountain Tennis Center when I was a seventeen-year-old high school student. This job supported me financially throughout my entire undergraduate career.

I want to acknowledge Sandy and Roger Moore. I met Sandy and her husband when I worked at Lost Mountain Tennis Center and they quickly became the parental figures I was always looking for. They both gave me so much love and support and I wouldn't be who I am today without them.

I have many people to thank at the University of Georgia. First I would like to acknowledge my graduate advisor, Vasant Muralidharan, who took me as his first graduate student in 2013. This has given me the unique opportunity to see a lab start from the very beginning. I have no doubt this will be very useful for me to have observed and experienced when I start my own lab. I want to thank all of my lab mates I have had over the past six years—specifically David Cobb, Manuel Fierro, Anat Florentin, Carrie Brooks, Dylon Stephens, and Michelle Krakowiak. I would like to thank Julie Nelson (flow cytometry core) who not only taught me how to use many cool instruments, but also became a great friend. I would like to thank my committee members Dr. Silvia Moreno, Dr. Boris Striepen, Dr. Drew Etheridge, and Dr. Karl Lechtreck.

I have made many incredible friends during graduate school who have helped make my PhD experience fun: David Cobb, Manashree Malpe, Madison Grant, Katie Reagin, Chris Slade, and Robert Ng.

Lastly I would like to acknowledge my amazing husband Karl and his family (Paul Kudyba II, Gigi Kudyba, Paul Kudyba III, George Kudyba, Joe Kudyba, and Sarah Kudyba). Their love and support during graduate school has made a significant impact on me.

TABLE OF CONTENTS

Page

LIST OF TABLES

Page

LIST OF FIGURES

Page

CHAPTER 1

INTRODUCTION AND LITERATURE REVIEW

1.1 Malaria is a major global health burden

Malaria is a potentially fatal disease caused by an infection with parasites from the genus *Plasmodium*. While several species infect humans, the vast majority of malaria-associated mortality and morbidity can be attributed to two species, *Plasmodium falciparum and Plasmodium vivax*. In 2017, there were 219 million cases of malaria and 435,000 deaths—mostly in children under the age of five[1]. The major populations most burdened by malaria are in some of the most impoverished regions of the world, making effective diagnosis and treatment of this disease extremely challenging. Moreover, resistance has emerged to all clinically available drugs, highlighting an important need for malaria research[2-8]

Plasmodium has an intricate life cycle that involves a mosquito vector and a vertebrate host[9,10]. Sporozoites are transmitted from an *Anopheles* mosquito to a human host during a blood meal. The parasites invade liver cells, where they form thousands of haploid merozoites. After approximately 10-14 days these merozoites are release into the blood stream, where they invade erythrocytes. As the parasite invades the red blood cell (RBC) it cocoons itself within a parasitophorous vacuole (PV), forming the ring stage of the parasite. Over the next 48 hours the parasite transitions from the ring stage to the metabolically active trophozoite stage, and lastly the parasite will undergo schizogony to form 16-32 new daughter merozoites that will egress and invade

new RBCs. A small portion of the parasites will develop into sexual stage gametocytes that can be ingested by another mosquito, allowing for transmission to a new host. During early malaria infections, the symptoms consist of high fever, chills, nausea and headache. If left untreated, the disease can cause severe complications such as respiratory distress, renal failure, cerebral damage, and placental damage[11]. All clinical symptoms of malaria arise from the parasite's asexual replication in the erythrocyte.

The World Health Organization's (WHO) global technical strategy for malaria aims to eliminate the disease as a global health issue by 2030[12]. While significant advancements have been made in the last decade, progress toward malaria elimination has plateaued. Several factors contribute to this hindrance of progress, including the circulation of drug resistant parasites and the lack of sensitive, cost effective diagnostics to detect low-density infections[12]. The establishment of affordable and sensitive molecular diagnostics, the advancement of tools used to study the biology of the parasite, and a better understanding of the proteins that drive the parasitic life cycle of *Plasmodium* will all be imperative to combat this deadly parasitic disease. The work presented in this dissertation will focus on each of these aspects of malaria research.

1.2 Malachite Green Loop Mediated Isothermal Amplification as a Malaria Molecular Diagnostic

A substantial proportion of the mortality and morbidity associated with human malaria infections are caused by infection with either *P. falciparum or P. vivax* [1,13,14]. In endemic areas, patients are predominantly diagnosed with malaria using light microscopy. This method of diagnosis is extremely time consuming and is limited in its ability to detect low-density infections. The sensitivity of microscopy typically ranges

between 30-100 parasites/μL and the accuracy of the diagnosis is contingent upon the training of the microscopist[15-17]. Furthermore, occasional misdiagnosis of mixed-species infections occurs using microscopy, which is detrimental to patient outcomes as treatment regimens differ for each *Plasmodium* species[18]. The introduction of rapid diagnostic tests (RDT's) for malaria diagnosis circumvented some of these issues with microscopy, as they are less subjective, user-friendly, and don't require expensive equipment. However, most RDTs have the same level of sensitivity as microscopy and are specific for *P. falciparum* infection[15,19]. Additionally, infections can be missed using current RDTs due to circulating parasites which have deleted the antigen that is being used for detection[20-23].

Molecular diagnostics offer increased sensitivity and specificity for the detection of *Plasmodium* parasites. However, implementation of these diagnostics in resource-limited laboratories in the field may be difficult due to the requirement of expensive equipment and trained personnel. The ideal molecular diagnostic tool would be user friendly and adaptable to field settings, while maintaining sensitivity and specificity. Several studies have reported on the use of loop-mediated isothermal amplification (LAMP) as a promising molecular diagnostic for malaria[24-30]. Unlike polymerase chain reaction (PCR), which requires temperature cycling to amplify DNA, LAMP reactions are performed at a single temperature (~63°C). If amplification of DNA occurs during the LAMP reaction, magnesium pyrophosphates are released which results in a change in the turbidity of the sample. However, this readout method can be subjective. Turbidimeters have been used with malaria LAMP assays but the need for this equipment decreases the versatility of LAMP in the field[26,28].

Recently, a colorimetric malaria LAMP assay using malachite green (MG-LAMP) was reported[31]. LAMP reactions containing malachite green turn a blue/green color after DNA amplification and appear colorless if DNA is not amplified. This colorimetric readout makes diagnosis extremely straightforward. The sensitivity of MG-LAMP, which depended on the species being tested, ranged from 1-8 parasites/μL[31]. The high sensitivity of MG-LAMP, coupled with the fact that multiple reactions can be performed in a 40-well mini heat block at a single temperature, demonstrated that MG-LAMP is a significant improvement over both microscopy and RDTs for malaria diagnosis. However, the data and conclusion made in this paper were based on MG-LAMP reactions performed in a laboratory in the United States, not in malaria endemic regions[31]. The data presented in Chapter 2 of this thesis evaluates MG-LAMP as a malaria diagnostic in the field in three municipalities of Roraima State, Brazil.

1.3 Advancements in genetic tools to study *P. falciparum* biology

Uncovering the factors which drive the life cycle of this deadly parasite is vital for the development of new drug targets, a requirement for combatting the disease and advancing the WHO's goal of malaria elimination. Genetic manipulation of *P. falciparum* allows researchers to investigate proteins and processes that are required for parasite survival. The recent introduction of CRISPR/Cas9 gene editing in *P. falciparum* has substantially expanded the molecular toolbox for establishing transgenic malaria parasites[32]. Prior to CRISPR/Cas9-mediated editing, the generation of mutants in *Plasmodium* was a 6 to 9 month process with an exceptionally low success rate. This technique involved multiple rounds of drugs selection, hinged on random double

stranded breaks in the genome, and relied on the ability of the parasite to utilize homologous directed repair to insert a repair template[33-37].

CRISPR/Cas9 gene editing works by expressing both a guide RNA (gRNA), that is complementary to the DNA region of interest, and the endonuclease Cas9 The gRNA directs Cas9 to the target DNA where it will introduce a double stranded break[38]. The DNA is usually repaired in one of two ways, either by non-homologous enjoining or homology directed repair[38]. *Plasmodium* lacks the machinery to facilitate non-homologous end joining[39-41]. Therefore, the malaria parasite relies solely on homologous recombination to insert DNA and repair the genome following a double stranded break induced by Cas9. Typically, the parasite requires approximately 500-800bp of homologous template to mend the genome[32,35]. Attempts to use smaller homology regions significantly decrease efficiency as shown in the manuscript presented in Chapter 3 of this dissertation.

Chapter 3 of this thesis is a published manuscript on the method our lab uses to generate CRISPR/Cas9 mutants in *Plasmodium falciparum*. The methods paper outlines the procedure for tagging an exported chaperone, PfHSP70x, with the *glmS* ribozyme[42,43]. The *glmS* ribozyme allows for knockdown of a protein when glucosamine is added to the culture medium. Glucosamine, which is covered to glucosamine-6-phosphate in the parasite, binds to and activates the *glmS* ribozyme. The active ribozyme cleaves the mRNA of the tagged protein of interest and targets it for degradation, thus allowing for a decrease in protein levels. Our lab has adopted this same transfection protocol to generate mutants using the TetR-DOZI system and to create gene knockouts[43,44].

1.4 The *P. falciparum* Endoplasmic Reticulum

The *Plasmodium* ER plays an essential role in parasite biology, serving as the point of origin for a complex protein trafficking network and an understudied stress response pathway. There are many outstanding questions about the molecular mechanisms that drive these cellular processes in the parasite. Understanding the basic biology of the *Plasmodium* ER may uncover potential drug targets, which would further progress the goal of malaria elimination. Chapter 4 of this dissertation is a manuscript on the first characterization of an ER chaperone, PfGRP170, and its role in this critical organelle.

Once the parasite invades the RBC, it manipulates its surface, so it will bind and sequester in the blood capillaries in order to avoid clearance in the spleen[9,11,45]. The accumulation and adhesion of infected RBCs in the microvasculature obstruct blood flow, induce hypoxia, and lead to organ damage. To be able to adhere to the capillaries and cause disease the parasite must drastically remodel the host RBC. These modifications are accomplished through protein transport into the host cell[46]. The majority of trafficked proteins begin their journey in the ER. While some export motifs have been characterized, such as the *Plasmodium* Export Element (PEXEL) and the apicoplast transit peptide, the mechanisms of recognition, sorting, and targeting of proteins in the ER are unknown[47-52]. Additionally, there are subsets of transported RBC proteins which lack any particular signal, adding yet another layer of complexity[53,54]. In model eukaryotes, such as yeast and mammalian cells, molecular chaperones play central roles in protein trafficking[55]. In *Plasmodium*, it has been suggested that PfGRP78 (BiP) plays a role in protein export due to its ability to interact with Plasmepsin V, the PEXEL-cleaving protease[56].

Protein trafficking from the ER to the apicoplast is also essential for parasite survival. In the blood stages, this organelle is primarily required for isoprenoid biosynthesis[57]. Proteins targeted to the apicoplast contain an N-terminal transit peptide that is revealed upon signal peptide cleavage in the ER[51]. These signal motifs vary in sequence length and typically contain a surplus of basic amino acids[52]. Once these proteins reach the apicoplast, the transit peptide is cleaved[58].

Interestingly, apicoplast transit peptides also have been shown to interact with HSP70s, suggesting HSP70s play a role in the targeting of apicoplast proteins[52]. To further support this claim, treatment of parasites with an HSP70 inhibitor blocked trafficking to the apicoplast[59,60].

In addition to being a hub for protein trafficking, the ER plays a critical role in the management of cellular stress[61]. In other eukaryotic organisms, ER chaperones and other proteins will attempt to fold substrates multiple times. If the protein cannot be folded, a process called ER associated degradation (ERAD) takes place[62]. This results in the transfer of the unfolded proteins out of the ER and into the cytosol, where they are degraded via the proteasome. When the rate of unfolded proteins in the ER increases to a certain level, Unfolded Protein Response (UPR) signaling pathways are activated[63]. These pathways, many of which are regulated by ER chaperones, lead to transcriptional and translational changes which aid in reducing cell stress. Several proteins involved in ERAD and UPR are missing from the *Plasmodium* genome[64,65]. The only conserved UPR pathway in *P. falciparum* is the pancreatic endoplasmic reticulum kinase (PERK) signaling pathway[65-67].

The ER chaperone BiP maintains PERK, a transmembrane protein in the ER, in an inactive state until there is ER stress[63,68,69]. When ER stress occurs, BiP is released from PERK, and PERK oligomerizes, leading to trans-autophosphorylation of the kinase[68]. This leads to the phosphorylation the cytoplasmic eukaryotic initiation factor 2 alpha (EIF2α), which in turns decreases translation and flux through the ER. The *Plasmodium* PERK homolog PK4 appears to operate in a similar mechanism[66,67]. PK4 has been shown to be essential for asexual development of *Plasmodium* parasites and the pathway is activated in artemisinin resistant parasites[66,67]. Inhibition of this pathway either pharmacologically or by the overexpression of a dominant-negative PK4 renders artemisinin resistant parasites sensitive to drug treatment[66]. Interestingly, it was also demonstrated that artemisinin treatment displaced the ER chaperone BiP from PK4, which is also important for PERK activation in other eukaryotes[66].

A key interest of my research was to better understand the function ER chaperones play in *Plasmodium* biology. The *Plasmodium* genome encodes a relatively reduced repertoire of predicted ER chaperones, but it does contain two members of the HSP70 ER chaperone complex, BiP and PfGRP170. BiP is documented in the other eukaryotic organisms as a multipurpose chaperone that is essential for the import of proteins into the ER, proper protein folding, prevention of protein aggregation, and several ER stress response mechanisms[55,70,71]. GRP78 interacts with client proteins through its C-terminal binding domain, which recognizes and binds peptides containing 7-11 hydrophobic amino acids[72,73]. The interaction of BiP with client proteins is regulated by whether it is bound to ATP or ADP[74]. When bound to ADP, the chaperone can bind proteins; when it is exchanged to ATP, the substrate is released[55,71,74]. Studies

in yeast have shown that the exchange of ADP to ATP is facilitated by the ER chaperone GRP170[75].

GRP170, or glucose-regulated protein 170, was first described in Chinese hamster ovary cells in the 1980s[76]. GRP170, along with two other chaperones, were shown to have increased expression during glucose starvation[76]. While GRP170 is most often documented as a nucleotide exchange factor for BiP, it has been reported that GRP170 can serve as a holdase and bind unfolded substrates, independent of ATP or BiP[77-79]. GRP170 in mammalian cells interacts directly with PERK and thus could be regulating the UPR pathway in some capacity[80-82]. It was shown that the yeast GRP170 homolog, Lhs1, is dispensable for growth[83]. Yeast null for Lhs1 were shown to constitutively activate the unfolded protein response via the IRE1 pathway[83]. The activation of this UPR pathway is essential, as yeast null for IRE1 and Lhs1 are nonviable. Overexpression of another nucleotide exchange factor, SIL1, rescues the IRE1/Lhs1 death phenotype[83]. Furthermore, double knockout mutants for Lhs1 and SIL1 are not viable[83]. SIL1 is missing from the *Plasmodium* genome and the role and essentiality of GRP170 in the malaria parasite has yet to be ascertained. The manuscript presented in Chapter 4 demonstrates for the first time that PfGRP170 is essential for parasite growth and that knockdown of this protein results in the activation of the only defined UPR pathway in *Plasmodium*.

1.5 References

1 World Health Organization. World Malaria Report. (World Health Organization, Geneva, 2018.

2 Winzeler, E. A. & Manary, M. J. Drug resistance genomics of the antimalarial drug artemisinin. *Genome biology* **15**, 544-544, doi:10.1186/s13059-014-0544-6 (2014).

3 Dondorp, A. M. *et al.* Artemisinin resistance in Plasmodium falciparum malaria. *N Engl J Med* **361**, 455-467, doi:10.1056/NEJMoa0808859 (2009).

4 Noedl, H. *et al.* Evidence of Artemisinin-Resistant Malaria in Western Cambodia. *New England Journal of Medicine* **359**, 2619-2620, doi:10.1056/NEJMc0805011 (2008).

5 Ashley, E. A. *et al.* Spread of Artemisinin Resistance in Plasmodium falciparum Malaria. *New England Journal of Medicine* **371**, 411-423, doi:10.1056/NEJMoa1314981 (2014).

6 Mita, T. *et al.* Limited geographical origin and global spread of sulfadoxine-resistant dhps alleles in Plasmodium falciparum populations. *J Infect Dis* **204**, 1980-1988, doi:10.1093/infdis/jir664 (2011).

7 Roper, C. *et al.* Intercontinental spread of pyrimethamine-resistant malaria. *Science* **305**, 1124 (2004).

8 Wootton, J. C. *et al.* Genetic diversity and chloroquine selective sweeps in Plasmodium falciparum. *Nature* **418**, 320-323 (2002).

9 Boddey, J. A. & Cowman, A. F. Plasmodium nesting: remaking the erythrocyte from the inside out. *Annu Rev Microbiol* **67**, 243-269, doi:10.1146/annurev-micro-

092412-155730 (2013).

10 Cowman, A. F., Healer, J., Marapana, D. & Marsh, K. Malaria: Biology and Disease. *Cell* **167**, 610-624, doi:https://doi.org/10.1016/j.cell.2016.07.055 (2016).

11 Miller, L. H., Baruch, D. I., Marsh, K. & Doumbo, O. K. The pathogenic basis of malaria. *Nature* **415**, 673-679 (2002).

12 WHO. Global Technical Strategy for Malaria 2016-2030. (2015).

13 Gething, P. W. *et al.* A long neglected world malaria map: Plasmodium vivax endemicity in 2010. *PLoS neglected tropical diseases* **6**, e1814-e1814, doi:10.1371/journal.pntd.0001814 (2012).

14 Gething, P. W. *et al.* A new world malaria map: Plasmodium falciparum endemicity in 2010. *Malaria Journal* **10**, 378, doi:10.1186/1475-2875-10-378 (2011).

15 Lucchi, N. W., Ndiaye, D., Britton, S. & Udhayakumar, V. Expanding the malaria molecular diagnostic options: opportunities and challenges for loop-mediated isothermal amplification tests for malaria control and elimination. *Expert Review or Molecular Diagnostics* **18**, 195-203 (2018).

16 A framework for malaria elmination. (World Health Organzation,Geneva, 2017)

17 WHO. Malaria diagnosis: memorandum from a WHO meeting. *Bulletin of the World Health Organization* **66**, 575-594 (1988).

18 WHO. Guidelines for the Treatment of Malaria. *WHO, Geneva*, 1-316 (2015).

19 WHO. Recommended selection criteria for procurement of malaria rapid diagnostic tests. (2018).

20 Watson, O. J. *et al.* Modelling the drivers of the spread of Plasmodium falciparum

hrp2 gene deletions in sub-Saharan Africa. *eLife* **6**, e25008, doi:10.7554/eLife.25008 (2017).

21 Berhane, A. *et al.* Major Threat to Malaria Control Programs by Plasmodium falciparum Lacking Histidine-Rich Protein 2, Eritrea. *Emerging infectious diseases* **24**, 462-470, doi:10.3201/eid2403.171723 (2018).

22 Parr, J. B. *et al.* Pfhrp2-Deleted Plasmodium falciparum Parasites in the Democratic Republic of the Congo: A National Cross-sectional Survey. *J Infect Dis* **216**, 36-44, doi:10.1093/infdis/jiw538 (2017).

23 Koita, O. A. *et al.* False-negative rapid diagnostic tests for malaria and deletion of the histidine-rich repeat region of the hrp2 gene. *The American journal of tropical medicine and hygiene* **86**, 194-198, doi:10.4269/ajtmh.2012.10-0665 (2012).

24 Cook, J. *et al.* Loop-mediated isothermal amplification (LAMP) for point-of-care detection of asymptomatic low-density malaria parasite carriers in Zanzibar. *Malar J* **14**, 43, doi:10.1186/s12936-015-0573-y (2015).

25 Han, E. Loop-mediated isothermal amplification test for the molecular diagnosis of malaria *Expert Review of Molecular Diagnostics* **13**, 205-218, doi:10.1586/erm.12.144 (2013).

26 Hopkins, H. *et al.* Highly sensitive detection of malaria parasitemia in a malaria-endemic setting: performance of a new loop-mediated isothermal amplification kit in a remote clinic in Uganda. *J Infect Dis* **208**, 645-652, doi:10.1093/infdis/jit184 (2013).

27 Lucchi, N. W. *et al.* Real-time fluorescence loop mediated isothermal amplification for the diagnosis of malaria. *PLoS One* **5**, e13733,

doi:10.1371/journal.pone.0013733 (2010).

28 Polley, S. D. *et al.* Mitochondrial DNA targets increase sensitivity of malaria detection using loop-mediated isothermal amplification. *J Clin Microbiol* **48**, 2866-2871, doi:10.1128/JCM.00355-10 (2010).

29 Britton, S., Cheng, Q., Sutherland, C. J. & McCarthy, J. S. A simple, high-throughput, colourimetric, field applicable loop-mediated isothermal amplification (HtLAMP) assay for malaria elimination. *Malar J* **14**, 335, doi:10.1186/s12936-015-0848-3 (2015).

30 Oriero, E. C., Jacobs, J., Van Geertruyden, J. P., Nwakanma, D. & D'Alessandro, U. Molecular-based isothermal tests for field diagnosis of malaria and their potential contribution to malaria elimination. *J Antimicrob Chemother* **70**, 2-13, doi:10.1093/jac/dku343 (2015).

31 Lucchi, N. W., Ljolje, D., Silva-Flannery, L. & Udhayakumar, V. Use of Malachite Green-Loop Mediated Isothermal Amplification for Detection of Plasmodium spp. Parasites. *PLoS One* **11**, e0151437, doi:10.1371/journal.pone.0151437 (2016).

32 Ghorbal, M. *et al.* Genome editing in the human malaria parasite Plasmodium falciparum using the CRISPR-Cas9 system. *Nat Biotechnol* **32**, 819-821, doi:10.1038/nbt.2925 (2014).

33 Meissner, M., Breinich, M. S., Gilson, P. R. & Crabb, B. S. Molecular genetic tools in Toxoplasma and Plasmodium: achievements and future needs. *Current Opinion in Microbiology* **10**, 349-356, doi:https://doi.org/10.1016/j.mib.2007.07.006 (2007).

34 Beck, J. R., Muralidharan, V., Oksman, A. & Goldberg, D. E. PTEX component

HSP101 mediates export of diverse malaria effectors into host erythrocytes. *Nature* **511**, 592-595, doi:10.1038/nature13574 (2014).

35 Florentin, A. *et al.* PfClpC Is an Essential Clp Chaperone Required for Plastid Integrity and Clp Protease Stability in Plasmodium falciparum. *Cell Rep* **21**, 1746-1756, doi:10.1016/j.celrep.2017.10.081 (2017).

36 Muralidharan, V., Oksman, A., Iwamoto, M., Wandless, T. J. & Goldberg, D. E. Asparagine repeat function in a Plasmodium falciparum protein assessed via a regulatable fluorescent affinity tag. *Proc Natl Acad Sci U S A* **108**, 4411-4416, doi:10.1073/pnas.1018449108 (2011).

37 Muralidharan, V., Oksman, A., Pal, P., Lindquist, S. & Goldberg, D. E. Plasmodium falciparum heat shock protein 110 stabilizes the asparagine repeat-rich parasite proteome during malarial fevers. *Nat Commun* **3**, 1310-1310 (2012).

38 Adli, M. The CRISPR tool kit for genome editing and beyond. *Nature Communications* **9**, 1911, doi:10.1038/s41467-018-04252-2 (2018).

39 Kirkman, L. A. & Deitsch, K. W. Antigenic variation and the generation of diversity in malaria parasites. *Curr Opin Microbiol* **15**, 456-462, doi:10.1016/j.mib.2012.03.003 (2012).

40 Kirkman, L. A., Lawrence, E. A. & Deitsch, K. W. Malaria parasites utilize both homologous recombination and alternative end joining pathways to maintain genome integrity. *Nucleic acids research* **42**, 370-379, doi:10.1093/nar/gkt881 (2014).

41 Lee, A. H., Symington, L. S. & Fidock, D. A. DNA Repair Mechanisms and Their Biological Roles in the Malaria

Parasite Plasmodium falciparum. *Microbiology and Molecular Biology Reviews* **78**, 469-486 (2014).

42 Prommana, P. *et al.* Inducible knockdown of Plasmodium gene expression using the glmS ribozyme. *PLoS One* **8**, e73783, doi:10.1371/journal.pone.0073783 (2013).

43 Cobb, D. W. *et al.* The Exported Chaperone PfHsp70x Is Dispensable for the Plasmodium falciparum Intraerythrocytic Life Cycle. *mSphere* **2**, doi:10.1128/mSphere.00363-17 (2017).

44 Ganesan, S. M., Falla, A., Goldfless, S. J., Nasamu, A. S. & Niles, J. C. Synthetic RNA-protein modules integrated with native translation mechanisms to control gene expression in malaria parasites. *Nat Commun* **7**, 10727, doi:10.1038/ncomms10727 (2016).

45 Arnot, D. E. & Jensen, A. T. R. in *Advances in Applied Microbiology* Vol. 74 (eds Allen I. Laskin, Sima Sariaslani, & Geoffrey M. Gadd) 77-96 (Academic Press, 2011).

46 Deponte, M. *et al.* Wherever I may roam: protein and membrane trafficking in P. falciparum-infected red blood cells. *Mol Biochem Parasitol* **186**, 95-116, doi:10.1016/j.molbiopara.2012.09.007 (2012).

47 Hiller, N. L. *et al.* A Host-Targeting Signal in Virulence Proteins Reveals a Secretome in Malarial Infection. *Science* **306** (2015).

48 Marti, M., Good, R. T., Rug, M., Knuepfer, E. & Cowman, A. F. Targeting malaria virulence and remodeling proteins to the host erythrocyte. *Science* **306**, 1930-1933 (2004).

49 Tonkin, C. J. *et al.* Evolution of malaria parasite plastid targeting sequences. *Proc Natl Acad Sci U S A* **105**, 4781-4785, doi:10.1073/pnas.0707827105 (2008).

50 Tonkin, C. J., Kalanon, M. & McFadden, G. I. Protein targeting to the malaria parasite plastid. *Traffic* **9**, 166-175, doi:10.1111/j.1600-0854.2007.00660.x (2008).

51 Waller, R. F., Reed, M. B., Cowman, A. F. & McFadden, G. I. Protein trafficking to the plastid of Plasmodium falciparum is via the secretory pathway. *EMBO J* **19**, 1794-1802 (2000).

52 Foth, B. J. *et al.* Dissecting Apicoplast Targeting in the Malaria Parasite Plasmodium falciparum. *Science* **299**, 705-708 (2003).

53 Gruring, C. *et al.* Uncovering common principles in protein export of malaria parasites. *Cell Host Microbe* **12**, 717-729, doi:10.1016/j.chom.2012.09.010 (2012).

54 Heiber, A. *et al.* Identification of new PNEPs indicates a substantial non-PEXEL exportome and underpins common features in Plasmodium falciparum protein export. *PLoS Pathog* **9**, e1003546, doi:10.1371/journal.ppat.1003546 (2013).

55 Gidalevitz, T., Stevens, F. & Argon, Y. Orchestration of secretory protein folding by ER chaperones. *Biochim Biophys Acta* **1833**, 2410-2424, doi:10.1016/j.bbamcr.2013.03.007 (2013).

56 Russo, I. *et al.* Plasmepsin V licenses Plasmodium proteins for export into the host erythrocyte. *Nature* **463**, 632-636, doi:10.1038/nature08726 (2010).

57 Yeh, E. & DeRisi, J. L. Chemical rescue of malaria parasites lacking an

apicoplast defines organelle function in blood-stage Plasmodium falciparum. *PLoS Biol* **9**, e1001138, doi:10.1371/journal.pbio.1001138 (2011).

58 van Dooren, G. G., Su, V., D'Ombrain, M. C. & McFadden, G. I. Processing of an apicoplast leader sequence in Plasmodium falciparum, and the identification of a putative leader cleavage enzyme. *J Biol Chem* **277**, 23612-23619 (2002).

59 Ramya, T. N., Karmodiya, K., Surolia, A. & Surolia, N. 15-deoxyspergualin primarily targets the trafficking of apicoplast proteins in Plasmodium falciparum. *J Biol Chem* **282**, 6388-6397, doi:10.1074/jbc.M610251200 (2007).

60 Ramya, T. N., Surolia, N. & Surolia, A. 15-Deoxyspergualin modulates Plasmodium falciparum heat shock protein function. *Biochem Biophys Res Commun* **348**, 585-592, doi:10.1016/j.bbrc.2006.07.082 (2006).

61 Araki, K. & Nagata, K. Protein folding and quality control in the ER. *Cold Spring Harb Perspect Biol* **3**, a007526, doi:10.1101/cshperspect.a007526 (2011).

62 Smith, M. H., Ploegh, H. L. & Weissman, J. S. Road to ruin: targeting proteins for degradation in the endoplasmic reticulum. *Science* **334**, 1086-1090 (2011).

63 Walter, P. & David, R. The unfolded protein response: from stress pathway to homeostatic regulation. *Science* **334**, 1081-1086 (2011).

64 Harbut, M. B. *et al.* Targeting the ERAD pathway via inhibition of signal peptide peptidase for antiparasitic therapeutic design. *Proc Natl Acad Sci U S A* **109**, 21486-21491 (2012).

65 Chaubey, S., Grover, M. & Tatu, U. Endoplasmic reticulum stress triggers gametocytogenesis in the malaria parasite. *J Biol Chem* **289**, 16662-16674, doi:10.1074/jbc.M114.551549 (2014).

66 Zhang, M. *et al.* Inhibiting the Plasmodium eIF2alpha Kinase PK4 Prevents Artemisinin-Induced Latency. *Cell Host Microbe* **22**, 766-776 e764, doi:10.1016/j.chom.2017.11.005 (2017).

67 Zhang, M. *et al.* PK4, a eukaryotic initiation factor 2α(eIF2α) kinase, is essential for the development of the erythrocytic cycle of Plasmodium. *PNAS* **109**, 3956–3961 (2012).

68 Harding, H. P., Zhang, Y. & Ron, D. Protein translation and folding are coupled by an endoplasmic-reticulum-resident kinase. *Nature* **397**, 271, doi:10.1038/16729 (1999).

69 Kumar, N., Koski, G., Harada, M., Aikawa, M. & Zheng, H. Induction and localization of Plasmodium falciparum stress proteins related to the heat shock protein 70 family. *Molecular and Biochemical Parasitology* **48**, 47-58, doi:https://doi.org/10.1016/0166-6851(91)90163-Z (1991).

70 Vogel, J. P., Misra, L. M. & Rose, M. D. Loss of BiP/GRP78 function blocks translocation of secretory proteins in yeast. *J Cell Biol* **110**, 1885-1895 (1990).

71 Gething, M. J. Role and regulation of the ER chaperone BiP. *Semin Cell Dev Biol* **10**, 465-472 (1999).

72 Flynn, G. C., Pohl, J., Flocco, M. T. & Rothman, J. E. Peptide-binding specificty of the molecular chaperone BiP. *Nature* **353**, 726-730 (1991).

73 Blond-Elguindi, S. *et al.* Affinity panning of a library of peptides displayed on bacteriophages reveals the binding specificity of BiP. *Cell* **75**, 717-728, doi:https://doi.org/10.1016/0092-8674(93)90492-9 (1993).

74 Dorner, A. J., Wasley, L. C. & Kaufman, R. J. Protein dissociation from GRP78

and secretion are blocked by depletion of cellular ATP levels. *Proc Natl Acad Sci U S A* **87**, 7429-7432 (1990).

75 Andreasson, C., Rampelt, H., Fiaux, J., Druffel-Augustin, S. & Bukau, B. The endoplasmic reticulum Grp170 acts as a nucleotide exchange factor of Hsp70 via a mechanism similar to that of the cytosolic Hsp110. *J Biol Chem* **285**, 12445-12453, doi:10.1074/jbc.M109.096735 (2010).

76 Shen, J. *et al.* Coinduction of glucose-regulated proteins and doxorubicin resistance in Chinese hamster cells. *Proceedings of the National Academy of Sciences of the United States of America* **84**, 3278-3282 (1987).

77 Behnke, J. & Hendershot, L. M. The large Hsp70 Grp170 binds to unfolded protein substrates in vivo with a regulation distinct from conventional Hsp70s. *J Biol Chem* **289**, 2899-2907, doi:10.1074/jbc.M113.507491 (2014).

78 Park, J. *et al.* The Chaperoning Properties of Mouse Grp170, a Member of the Third Family of Hsp70 Related Proteins. *Biochemistry* **42**, 14893-14902 (2003).

79 Buck, T. M. *et al.* The Lhs1/GRP170 chaperones facilitate the endoplasmic reticulum-associated degradation of the epithelial sodium channel. *J Biol Chem* **288**, 18366-18380, doi:10.1074/jbc.M113.469882 (2013).

80 Wang, H. *et al.* The Endoplasmic Reticulum Chaperone GRP170: From Immunobiology to Cancer Therapeutics. *Front Oncol* **4**, 377, doi:10.3389/fonc.2014.00377 (2014).

81 Sanson, M. *et al.* Oxidized low-density lipoproteins trigger endoplasmic reticulum stress in vascular cells: prevention by oxygen-regulated protein 150 expression. *Circ Res* **104**, 328-336, doi:10.1161/CIRCRESAHA.108.183749 (2009).

82 Wang, Y. *et al.* Involvement of oxygen-regulated protein 150 in AMP-activated protein kinase-mediated alleviation of lipid-induced endoplasmic reticulum stress. *J Biol Chem* **286**, 11119-11131, doi:10.1074/jbc.M110.203323 (2011).

83 Tyson, J. R. & Stirling, C. J. LHS1 and SIL1 provide a lumenal function that is essential for protein translocation into the endoplasmic reticulum. *The EMBO Journal* **19**, 6440-6452 (2000).

CHAPTER 2

Field evaluation of malaria malachite green loop-mediated isothermal amplification in health posts in Roraima state, Brazil

Kudyba, H. M., Louzada, J., Ljolje, D., Kudyba, K. A., Muralidharan, V., Oliveira-Ferreira, J., Lucchi, N.W. 2019. *Malaria Journal*. Reprinted here with permission of the publisher

ABSTRACT

Background

Microscopic detection of malaria parasites is the standard method for clinical diagnosis of malaria in Brazil. However, malaria epidemiological surveillance studies specifically aimed at the detection of low-density infection and asymptomatic cases will require more sensitive and field usable tools. We evaluated the diagnostic accuracy of the colorimetric malachite green loop-mediated isothermal amplification (MG-LAMP) assay remote health posts in Roraima state, Brazil.

Methods

Study participants were prospectively enrolled from health posts (health care seeking patients) and from nearby villages (healthy participants) in three different study sites. The MG-LAMP assay and microscopy were performed in the health posts. Two independent readers scored the MG-LAMP tests as positive (blue/green) or negative (clear). Sensitivity and specificity of local microscopy and MG-LAMP were calculated using results of PET-PCR as a reference.

Results

A total of 91 participants were enrolled. There was 100% agreement between the two MG-LAMP readers (Kappa=1). The overall sensitivity and specificity of MG-LAMP were 90.0% (95% confidence interval [1]: 76.34%- 97.21%) and 94% (95% CI: 83.76%- 98.77%), respectively. The sensitivity and specificity of local microscopy were 83% (95% CI: 67.22%- 92.66% and 100% (95% CI: 93.02%- 100.00%), respectively. PET-PCR detected six mixed infections (infection with both *P. falciparum* and *P. vivax*); two of these were also detected by MG-LAMP and one by microscopy. Microscopy did not

detect any *Plasmodium* infection in the 26 healthy participants; MG-LAMP detected Plasmodium in five of these and PET-PCR assay detected infection in three. Overall, implementation of the MG-LAMP in this setting was

Conclusion

MG-LAMP is a sensitive and specific assay that may be useful for the detection of malaria parasites in remote health care settings.

INTRODUCTION

Malaria is a devastating disease that remains a major global health burden. The illness arises from infection with parasites of the genus *Plasmodium*. Cases of the most significant morbidity and mortality in humans are caused by the most prevalent species, *P. vivax* and *P. falciparum*. *P. ovale* and *P. malariae* also cause human malaria, but the infections are typically associated with milder symptoms. In 2017, an estimated 219 million cases of malaria occurred worldwide [2]. Most malaria cases in 2017 were reported in sub-Saharan Africa (200 million, 92%). The WHO Region of the Americas recorded a rise, largely due to increases in malaria transmission in Brazil, Nicaragua and Venezuela[2]. In Brazil, the vast majority of malaria cases are concentrated in the Brazilian Amazon Region. The state of Roraima in Brazil is located in the Amazon region in the far north on the border with Venezuela and Guyana. In 2017, Roraima reported 11,966 cases of malaria which was a 44% increase compared to 2016 (8,307)[3]. Based on data from the Brazilian Secretariat of Health Surveillance, 50% of patients seen in the State of Roraima were residents of Venezuela and Guyana. There is frequent movement of the population and vectors in the border region, and access to preventive health care in Venezuela and Guyana is limited. Thus, control of malaria in

Roraima is endangered and the border area is vulnerable to malaria outbreaks and epidemics.

One of the challenges for malaria surveillance and control programs is the timely identification of low-density infections not detected by the routine diagnostic tests: microscopy and standard rapid diagnostic tests (RDTs). Currently, the primary method used in Brazil for the diagnosis of malaria is microscopy of a Giemsa-stained thick or thin blood smear, but there are limitations of microscopy, including inability to detect very low density (sub-microscopic) parasitemia, occasional misdiagnosis of mixed-species infection, and the fact that it is time consuming[1,4-7]. A majority of submicroscopic infections are asymptomatic. Individuals who are asymptomatic do not seek treatment resulting in a population of individuals with persistent infections, capable of transmitting malaria in the population, (reviewed in[8]). It is important to identify and treat persons with these low-level parasitemia's during malaria epidemiological surveys. Furthermore, the elimination of malaria will require active case detection in low transmission areas as well as the ability to detect sub-microscopic infections[9]. Thus, there is a need to develop and validate sensitive diagnostic tools. Molecular-based diagnostic tools provide more sensitive and specific methods for detecting *Plasmodium* infections than microscopy and RDTs. To be a "significant improvement" over expert microscopy, it is recommended that molecular tests be at least one log more sensitive than microscopy; preferably have a detection limit of 2 parasites/μl or less [10]. The use of molecular-based diagnostic tools in research and in epidemiological surveys has expanded in recent years. However, their use is still limited to laboratories with more sophisticated facilities due to the requirement of specialized equipment and technical

expertise. Simpler molecular tests, such as the loop-mediated isothermal amplification (LAMP) assays, promise to facilitate the use of molecular tests even in facilities with limited resources[11-15].

As recently reviewed [16], several malaria LAMP-based assays have been described to date. Many of these have excellent diagnostic performances, e.g. detecting as few as 1 parasite/μl (***illumi***gene LAMP), or 1-5 parasites/μl (EIKEN LAMP), however, they are not without limitations. These include the requirement for additional equipment for the read-out, the limited number of samples tested per run, and the fact that some are capable of detecting the malaria parasites at the genus level only. Recently, we reported on the development of a malaria malachite green loop-mediated isothermal amplification (MG-LAMP) as a LAMP method for diagnosing *Plasmodium* infection[17]. Three factors make the MG-LAMP assay appealing: 1) performance of the MG-LAMP assay requires only a small portable heat block and mini-centrifuge, 2) it is a colorimetric assay that does not require any special read-out equipment, and 3) the heat block used has a 38-sample capacity allowing for the testing of many samples at once therefore has the potential for use in large scale studies. To date, only two other high throughput (HTP) colorimetric malaria LAMP assays have been described[18,19].

In this study, we field-tested the performance of the MG-LAMP assay in health posts in three municipalities of Roraima, Brazil using freshly isolated patient samples. The MG-LAMP diagnosis was compared to results provided by the local microscopists at the sites of study. The sensitivity and specificity of MG-LAMP performed in these remote health posts with limited laboratory infrastructure was compared to that of a real-time PCR (PET-PCR) [20] assay.

MATERIALS AND METHODS

Ethical considerations

This study was part of a larger study approved by the Federal University of Roraima Ethical Committee (CAAE: 44055315.0.0000.5302). Written informed consent was obtained from all participants. The Centers for Disease Control and Prevention (CDC) investigators provided technical advice but did not have direct contact with study participants or access to any personally identifiable information and were considered not to be engaged in the research (protocol 2017-105).

Collection of clinical samples

This prospective study was carried out between July and August 2017 in malaria heath posts in three municipalities of Roraima, Brazil (Boa Vista, Pacaraima, and Rorainopolis). Patients attending the health posts for malaria screening and treatment were eligible to be enrolled in the study. In addition, healthy controls were enrolled from houses near the health posts. Blood samples were obtained from all enrolled patients by venipuncture. Enrolled patients were tested for malaria by a trained local microscopist using 10% Giemsa-stained thick blood smear, and the diagnosis and parasitemia level were recorded for each patient. Additionally, all consenting patients filled out a clinical questionnaire that addressed whether patient had symptoms, their age and sex, their residence and whether they had prior *Plasmodium* infections.

LAMP logistics

Blood sample collection and processing, microscopy, DNA extraction and MG-LAMP assays were all performed in the malaria health posts in Roraima by a US-based

graduate student with some training in molecular biology but with no field experience. Two laboratory technicians with no previous experience with LAMP were trained to read the MG-LAMP results. To simplify the MG-LAMP procedure, a three-component ready-to-use kit was used: component I contained all the necessary reaction components for the assay (LAMP buffer: 40 mM Tris-HCL pH 8.8, 20 mM KCl, 16 mM MgSO4, 20 mM (NH4)SO4, 0.2% Tween-20, 0.8 M Betaine, and 2.8 mM of dNTPs and the primers (stored in a 4^{o}C refrigerator); component II contained the Bst polymerase (stored at -20^{o}C) and component III contained 0.2% malachite green dye. To perform the assay, 13.8µL of Component I was mixed with 0.8µL of the Bst polymerase and 0.4uL of the malachite green dye for a final concentration of malachite green of 0.008%. Five µL of DNA template was added and tubes place in the preheated heat-block.

DNA Extraction

The DNA extraction was performed in small rooms within health posts. DNA was extracted from 200µL of whole blood using the QIAamp DNA Mini Kit (Qiagen). The manufacturer's provided DNA extraction protocol was slightly modified in that all of the spins were performed at 2,000g using a mini-centrifuge (Myfuge^{TM}) that was easily transported in the field setting.

LAMP method

All samples were screened for *Plasmodium* using the genus assay as described previously[17] in a final reaction volume of 20µL. Samples were incubated for 1 hour at 63^{o}C in a mini heat block (GeneMate, Bioexpress) to amplify the DNA. Following the 1-hour incubation, samples were removed from the heat block and allowed to cool for 15

minutes, the results were then scored by two independent readers as being positive (light blue/green) or negative (clear/colorless). Positive and negative controls were included during each run using *P. falciparum* 3D7 DNA or nuclease free water, respectively. *P. falciparum a*nd *P. vivax* species-specific MG-LAMP assays were carried out on all samples that were positive by the genus assay. These assays were performed using the 3-component ready-to-use in-house kits prepared using previously published *P. falciparum* and *P. vivax* primers[21,22]. Each reaction contained 5µL of isolated DNA in a final reaction volume of 20µL. Positive controls included a *P. falciparum* positive sample and a *P. vivax* positive sample. Nuclease free water was included as a negative control.

PET-PCR method

DNA samples were shipped to the malaria branch laboratory at the CDC using cold-packs. *Plasmodium* genus-specific PET-PCR was performed in duplicate as described previously except that 5µL of DNA was used instead of 2µl[20]. The reactions contained 2X TaqMan Environmental Master Mix 2.0 (Applied Biosystems, Foster City, CA, USA), 250nM of Genus forward Primer and FAM-Genus reverse primer, and 5µL of isolated DNA for a final volume of 20µL. The PET-PCR reaction was run using an Agilent Mx3005pro thermocycler (Agilent Technologies, Santa Clara, CA, USA) using the following cycling parameters ed: 15 minutes initial hot-start at 95ºC followed by 45 cycles of denaturing at 95ºC for 20 seconds, annealing at 63ºC for 40 seconds, and an extension of 30 seconds at 72ºC. A positive and negative control, 3D7 and nuclease free water respectively, were included in each run. Samples were designated as positive if they had a threshold cycle (Ct) value below 40.0 and negative if they had No

Ct value or Ct values above 40.0. Species-specific PET-PCR was performed in duplicate on all samples that were positive by the genus specific PET-PCR, using species-specific primers (Table 2.1). Two duplex reactions were set up to detect *P. ovale* together with *P. falciparum* and *P. malariae* together with *P. vivax.* The duplexed reactions were 20µL containing 2X TaqMan Environmental Master Mix 2.0 (Applied Biosystems), 250nM of FAM-*P. ovale* forward primer, 250nM *P. ovale* reverse primer, 250nM of *P. falciparum* forward primer, 125nM of HEX-*P. falciparum* reverse primer, 250nM *P. malariae* forward primer, 250nM FAM-*P. malariae*, 125nM *P. vivax* forward primer, 125nM HEX-*P. vivax* reverse primer and 5µL of isolated DNA. Reactions were run using the same cycling conditions as the Genus PET-PCR. Positive controls consisting of samples with known *Plasmodium* species and nuclease free water as a negative control were included in each run.

Statistical analyses

The percentage specificity and sensitivity were calculated as follows: Sensitivity=true positives/(true positives+false negatives) × 100. Specificity=true negatives/(true negatives+false positives) × 100. In addition, 95% Confidence Intervals (95% CI) for both sensitivity and specificity were calculated. The agreement between the human readers and diagnostic tests was assessed by calculating the kappa coefficients. 95% confidence intervals were calculated using MEDCALC® and GraphPad.

RESULTS

Patient enrollment

A total of 91 participants were enrolled during the two months of the study: 65 patients presenting with malaria symptoms (axillary temperature ≥ 37.5°C) at the health posts and 26 healthy participants from nearby villages, Figure 2.1. None of the 26 healthy participants exhibited any symptoms of malaria. Of the 91 enrolled participants, 86 (94.5%) reported having had previous malaria infections while 4 (4.4%) had no previous malaria and 1 (1.1%) did not provide this information.

Agreement between human readers for the MG-LAMP assay

Two independent human readers scored the MG-LAMP tests as positive or negative. There was 100% agreement between the two readers (Kappa=1).

Overall results of microscopy, MG-LAMP, and PET-PCR

Of the 91 samples, 33 (36%) were malaria positive by microscopy, 39 (43%) were positive by MG-LAMP, and 40 (44%) were positive by PET-PCR, Figure 2.2. All samples were negative for *P. malariae* and *P. ovale*.

Specificity and sensitivity of MG-LAMP and microscopy compared to PET-PCR

The sensitivity and specificity of the MG-LAMP assays and microscopy were calculated using PET-PCR as a reference test, Table 2.2.

Agreement of MG-LAMP with PET-PCR

We found that *Plasmodium* genus assay for MG-LAMP and PET-PCR agreed 92.3% of the time (Kappa=0.84, 95% CI: 0.732 to 0.955). When comparing the *P. falciparum* and *P. vivax* MG-LAMP and PET-PCR assays we found 97.8%

(Kappa=0.89, 95% CI: 0.735 to 1.000) and 96.7% (Kappa=0.92, 95% CI: 0.839 to 1.000) agreement between the two tests, respectively.

Detection of mixed infections

Microscopy detected one mixed *P. falciparum* and *P. vivax* infection. This infection was detected to be a *P. falciparum* only infection by both the MG-LAMP and PET-PCR assays. There were two mixed infections detected by MG-LAMP and six detected by PET-PCR (Table 2.3). In the four cases where the MG-LAMP did not detect the mixed infections identified by the PET-PCR, the Ct values were high, suggesting low parasite density infections, Table 2.3.

Detection of parasitemia in asymptomatic patients

Of the twenty-six enrolled healthy participants, five were positive for *Plasmodium* by MG-LAMP and three were positive for *Plasmodium* by PET-PCR assay. None of these were positive by microscopy (Table 2.4). Four of the five cases that were positive by MG-LAMP were only positive at the genus level and the infecting species could not be determined, Table 2.4. Two of these samples were positive by both MG-LAMP and PET-PCR, one only at the genus level.

Discordant Results

Seven samples were found to have discordant results among the three tests, Table 2.5. Four of these samples were negative by microscopy and MG-LAMP but positive by PET-PCR. Three of these samples were positive by PET-PCR genus test and negative by species tests, while one was positive by PET-PCR *P. vivax* (Table 2.5). In these four cases, the Ct values by PET-PCR were all above 35.0 Three samples

yielded a positive MG-LAMP genus test but were negative for the MG-LAMP *P. falciparum* and *P. vivax* tests and by both microscopy and PET-PCR (Table 2.5).

DISCUSSION

The findings presented in this study demonstrate the accuracy of the MG-LAMP as a malaria diagnostic test in remote health posts in a malaria endemic country. Importantly our data demonstrate that the MG-LAMP is sensitive at identifying infections not detectable by microscopy. Additionally, we demonstrate that this assay, like the PET-PCR assay used as a reference test in this study, is capable of detecting mixed infections that microscopy missed. However, the MG-LAMP assay missed four positive samples and four mixed infections detected by PET-PCR. These missed infections were all shown to be of much lower parasite densities (based on the high Ct values (between 35 and 39) in the PET-PCR assay. Extrapolation using our previously obtained PET-PCR data shows that a Ct value of 35.0 corresponds to about 16 parasites/μl[20] therefore, the missed samples likely had parasite densities of about 16 parasites/μl (3 samples) and below (5 samples). While a detection limit of 16 parasites/μl is much better than that for routine microscopy, it is within the detection limits of many PCR-based assays and some previously published LAMP-based assays. Previously, the malaria MG-LAMP assay was shown to have a limit of detection of 1-8 parasites/μl [17] using quantified standard curves, however, this limit of detection did not hold when the assay was performed in a field setting. More sensitive MG-LAMP primers or a change in assay conditions may be required to achieve the same level of diagnostic accuracy as the PET-PCR assay. In addition, there were three cases where MG-LAMP yielded a positive genus result, while microscopy and PET-PCR were negative. It is likely that

these are false positives by the MG-LAMP assay, however, we cannot rule out that these are indeed true positives missed by PET-PCR, a phenomenon that has been observed before in evaluation studies using low-density infection samples [11,12].

However, while PCR-based assays such as PET-PCR have superior sensitivity for diagnosing low-density infections, they are far more complicated procedurally compared to the MG-LAMP, as they require costly equipment and supplies. The MG-LAMP assay evaluated in this study can be performed using a small portable heat block and mini-centrifuge and does not require any special read-out equipment since it is a colorimetric assay. Thus, it is an appealing test for use in resource-limited facilities. In addition, it has a 38-sample capacity allowing for high-throughput (HTP) testing therefore has the potential for use in large-scale studies. Further investment in refining simple molecular tests to increase sensitivity would allow them to be used in resource-limited settings for the detection of low-density infections.

A limitation of the current format of the MG-LAMP is the fact that the LAMP buffers and polymerase require cold chain, which is not ideal in more resource-limited settings. Currently, there are two available malaria LAMP assays that do not require a cold chain: the EIKEN LAMP and ***illumi***gene LAMP, but each of these have limitations, reviewed in [16]. For example, the ***illumi***gene LAMP assay is only a genus-specific test and is only capable of testing 10 samples per run. Elimination of the need for a cold chain will be required if the MG-LAMP assay is to be used in the settings without a laboratory. However, in facilities similar to the health post used in this study, the current format of MG-LAMP assay can be performed. The use of DNA extracted using commercially available blood kits should be avoided as this adds extra steps and cost to

the test; the use of boil-and-spin DNA isolation should be further explored in future field studies.

Although we enrolled healthy participants in an effort to estimate the ability of the MG-LAMP to detect asymptomatic parasitemia, the number of healthy participants was too low to draw firm conclusions

Overall, MG-LAMP evaluated in this study provided a portable, sensitive and specific assay for the detection of malaria parasites in a remote health clinic in Brazil when compared to microscopy. However, the current format of the assay was not sensitive enough to be recommended for detection of low-density infections and improvements will be required to enhance its sensitivity and if possible, to make it a more field usable tool that does not require a cold-chain.

ACKNOWLEDGMENTS

We would like to thank all the patients who enrolled in this study and made this work possible and the Secretary of Health of Roraima and the local malaria control program team of Boa Vista, Pacaraima and Rorainopolis for their logistical support. This work was supported by the US National Institutes of Health to H.M.K (T32AI060546). JOF is recipient of Research Productivity Fellowships from the Conselho Nacional de Desenvolvimento Científico e Tecnológico (CNPq). The findings and conclusions in this report are those of the author(s) and do not necessarily represent the official position of the Centers for Disease Control and Prevention

References

1 Tajebe, A., Magoma, G., Aemero, M. & Kimani, F. Detection of mixed infection level of Plasmodium falciparum and Plasmodium vivax by SYBR GreenI-based real-time PCR in North Gondar, north-west Ethiopia. *Malaria Journal* **13**, 1-8 (2014).

2 World Health Organization. World Malaria Report. (World Health Organization, Geneva, 2018).

3 Epidemiological Alert: Increase of malaria in the Americas. (Pan American Health Organization 2018).

4 Wongsrichanalai, C., Barcus, M. J., Muth, S., Sutamihardja, A. & Wernsdorfer, W. H. A Review of Malaria Diagnostic Tools: Microscopy and Rapid Diagnostic Test (RDT). *The American Journal of Tropical Medicine and Hygiene* **77**, 119-127 (2007).

5 Ehtesham, R., Fazaeli, A., Raeisi, A., Keshavarz, H. & Heidari, A. Detection of mixed-species infections of Plasmodium falciparum and Plasmodium vivax by nested PCR and rapid diagnostic tests in southeastern Iran. *Am J Trop Med Hyg* **93**, 181-185, doi:10.4269/ajtmh.14-0650 (2015).

6 Krishna, S. *et al.* Detection of Mixed Infections with Plasmodium spp. by PCR, India, 2014. *Emerg Infect Dis* **21**, 1853-1857, doi:10.3201/eid2110.150678 (2015).

7 Roth, J. M., Korevaar, D. A., Leeflang, M. M. & Mens, P. F. Molecular malaria diagnostics: A systematic review and meta-analysis. *Crit Rev Clin Lab Sci* **53**, 87-105, doi:10.3109/10408363.2015.1084991 (2016).

8 Okell, L. C., Ghani, A. C., Lyons, E. & Drakeley, C. J. Submicroscopic infection in Plasmodium falciparum-endemic populations: a systematic review and meta-analysis. *The Journal of infectious diseases* **200**, 1509-1517, doi:10.1086/644781 (2009).

9 A framework for malaria elimination. (World Health Organization, Geneva, 2017).

10 WHO Evidence Review Group on Malaria Diagnosis in Low Transmission Settings<http://www.who.int/malaria/mpac/mpac_mar2014_diagnosis_low_transmission_settings_report.pdf> (2014).

11 Cook, J. *et al.* Loop-mediated isothermal amplification (LAMP) for point-of-care detection of asymptomatic low-density malaria parasite carriers in Zanzibar. *Malar J* **14**, 43, doi:10.1186/s12936-015-0573-y (2015).

12 Hopkins, H. *et al.* Highly sensitive detection of malaria parasitemia in a malaria-endemic setting: performance of a new loop-mediated isothermal amplification kit in a remote clinic in Uganda. *J Infect Dis* **208**, 645-652, doi:10.1093/infdis/jit184 (2013).

13 Lucchi, N. W. *et al.* Real-time fluorescence loop mediated isothermal amplification for the diagnosis of malaria. *PLoS One* **5**, e13733, doi:10.1371/journal.pone.0013733 (2010).

14 Polley, S. D. *et al.* Mitochondrial DNA targets increase sensitivity of malaria detection using loop-mediated isothermal amplification. *J Clin Microbiol* **48**, 2866-2871, doi:10.1128/JCM.00355-10 (2010).

15 Oriero, E. C., Jacobs, J., Van Geertruyden, J. P., Nwakanma, D. & D'Alessandro, U. Molecular-based isothermal tests for field diagnosis of malaria and their

potential contribution to malaria elimination. *J Antimicrob Chemother* **70**, 2-13, doi:10.1093/jac/dku343 (2015).

16 Lucchi, N. W., Ndiaye, D., Britton, S. & Udhayakumar, V. Expanding the malaria molecular diagnostic options: opportunities and challenges for loop-mediated isothermal amplification tests for malaria control and elimination. *Expert Rev Mol Diagn* **18**, 195-203, doi:10.1080/14737159.2018.1431529 (2018).

17 Lucchi, N. W., Ljolje, D., Silva-Flannery, L. & Udhayakumar, V. Use of Malachite Green-Loop Mediated Isothermal Amplification for Detection of Plasmodium spp. Parasites. *PLoS One* **11**, e0151437, doi:10.1371/journal.pone.0151437 (2016).

18 Britton, S. *et al.* A Sensitive, Colorimetric, High-Throughput Loop-Mediated Isothermal Amplification Assay for the Detection of Plasmodium knowlesi. *The American journal of tropical medicine and hygiene* **95**, 120-122, doi:10.4269/ajtmh.15-0670 (2016).

19 Britton, S., Cheng, Q., Sutherland, C. J. & McCarthy, J. S. A simple, high-throughput, colourimetric, field applicable loop-mediated isothermal amplification (HtLAMP) assay for malaria elimination. *Malaria journal* **14**, 335, doi:10.1186/s12936-015-0848-3 (2015).

20 Lucchi, N. W. *et al.* Molecular diagnosis of malaria by photo-induced electron transfer fluorogenic primers: PET-PCR. *PLoS One* **8**, e56677, doi:10.1371/journal.pone.0056677 (2013).

21 Yamamura, M., Makimura, K. & Ota, Y. Evaluation of a New Rapid Molecular Diagnostic System for Plasmodium falciparum Combined with DNA Filter Paper,

Loop-Mediated Isothermal Amplification, and Melting Curve Analysis *Jpn. J. Infect. Dis* **62**, 20-25 (2009).

22 Patel, J. C. *et al.* Real-time loop-mediated isothermal amplification (RealAmp) for the species-specific identification of Plasmodium vivax. *PLoS One* **8**, e54986, doi:10.1371/journal.pone.0054986 (2013).

Table 2.1: PET-PCR Primers utilized in the evaluation

Primer	Sequence
P. vivax Forward	5'- ACT GAC ACT GAT GAT TTA GAA CCC ATT T -3'
HEX-*P. vivax* Reverse	5'-agg cgc ata gcg cct ggT GGA GAG ATC TTT CCA TCC TAA ACC T-3'

(HEX-labeled: based on the *plasmepsin* gene)

Primer	Sequence
P. malariae Forward	5'-AAGGCAGTAACACCAGCAGTA-3'
FAM-*P. malariae* Reverse	5'-agg cgc ata gcg cct ggTCCCATGAAGTTATATTCCCGCTC-3'

(FAM-labeled: based on *dihydofolate reductase-thymidylate synthase* (DHFR-TS) gene)

Table 2.2: Sensitivity and specificity of MG-LAMP and microscopy using PET-PCR as a reference.

	Method	Sensitivity	Specificity
Genus	**Microscopy**	83% (95% CI:67.22%-92.66%	100% (95% CI: 93.02%-100.00%)
	MG-LAMP	90% (95% CI: 76.34%-97.21%)	94% (95% CI: 83.76%-98.77%)
P. falciparum	**Microscopy**	64% (95% CI: 93.02%-100.00%)	99% (95% CI: 93.23%-99.97%)
	MG-Lamp	82% (95% CI: 48.22%-97.72%)	100% (95% CI: 95.49%-100.00%)
P. vivax	**Microscopy**	83% (95% CI: 65.28% - 94.36%)	98% (95% CI: 91.20%-99.96%)
	MG-LAMP	90% (95% CI: 73.47%-97.89%)	100% (95% CI: 94.13% - 100.00%)

Table 2.3: Detection of mixed infections by microscopy, MG-LAMP and PET-PCR

Sample	Microscopy diagnosis	MG-LAMP diagnosis	PET-PCR diagnosis	PET-PCR CT value for *P. falciparum*	PET-PCR CT value for *P. vivax*
PC121	*P. vivax*	Mixed	Mixed	22.68	28.5
PC123	*P. falciparum*	Mixed	Mixed	26.56	39.9
BV237	*P. vivax*	*P. vivax*	Mixed	35.1	29.12
BV217	*P. vivax*	*P. vivax*	Mixed	36.24	32.23
BV239	*P. vivax*	*P. falciparum*	Mixed	31.37	35.38
BV241	*P. falciparum*	*P. falciparum*	Mixed	29.43	39.92
BV240	Mixed*	*P. falciparum*	*P. falciparum*	37.82	No Ct

*****Only one *P. vivax* parasite was seen under the microscopy

Table 2.4: Asymptomatic patients detected by MG-LAMP and PET-PCR.

Sample	**Microscopy Diagnosis**	**MG-LAMP diagnosis**	**PET-PCR Genus (Ct value)**	**PET-PCR *P. vivax* (Ct value)**	**PET-PCR *P. falciparum* (Ct value)**
RR09	Negative	Genus only	Negative (40.7)	Negative (No Ct)	Negative (No Ct)
RR10	Negative	Genus only	Negative (41.76)	Negative (No Ct)	Negative (No Ct)
RR37*	**Negative**	***P. vivax***	**Positive (32.74)**	**Positive (35.96)**	**Negative (No Ct)**
RR41	Negative	Genus only	Positive (38.76)	Negative (41.99)	Negative (No Ct)
RR42	Negative	Genus only	Negative (40.74)	Negative (41.69)	Negative (No Ct)
RR53	Negative	Negative	Positive (34.99)	Positive (39.09)	Negative (No Ct)

* The only sample shown to be positive by both MG-LAMP and PET-PCR.

Table 2.5: Summary of discordant results.

Sample	Microscopy diagnosis	MG-LAMP Genus diagnosis	PET-PCR Genus (Ct value)	PET-PCR *P. vivax* (Ct value)	PET-PCR *P. falciparum* (Ct value)
RR53	Negative	Negative	Positive (34.99)	Positive (39.09)	Negative (No Ct)
BV235	Negative	Negative	Positive (35.78)	Negative (No Ct)	Negative (No Ct)
RR01	Negative	Negative	Positive (37.96)	Negative (No Ct)	Negative (No Ct)
BV236	Negative	Negative	Positive (39.34)	Negative (No Ct)	Negative (No Ct)
RR09	Negative	Positive	Negative (40.7)	Negative (No Ct)	Negative (No Ct)
RR10	Negative	Positive	Negative (41.76)	Negative (No Ct)	Negative (No Ct)
RR42	Negative	Positive	Negative (40.74)	Negative (41.69)	Negative (No Ct)

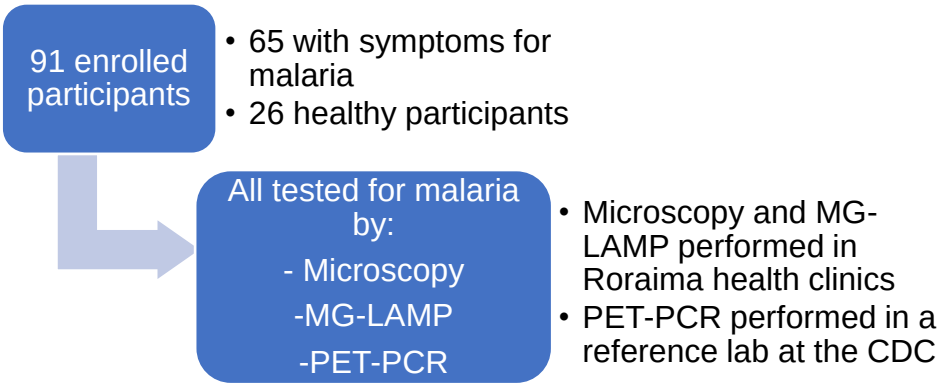

Figure 2.1: Summary of enrolled patients

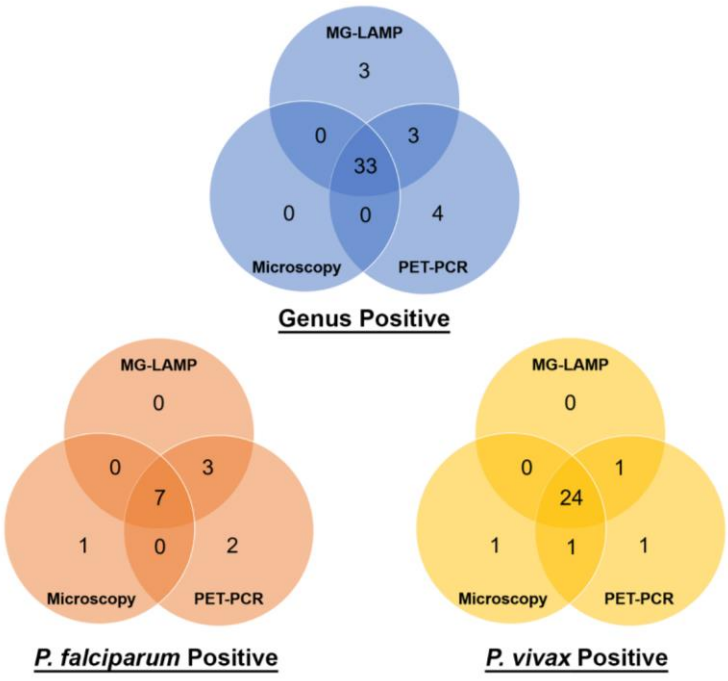

Figure 2.2: Summary of results for microscopy, MG-LAMP, and PET-PCR.

CHAPTER 3

CRISPR/Cas9 Gene Editing to Make Conditional Mutants of the Human Malaria Parasite *Plasmodium Falciparum*

Kudyba, H.M.*, Cobb, D.W.*, Florentin, A., Krakowiak, M., and Muralidharan, V. 2018. *Journal of Visualized Experiments*. Reprinted here with permission of the publisher

Short Abstract

We describe here a method for generating *glmS*-based conditional knockdown mutants in *P. falciparum* using CRISPR/Cas9 genome editing.

Long Abstract:

Malaria is a significant cause of morbidity and mortality worldwide. This disease, which primarily affects those living in tropical and subtropical regions, is caused by infection with *Plasmodium* parasites. The development of better drugs to combat malaria can be accelerated by improving our understanding of the biology of this complex parasite. Genetic manipulation of these parasites is key to understanding their biology, but historically, the genome of *P. falciparum* has been difficult to manipulate. Recently, CRISPR/Cas9 genome editing has been utilized in malaria parasites, allowing for easier protein tagging, generation of conditional protein knockdowns, and deletion of genes. CRISPR/Cas9 genome editing has proven to be a powerful tool for advancing the field of malaria research. Here, we describe a CRISPR/Cas9 method for generating *glmS*-based conditional knockdown mutants in *P. falciparum*. The method is highly adaptable to other types of genetic manipulations, including protein tagging and gene knockouts.

Introduction

Malaria is a devastating disease caused by protozoan parasites of the genus *Plasmodium*. *P. falciparum*, the most deadly human malaria parasite, causes approximately 445,000 deaths per year, mostly in children under the age of five[1]. *Plasmodium* has an intricate life cycle involving a mosquito vector and a vertebrate host. Humans become infected when an infected mosquito takes a blood meal. The parasite first invades the liver where they grow, develop, and divide for approximately one week. After this time, the parasites are released in the bloodstream where they undergo asexual replication in red blood cells (RBC). Growth of the parasites within the red blood cells are directly responsible for all of the clinical symptoms associated with malaria[2].

Until recently, production of transgenic *P. falciparum* was a laborious process, involving several rounds of drug selection that took many months and had a high rate of failure. This time-consuming procedure relies on the generation of random DNA breaks in the region of interest and the endogenous ability of the parasite to mend its genome though homologous repair[3-6]. Recently, Clustered Regularly Interspaced Palindromic Repeat/Cas9 (CRISPR/Cas9) genome editing has been successfully utilized in *P. falciparum*[7,8]. The introduction of this new technology in malaria research has been critical for advancing understanding of the biology of these deadly *Plasmodium* parasites. CRISPR/Cas9 allows for specific targeting of genes through the use of guide RNAs (gRNAs) that are homologous to the gene of interest. The gRNA/Cas9 complex recognizes the gene through the gRNA and Cas9 introduces a double-strand break, forcing the organism to initiate repair mechanisms[9,10]. Because *P. falciparum* lacks the

machinery to repair DNA breaks via non-homologous end joining, it utilizes homologous recombination mechanisms and integrates transfected homologous DNA templates to repair the Cas9/gRNA induced double-strand break[11,12].

Here we present a protocol for the generation of conditional knockdown mutants in *P. falciparum* using CRISPR/Cas9 genome editing. The protocol demonstrates usage of the *glmS* ribozyme to conditionally knockdown protein level of PfHsp70x (PF3D7_0831700), a chaperone exported by *P. falciparum* into the host red blood cell (RBC)[13,14]. The *glmS* ribozyme is activated by treatment with glucosamine (which is converted to glucosamine-6-phosphate within cells) to cleave its associated mRNA, leading to reduction in protein[14]. This protocol is easily adapted to utilize other conditional knockdown tools such as destabilization domains or RNA aptamers[4,5,15]. Our protocol details the generation of a repair plasmid consisting of a hemagglutinin (HA) tag and *glmS* ribozyme coding sequence flanked by sequences homologous to the PfHsp70x open reading frame (ORF) and 3'UTR. We also describe the generation of a second plasmid to drive expression of the gRNA. These two plasmids, along with a third plasmid that drives expression of Cas9, are transfected into RBCs and used to modify the genome of *P. falciparum* parasites. Finally, we describe a polymerase chain reaction (PCR)-based technique to verify integration of the tag and *glmS* ribozyme. This protocol is highly adaptable for the modification or complete knockout of any *P. falciparum* genes, enhancing our ability to generate new insights into the biology of the malaria parasite.

Protocol:

1. Choose gRNA sequence

1.1. Go to CHOP CHOP (http://chopchop.cbu.uib.no/) and select FASTA target**.** Under "Target", paste the 200 base pairs from the 3' end of the open reading frame (ORF) of a gene and 200 base pairs from the start of the gene's 3'UTR. Under "In", select the species to be *P. falciparum* (3D7 v3.0) and select CRISPR/Cas9 under "Using". Next, click "Find Target Sites".

1.2. Select a gRNA sequence from the options presented, giving preference to the most efficient gRNA that is closest to your site of modification and that has the fewest off-target sites.

Note: Potential gRNA sequences are identified because they are immediately upstream of a Protospacer Adjacent Motif (PAM), which is required for recruitment of Cas9 to DNA. The sequence that is cloned into pMK-U6, the vector that drives gRNA expression, is the 20 bases immediately upstream of the PAM. The PAM specific for *S. pyogenes* Cas9 is the nucleotide sequence NGG and should not be included in the sequence that is cloned into pMK-U6.

CHOP CHOP visually ranks the gRNA sequences, displaying the best options in green, the less ideal options in amber, and the worst options in red. CHOP CHOP gives each gRNA sequence an efficiency score that is calculated using the most up-to-date parameters found in the literature, and they predict off-target sites that could be

recognized by the gRNA. Two or three gRNA sequences may need to be tried to find the gRNA best suited to a particular gene.

1.3. Purchase the gRNA sequence and its reverse-complement as Polyacrylamide Gel Electrophoresis-purified oligos; the gRNA sequence used to target PfHSP70x can be found in **Figure 3.1B**.

Note: This oligo should include 15 base pairs homologous to the gRNA-expressing plasmid, which are necessary for sequence and ligation-independent cloning (SLIC) into the pMK-U6 vector[16].

2. Clone gRNA sequence into pMK-U6

2.1. Digest pMK-U6 with BtgZI.

2.1.1. Digest 10 µg of pMK-U6 with 5 µL of BtgZI enzyme (5000 units/mL) for 3 h at 60 °C. Follow the enzyme manufacturer's protocol for reaction conditions.

2.1.2. After the 3 h incubation, add an additional 3 µL BtgZI to the reaction to ensure complete digestion of the plasmid. Digest for an additional 3 h, again following manufacturer's instructions for ensuring the correct reaction condition.

2.1.3. To purify the digested pMK-U6 from the reaction, use a column-based PCR cleanup kit according to manufacturer's instructions.

2.1.4. Separate the digested DNA using a 0.7% agarose gel and extract the 4,200 base pair band.

2.2. Anneal the oligos containing the gRNA sequence.

2.2.1. Reconstitute the PAGE-purified oligos to a concentration of 100 µM using nuclease free water.

2.2.2. Combine 10 µL of each oligo with 2.2 µL 10x buffer 2 (see Table of Materials, Table 3.1); the total reaction volume will be 22.2 µL.

2.2.3. Run the gRNA annealing program in a thermocycler: Step 1- 95 °C, 10 min; step 2- 95 °C, 1 s, with a reduction in temperature of 0.6 °C/cycle; step 3- Go to step 2, 16 times; step 4- 85 °C, 1 min; step 5- 85 °C, 1 s, with a reduction in temperature of 0.6°C/cycle; step 6- Go to step 5, 16 times; step 7- 75 °C, 1 min; step 8- 75 °C, 1 s, with a reduction in temperature of 0.6 °C/cycle; step 9- Go to step 8, 16 times. Steps 10-21- Repeat the procedure used in Steps 4-9 until the temperature reaches 25 °C; step 22- 25 °C, 1 min.

2.3. Insert the annealed gRNA oligos into the BtgZI-digested and gel-purified pMK-U6 plasmid.

2.3.1. Combine 100 ng digested pMK-U6 with 1 µL 10x buffer 2.1 and 3 µL annealed gRNA oligos. Bring the volume up to 9.5 µL with nuclease-free water.

2.3.2. Add 0.5 µL T4 polymerase and incubate reaction at room temperature for 2 min 30 s.

2.3.3. Move the reaction to ice and incubate for 10 min.

2.3.4. Immediately transform 5 µL of the reaction into competent *E. coli* according to manufacturer's instructions and plate bacteria on Lysogeny Broth (LB) agar plates containing 100 µg/mL Ampicillin.

2.3.5. Allow transformed bacteria to grow at 37 °C overnight, then select colonies for DNA extraction with a commercially available plasmid miniprep kit.

3. Design homology regions of the repair template

3.1. Design shield mutations within the homology repair template to prevent re-cutting of DNA that is integrated into the genome.

Note: The shield mutation typically consists of introducing a silent mutation to alter the protospacer adjacent motif (PAM) so that Cas9 will not induce a break in the repair template. The PAM required for the Cas9 used here is the nucleotide sequence NGG, where N is any nucleotide. If possible, change one of the G nucleotides to an A, C, or T.

3.1.1. If the PAM cannot be silently mutated, introduce at least two silent mutations into the six base pairs directly adjacent to the PAM[7,8].

Note: These mutations will prevent recognition of the repair template by the gRNA and prevent re-cutting of the repaired locus by the Cas9/gRNA complex. The shield mutations can be introduced into the homology region by amplifying the DNA with primers that contain the mutation.

3.2. Amplify the ORF homology region for the repair template.

3.2.1. Using PCR, amplify 800 base pairs from the 3' end of the target gene's ORF. Design the primers to be used to exclude the stop codon from this amplicon.

3.2.2. Additionally, design the primers to insert this amplicon into pHA-*glmS* that has been digested with SacII and AfeI, either through a DNA ligation reaction or SLIC[16]

3.3. Amplify the 3'UTR homology region for the repair template.

3.3.1. Using PCR, amplify the 800 base pairs immediately following the stop codon of the target gene. The primers used should be designed to insert this amplicon into pHA-*glmS* that has been digested with HindIII and NheI, either through a DNA ligation reaction or SLIC[16].

Note: The high AT content of the *P. falciparum* genome often makes amplification of regions such as UTRs difficult. An alternative approach to using PCR is to synthesize the homology regions.

4. Clone homology regions into the repair plasmid

4.1. Insert ORF homology region into pHA-*glmS*.

4.1.1. Digest pHA-*glmS* with SacII and AfeI, according to enzyme manufacturer's instructions, and insert the ORF homology region PCR product into the digested plasmid using SLIC [16].

4.1.2. Transform into competent *E. coli*.

4.2. Insert 3'UTR homology region into pHA-glmS plasmid that already contains the ORF homology region (see 4.1).

4.2.1. Digest the plasmid with HindIII and NheI according to enzyme manufacturer's instructions, and then insert the 3'UTR homology region amplicon into the digested plasmid using SLIC[16].

4.2.2. Transform into competent *E. coli*. See steps 2.3.4 and 2.3.5 above.

5. Precipitate DNA for transfection

5.1. Add 40 µg each of pMK-U6, pUF1-Cas9, and pHA-*glmS* DNA (for a total of 120 µg of DNA) into a sterile 1.5 mL microcentrifuge tube.

5.2. Add 1/10th the volume of DNA of 3M sodium acetate in water (pH 5.2) to the tube and mix well using a vortex. For example, if the volume in step 5.1 was 100 µL, add 10 µL sodium acetate.

5.3. Add 2.5 volumes of 100% ethanol to the tube and mix well using a vortex for at least 30 s. For example, if the volume in 5.1 was 100 µL, add 250 µL 100% ethanol.

5.4. Place the tube on ice or at -20 °C for 30 min.

5.5. Centrifuge the tube at 18,300g for 30 min at 4 °C.

5.6. Carefully remove the supernatant from the tube. Do not disturb the pellet.

5.7. Add 3 volumes of 70% ethanol to the tube and mix briefly using a vortex. For example, if the volume in 5.1 was 100 µL, add 300 µL 70% ethanol.

5.8. Centrifuge the tube at 18,300g for 30 min at 4 °C.

Note: This step should be performed under sterile conditions in a biological safety cabinet.

5.9. Carefully remove the supernatant from the tube. Do not disturb the pellet. Leave the tube open and allow the pellet to air dry for 15 min.

5.10. Store the precipitated DNA at -20 °C until it is needed for transfection.

6. Isolate RBCs from whole blood in preparation for transfection.

6.1. Aliquot fresh blood into sterile 50 mL conical tubes (approximately 25 mL per tube).

6.2. Centrifuge tubes at 1088g for 12 min, with centrifuge brakes set to 4.

6.3. Aspirate off supernatant and buffy coat.

6.4. Resuspend RBC pellet with equal volume incomplete RPMI.

Note: Incomplete RPMI is prepared by supplementing RPMI 1640 with 10.32 μM thymidine, 110.2 μM hypoxanthine, 1 mM sodium pyruvate, 30 mM sodium bicarbonate, 5 mM HEPES, 11.1 mM glucose, and 0.02% (v/v) gentamicin.

6.5. Repeat steps 6.2-6.4 twice.

6.6. After the last wash, resuspend RBCs in equal volume incomplete RPMI and store at 4 °C.

7. Transfect RBCs with the CRISPR/Cas9 plasmids (to be done aseptically)

Note: Plasmodium falciparum cultures are maintained as described[17]. Whenever blood is used in the protocol, it is referring to pure red blood cells prepared in Step 6. Blood used should not be older than 6 weeks, as we see a decrease in parasite proliferation in older blood. We describe here a protocol for pre-loading RBCs with DNA and then adding parasite culture to the transfected cells. Other established transfection protocols would be compatible with transfecting these constructs[18,19].

7.1. Prepare 1x cytomix buffer in water (120 mM KCl, 0.15 mM $CaCl_2$, 2mM EGTA, 5mM $MgCl_2$, 10mM K_2HPO_4, 25mM HEPES, pH 7.6). Filter-sterilize the buffer using a 0.22 µM filter.

7.2. Add 380 µL of 1x cytomix to the DNA precipitated in step 5 and vortex to dissolve. Allow the DNA to dissolve in 1x cytomix for 10 minutes, vortexing every 3 minutes for 10 seconds.

7.3. In a sterile 15 mL conical tube, combine 300 µL of red blood cells (RBCs, 50% hematocrit, from Step 6) in incomplete RPMI with 4 mL of 1x cytomix.

7.4. Centrifuge the RBCs from 7.3 at 870g for 3 min, then remove the supernatant from the RBC pellet.

7.5. Resuspend the RBC pellet with DNA/cytomix mixture from step 6.2 and transfer to a 0.2 cm electroporation cuvette.

7.6. Electroporate the RBCs using the following conditions: 0.32kV, 925 µF, capacitance set to “High Cap”, and resistance set to “infinite”.

7.7. Following electroporation, transfer the contents from the cuvette to a 15 mL conical containing 5 mL of complete RPMI (cRPMI). Centrifuge the tube at 870g for 3 min at 20 °C, then decant the supernatant.

Note: cRPMI is prepared as described for incomplete RPMI in 7.4 with the addition of 0.25% (w/v) lipid-rich bovine serum albumin.

7.8. Resuspend the pellet in 4 mL cRPMI and transfer to a well of a 6-well tissue culture plate. Add 400 µL of a high-schizont culture (7-10% schizont parasitemia is ideal) to the transfected RBCs.

Note: Parasitemia is defined as the percentage of parasite-infected RBCs.

7.9. The next day, wash the culture with 4 mL of cRPMI.

7.9.1. Centrifuge the culture at 870g for 3 min and aspirate the supernatant. Resuspend the culture in 4 mL cRPMI.

7.10. 48 h after step 7.6, wash the culture with 4 mL of cRPMI, then resuspend the culture in cRPMI containing 1 μM DSM1 to select for the Cas9 plasmid.

7.11. Continue washing the cultures each day with cRPMI until parasites are no longer visible by blood smear. After this point, the culture medium should be replaced with fresh cRPMI + 1 μM DSM1 every 48 h.

7.11.1. To make a blood smear, pipette 150 μL of culture into an 0.6 mL eppendorf tube. Pellet the cells by centrifugation at 1700g for 30 s.

7.11.2. Aspirate off the supernatant. Use a pipette to transfer the pelleted cells to a glass slide. Using a second glass slide, held at a 45° angle to the first slide, smear the blood droplet. Stain the slide using a commercially available staining kit according to the manufacturer's protocol.

7.11.3. View parasites using a 100x oil immersion objective.

7.12. Beginning 5 days post-transfection (Step 7.6), remove 2 mL of the culture, with RBCs resuspended in the culture medium, and add back 2 mL fresh medium (cRPMI + 1 μM DSM1) and blood at 2% hematocrit. Add fresh blood in this manner once a week until parasites reappear, as determined by thin blood smear.
Note: If integration is successful, parasites generally reappear in culture by one-month post-transfection.

7.13. Once parasites reemerge, remove drug pressure. Alternatively, remove drug pressure after parasites have been cloned out.

8. Check parasites for integration of the repair template

8.1. When parasites are visible again by thin blood smear, isolate DNA from the culture.

8.2. Use PCR to amplify the modified region of the genome to determine whether the targeted locus has been successfully altered and whether the unmodified *wild-type* locus (indicative of *wild-type* parasites) is detectable.

8.2.1. To detect parasites that have integrated the repair template, use a forward primer that sits at the beginning of the ORF, outside of the cloned homology region. Use a reverse primer that sits in the 3'UTR.

Note: As this amplification includes the sequences of the HA tags and *glmS* ribozyme, amplicons from integrated parasites will be longer than the same region amplified in *wild-type* parasites.

9. Clone parasites by limiting dilution

9.1 Perform serial dilutions of the parasite culture from step 7.13 to achieve a final concentration of 0.5 parasites/200 µL.

9.1.1. Prepare 1 mL culture in cRPMI at 5% parasitemia and 2% hematocrit; at this parasitemia and hematocrit, the culture contains $1x10^7$ parasites/mL.

9.1.2. Dilute this culture 1:100 with cRPMI. Dilute again 1:100 with cRPMI.

9.1.3. Dilute 1:400. Perform this dilution by adding 62.5 µL culture to 25 mL cRPMI and 1 mL blood. This dilution results in the desired concentration of 0.5 parasites/200 µL.

9.1.5. Add 200 µL of the diluted culture to the wells of a 96-well tissue culture plate.

9.2. Maintain the cloning plate until parasites are detectable in the wells.

9.2.1. Every 48 h replace the medium in the 96-well plate with fresh medium.

9.2.2. Once a week, starting 5 days after beginning the cloning plate (Step 8.1.5), remove 100 µL from each well and add back 100 µL of fresh medium + blood (2% hematocrit).

9.3. Identify wells containing parasites.

9.3.1. Place the 96-well plate at a 45° angle for approximately 20 min, allowing the blood to settle at an angle within the plate.

9.3.2. Place the 96-well plate on a light box. Observe that the wells containing parasites will contain medium that is yellow in color, compared to the pink medium of parasite-free wells, due to acidification of the medium by the parasites.

9.3.3. Using a serological pipette, move the contents of the parasite-containing wells to a 24-well tissue culture plate to allow expansion of parasitemia.

9.3.4. Using PCR analysis as described in Step 8, check these clonal parasite lines for correct integration.

10. Knockdown protein by treating parasites with GlcN and confirm knockdown by Western blot analysis.

10.1. Prepare 0.5 M GlcN stock solution; the stock can be stored at -20° C.

10.2. Add GlcN to *glmS* parasite cultures and allow to grow in the presence of GlcN.

Note: The final concentration and timing of GlcN treatment to be used is dependent upon the experiment and parasite line. GlcN can impact parasite growth, so the parental parasite strain should be exposed to a range of GlcN concentrations to determine sensitivity to the compound. Often, a concentration of 2.0-7.5 mM GlcN is used[13,14,20].

10.3. Isolate protein samples from GlcN-treated parasites[13].

10.4. Use protein samples for Western blot analysis to detect reduction in protein[13].

10.4.1. Use an anti-HA antibody according to manufacturer's instructions to detect the HA-glmS-tagged protein, and compare the HA band to a loading control, such as PfEF1α.

Representative Results:

A schematic of the plasmids used in this method as well as an example of a shield mutation are shown in **Figure 3.1**. As an example of how to identify mutant parasites after transfection, results from PCRs to check integration of the HA-*glmS* construct is shown in **Figure 3.2**. A representative image of a cloning plate is shown in **Figure 3.3** to demonstrate the color change of the medium in the presence of parasites. Results from an immunofluorescence assay and Western blotting experiments are shown in **Figure 3.4** to demonstrate the functionality of the HA tag and *glmS*-based reduction of protein in the parasites. **Figure 3.5** demonstrates the inability of short homology arms on PCR products to modify the parasites genome and obtain viable mutants.

Discussion

The implementation of CRISPR/Cas9 in *P. falciparum* has both increased the efficiency of and decreased the amount of time needed for modifying the parasite's genome, in comparison to previous methods of genetic manipulation. The comprehensive protocol described in this manuscript outlines the steps taken to generate conditional mutants using CRISPR/Cas9 in *Plasmodium falciparum*. While the method here is written specifically for the generation of HA-*glmS* mutants, this strategy can be adapted for a variety of purposes, including the tagging of genes, gene knockouts, and introduction of point mutations.

A critical early step in this protocol is the selection of a gRNA sequence. When selecting a gRNA, there are several considerations to keep in mind in regards to where the gRNA sits, how efficient it is, and whether it has the potential for off-target effects. Typically, the gRNA sequence should be as close as possible to the site of modification, ideally within 200 bp. This will decrease the likelihood of the parasites using the repair template to fix their genome without integrating the tag. The tool used here to locate a gRNA was a free online service called CHOP CHOP[22]. Another online tool, Eukaryotic Pathogen CRISPR guide RNA/DNA Design Tool (EuPaGDT, http://grna.ctegd.uga.edu/), can also be used[23]. EuPaGDT provides additional characterization of gRNA sequences, including prediction of off-target hits and potential issues that may prevent transcription of the gRNA. EuPaGDT also has tools for batch processing of gRNAs to target multiple genes or whole genomes. The gRNA chosen should be one that sits closest to the site of modification with the highest efficiency and minimal off-target hits. An important limitation to CRISPR/Cas9 gene editing that may arise is the inability to design a suitable gRNA to target the gene of interest. In such cases, a trial-and-error approach may be needed, using multiple sub-optimal gRNA sequences until the best one is found and successful gene editing has occurred.

Another important consideration for generating *P. falciparum* mutants using CRISPR/Cas9 is the length of the homology regions used in the repair template. The protocol here states that the homology regions should be approximately 800 base pairs each, but we have also been successful in using smaller regions (500 base pairs)[3]. Successful genome modification using CRISPR/Cas9 and short homology arms on PCR products have been used in other protozoan parasites such as *Toxoplasma gondii*

and *Trichomonas vaginalis*[24,25]. We tested the feasibility of using smaller homology arms on PCR products (50, 75, or 100 base pairs) by attempting to knockout GFP in B7 parasites using a blasticidin resistance cassette[21]. We saw some integration of the blasticidin resistance cassette at five days post transfection; however, these parasites never recovered from transfection. For these transfections, we selected for the Cas9-expressing plasmid using DSM1. A different selection method, such as treating transfected cultures with blasticidin S alone or in combination with DSM1, may improve the chances of parasites reappearing when using shorter homology regions for repairing the Cas9/gRNA induced break. We did not select with blasticidin S in this case because we wanted to test whether short homology arms could be used in instances where a drug resistance cassette is not being integrated into the genome, such as when a protein is being tagged.

The core components of CRISPR/Cas9 gene editing discussed here are the Cas9 endonuclease, the gRNA, and the repair template. We describe a three-plasmid approach to introduce these components into the parasites, where Cas9, the gRNA, and the repair template are found in separate plasmids. In addition to this approach, our lab has been successful in using a two-plasmid approach where Cas9 and gRNA expression are driven by a single plasmid and the repair template is found in a second plasmid[3]. Similar two-plasmid approaches have been successfully employed by other labs to generate mutants[7,8,26-29]. Furthermore, a few labs are using a strain of *Plasmodium (*NF54^{attB}*)* which constitutively expresses Cas9 and a T7 RNA polymerase to drive expression of gRNA's[30]. In this case, a single plasmid containing the repair template and the gRNA are transfected into NF54^{attB} parasites[31,32]. A plasmid-free

approach, utilizing a purified Cas9-gRNA ribonucleoprotein complex, has been used to insert mutations into the genome as well[33]. The success of these different approaches demonstrates flexibility in how researchers can introduce the Cas9/gRNA components into the parasite.

Finally, the choice of drug pressure to apply to transfected parasites can be altered depending on constructs used. Here, we show successful generation of mutants by transiently selecting for the Cas9 expressing plasmid using DSM1 until parasites reappear. To generate PfHsp70x knockout parasites, *pfhsp70x* was replaced with the human dihydrofolate reductase gene, and parasites were selected using WR99210[13].The recently described TetR-PfDOZI knockdown system relies on integration of a plasmid containing a blasticidin S resistance gene, allowing for selection of parasites using blasticidin S[15,31].

CRISPR/Cas9 gene editing of *P. falciparum* has proven to be a powerful tool in malaria research, and we have detailed here a method for generating conditional knockdown mutants[3,7,8,13,20,28]. The protocol is highly adaptable to individual research interests.

References

1 World Health Organization. World Malaria Report. *WHO, Geneva.* (2017).

2 Miller, L. H., Baruch, D. I., Marsh, K. & Doumbo, O. K. The pathogenic basis of malaria. *Nature.* **415** (6872), 673-679, (2002).

3 Florentin, A. *et al.* PfClpC Is an Essential Clp Chaperone Required for Plastid Integrity and Clp Protease Stability in Plasmodium falciparum. *Cell Rep.* **21** (7), 1746-1756, (2017).

4 Muralidharan, V., Oksman, A., Pal, P., Lindquist, S. & Goldberg, D. E. Plasmodium falciparum heat shock protein 110 stabilizes the asparagine repeat-rich parasite proteome during malarial fevers. *Nat Commun.* **3** 1310-1310, (2012).

5 Muralidharan, V., Oksman, A., Iwamoto, M., Wandless, T. J. & Goldberg, D. E. Asparagine repeat function in a Plasmodium falciparum protein assessed via a regulatable fluorescent affinity tag. *Proc Natl Acad Sci U S A.* **108** (11), 4411-4416, (2011).

6 Beck, J. R., Muralidharan, V., Oksman, A. & Goldberg, D. E. PTEX component HSP101 mediates export of diverse malaria effectors into host erythrocytes. *Nature.* **511** (7511), 592-595, (2014).

7 Ghorbal, M. *et al.* Genome editing in the human malaria parasite Plasmodium falciparum using the CRISPR-Cas9 system. *Nat Biotechnol.* **32** (8), 819-821, (2014).

8 Wagner, J. C., Platt, R. J., Goldfless, S. J., Zhang, F. & Niles, J. C. Efficient CRISPR-Cas9-mediated genome editing in Plasmodium falciparum. *Nat*

Methods. **11** (9), 915-918, (2014).

9 Doudna, J. A. & Charpentier, E. Genome editing. The new frontier of genome engineering with CRISPR-Cas9. *Science.* **346** (6213), 1258096, (2014).

10 Wang, H., La Russa, M. & Qi, L. S. CRISPR/Cas9 in Genome Editing and Beyond. *Annu Rev Biochem.* **85** 227-264, (2016).

11 Kirkman, L. A. & Deitsch, K. W. Antigenic variation and the generation of diversity in malaria parasites. *Curr Opin Microbiol.* **15** (4), 456-462, (2012).

12 Lee, A. H., Symington, L. S. & Fidock, D. A. DNA Repair Mechanisms and Their Biological Roles in the Malaria

Parasite Plasmodium falciparum. *Microbiology and Molecular Biology Reviews.* **78** (3), 469-486, (2014).

13 Cobb, D. W. *et al.* The Exported Chaperone PfHsp70x Is Dispensable for the Plasmodium falciparum Intraerythrocytic Life Cycle. *mSphere.* **2** (5), (2017).

14 Prommana, P. *et al.* Inducible knockdown of Plasmodium gene expression using the glmS ribozyme. *PLoS One.* **8** (8), e73783, (2013).

15 Ganesan, S. M., Falla, A., Goldfless, S. J., Nasamu, A. S. & Niles, J. C. Synthetic RNA-protein modules integrated with native translation mechanisms to control gene expression in malaria parasites. *Nat Commun.* **7** 10727, (2016).

16 Li, M. Z. & Elledge, S. J. Harnessing homologous recombination in vitro to generate recombinant DNA via SLIC. *Nat Methods.* **4** (3), 251-256, (2007).

17 Drew, M. E. *et al.* Plasmodium food vacuole plasmepsins are activated by falcipains. *J Biol Chem.* **283** (19), 12870-12876, (2008).

18 WU, Y., SIFRI, C. D., LEI, H.-H., SU, X.-Z. & WELLEMS, T. E. Transfection of

Plasmodium falciparum within human red blood cells. *Proc Natl Acad Sci U S A.* **92** 973-977, (1995).

19 Janse, C. J. *et al.* High efficiency transfection of Plasmodium berghei facilitates novel selection procedures. *Mol Biochem Parasitol.* **145** (1), 60-70, (2006).

20 Counihan, N. A. *et al.* Plasmodium falciparum parasites deploy RhopH2 into the host erythrocyte to obtain nutrients, grow and replicate. *Elife.* **6**, (2017).

21 Klemba, M., Beatty, W., Gluzman, I. & Goldberg, D. E. Trafficking of plasmepsin II to the food vacuole of the malaria parasite Plasmodium falciparum. *J Cell Biol.* **164** (1), 47-56, (2004).

22 Labun, K., Montague, T. G., Gagnon, J. A., Thyme, S. B. & Valen, E. CHOPCHOP v2: a web tool for the next generation of CRISPR genome engineering. *Nucleic Acids Res.* **44** (W1), W272-276, (2016).

23 Peng, D. & Tarleton, R. EuPaGDT: a web tool tailored to design CRISPR guide RNAs for eukaryotic pathogens. *Microb Genom.* **1** (4), e000033, (2015).

24 Shen, B., Brown, K. M., Lee, T. D. & Sibley, L. D. Efficient Gene Disruption in Diverse Strains of Toxoplasma gondii Using CRISPR/CAS9. *MBio.* **5** (3), (2014).

25 Janssen, B. D. *et al.* CRISPR/Cas9-mediated gene modification and gene knock out in the human-infective parasite Trichomonas vaginalis. *Sci Rep.* **8** (1), 270, (2018).

26 Spillman, N. J., Beck, J. R., Ganesan, S. M., Niles, J. C. & Goldberg, D. E. The chaperonin TRiC forms an oligomeric complex in the malaria parasite cytosol. *Cell Microbiol.* **19** (6), (2017).

27 Brancucci, N. M. B. *et al.* Lysophosphatidylcholine Regulates Sexual Stage Differentiation in the Human Malaria Parasite Plasmodium falciparum. *Cell.* 10.1016/j.cell.2017.10.020, (2017).

28 Ng, C. L. *et al.* CRISPR-Cas9-modified pfmdr1 protects Plasmodium falciparum asexual blood stages and gametocytes against a class of piperazine-containing compounds but potentiates artemisinin-based combination therapy partner drugs. *Mol Microbiol.* **101** (3), 381-393, (2016).

29 Lim, M. Y. *et al.* UDP-galactose and acetyl-CoA transporters as Plasmodium multidrug resistance genes. *Nat Microbiol.* 10.1038/nmicrobiol.2016.166 16166, (2016).

30 Adjalley, S. H. *et al.* Quantitative assessment of Plasmodium falciparum sexual development reveals potent transmission blocking activity by methylene blue. *PNAS.* **108** (47), E1214-E1223, (2011).

31 Sidik, S. M. *et al.* A Genome-wide CRISPR Screen in Toxoplasma Identifies Essential Apicomplexan Genes. *Cell.* **166** (6), 1423-1435 e1412, (2016).

32 Amberg-Johnson, K. *et al.* Small molecule inhibition of apicomplexan FtsH1 disrupts plastid biogenesis in human pathogens. *Elife.* **6**, (2017).

33 Crawford, E. D. *et al.* Plasmid-free CRISPR/Cas9 genome editing in Plasmodium falciparum confirms mutations conferring resistance to the dihydroisoquinolone clinical candidate SJ733. *PLoS One.* **12** (5), e0178163, (2017).

Table 3.1: Summary of materials

Name of Material/ Equipment	Company	Catalog Number
Gene Pulser Xcell Electroporator	Bio-Rad	1652660
Gene Pulser®/MicroPulser Electroporation Cuvettes, 0.2 cm gap	Bio-Rad	165-2086
Sodium Acetate	Sigma-Aldrich	S2889-250g
DSM1	Gift from Akhil Vaidya lab	Ganesan et al. Mol. Biochem. Parasitol. 2011 177:29-34
TPP Tissue Culture 6 Well Plates	MIDSCI	TP92006
TPP 100mm Tissue Culture Dishes (12 mL Plate)	MIDSCI	TP93100
TPP Tissue Culture 96 Well Plates	MIDSCI	TP92096
TPP Tissue Culture 24 Well Plates	MIDSCI	TP92024
NEBuffer 2	New England Biolabs	#B7002S
NEBuffer 2.1	New England Biolabs	#B7202S
BtgZI	New England Biolabs	#R0703L
SacII	New England Biolabs	#R0157L
HindIII-HF	New England Biolabs	#R3104S
Afe1	New England Biolabs	#R0652S
Nhe1-HF	New England Biolabs	#R3131L

T4 DNA Polymerase	New England Biolabs	#M0203S
500 mL Steritop bottle top filter unit	Millipore	SCGPU10RE
EGTA	Sigma	E4378-100G
KCl	Sigma-Aldrich	P9333-500g
CaCl2	Sigma-Aldrich	C7902-500g
MgCl2	Sigma-Aldrich	M8266-100g
K2HPO4	Fisher	P288-500
HEPES	Sigma-Aldrich	H4034-500g
pMK-U6	Generated by the Muralidharan Lab	n/a
pHA-glmS	Generated by the Muralidharan Lab	n/a
pUF1-Cas9	Gift from the Jose-Juan Lopez-Rubio Lab	Ghorbal et al. Nature Biotech 2014
Glucose	Sigma-Aldrich	G7021-1KG
Sodium bicarbonate	Sigma-Aldrich	S5761-500G
Sodium pyruvate	Sigma-Aldrich	P5280-100G
Hypoxanthine	Sigma-Aldrich	H9636-25g
Gentamicin Reagent	Gibco	15710-064
Thymidine	Sigma-Aldrich	T1895-1G
PL6-eGFP BSD	Generated by the Muralidharan Lab	N/A

Puf1-cas9 eGFP gRNA	Generated by the Muralidharan Lab	N/A
NucleoSpin Gel and PCR Clean-up	Macherey-Nagel	740609.250
Albumax I	Life Technologies	N/A
Human Red Blood Cells	Interstate Blood Bank, Inc	Email or call them directly for ordering
3D7 parasite line	Available upon request	N/A
Lysogeny Broth (LB)	Fisher	BP1426-2
Ampicilin	Fisher	BP1760-25
PrimeSTAR® GXL DNA Polymerase	Clonetech	R050A
Anti-EF1alpha	Dr. Daniel Goldberg's Lab	Washington University in St. Louis
Rat Anti-HA Clone 3F10, monoclonal	Made by Roche, sold by Sigma	11867423001
0.6 mL tubes	Fisher	AB0350
Fisher HealthCare* PROTOCOL* Hema 3* Manual Staining System (Fixative+Solution I and II)	Fisher	22-122-911
Fisherfinest™ Premium Frosted Microscope Slides - Size: 3 x 1 in.	Fisher	12-544-3

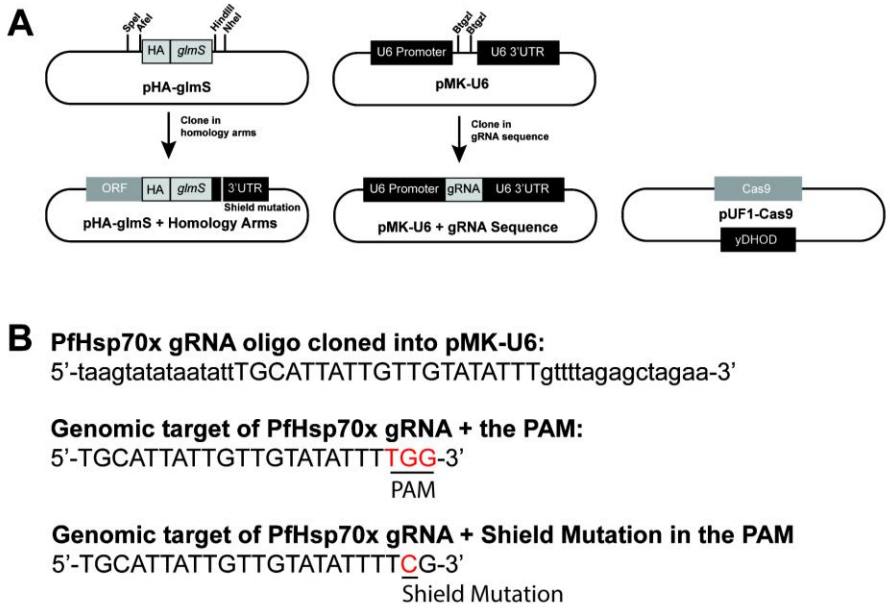

Figure 3.1: Summary of our three-plasmid approach to CRISPR/Cas9 and examples of a gRNA oligo and shield mutation. A) Schematics of empty pHA-glmS and pMK-U6 are shown with the restriction enzyme sites used for cloning. Also shown are pHA-glmS and pMK-U6 after the homology arms and gRNA sequences have been cloned into them, respectively. Finally, pUF1-Cas9 is shown. yDHOD: yeast dihydrofolate reductase, the resistance marker to DSM1. B) The forward oligo used for cloning the PfHsp70x gRNA sequence into pMK-U6 is shown, with the gRNA sequence in capital letters and the pMK-U6 homology arms necessary for cloning shown in lower case (Top). The genomic target of the PfHsp70x gRNA is shown as well as the downstream PAM, in red (Middle). The shield mutation in the PfHsp70x gRNA PAM is shown in red (Bottom).

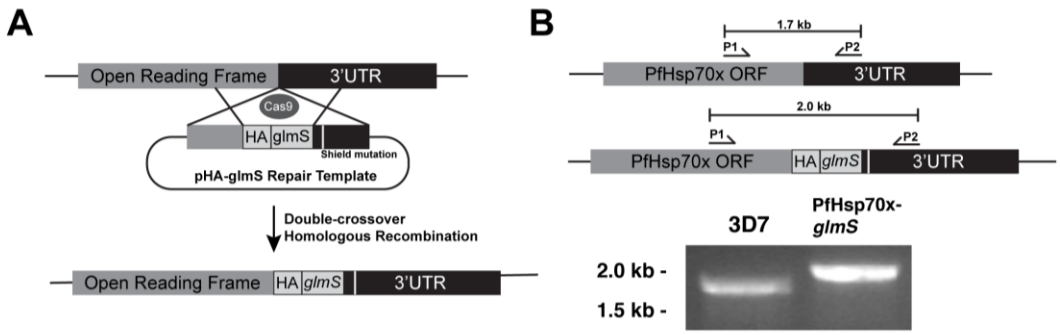

Figure 3.2: Schematic of CRISPR/Cas9 genome modification using pHA-glmS and strategy for confirming integration. A) Cas9, guided to a genomic locus by a gRNA, induces a double strand break in the DNA. The parasite repairs the damage through double crossover homologous repair, using the pHA-glmS plasmid as a template and introducing the HA-glmS sequence into the genome. B) A PCR test to identify correct integration of the HA-glmS sequence. Using primers P1 and P2, the 3' ORF of *wild-type* PfHsp70x and PfHsp70x-*glmS* mutants are amplified[13]. The amplicon from PfHsp70x-glmS is longer than *wild-type* due to insertion of the HA-glmS sequence.

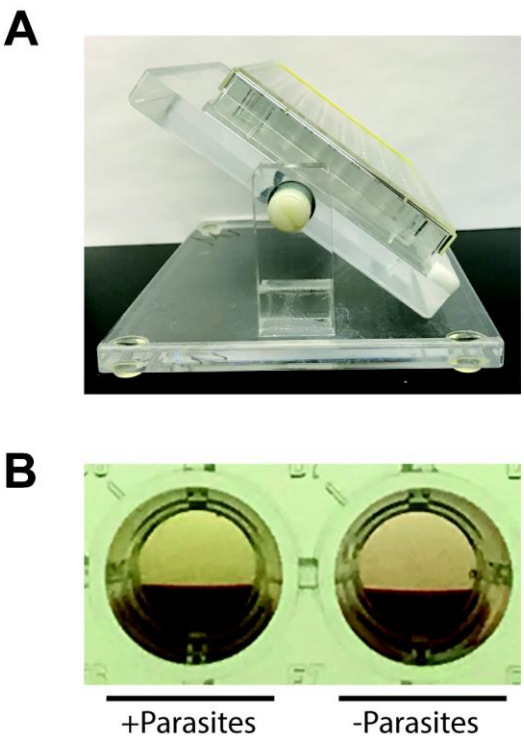

Figure 3.3: Identification of wells containing parasites in a 96-well cloning plate. A) The 96-well plate is set at a 45° angle for approximately 20 minutes to allow the blood to settle at an angle in the plate. B) The well on the left contains a parasite culture, indicated by the yellow color of the medium in comparison to the pink medium of the parasite-free well on the right.

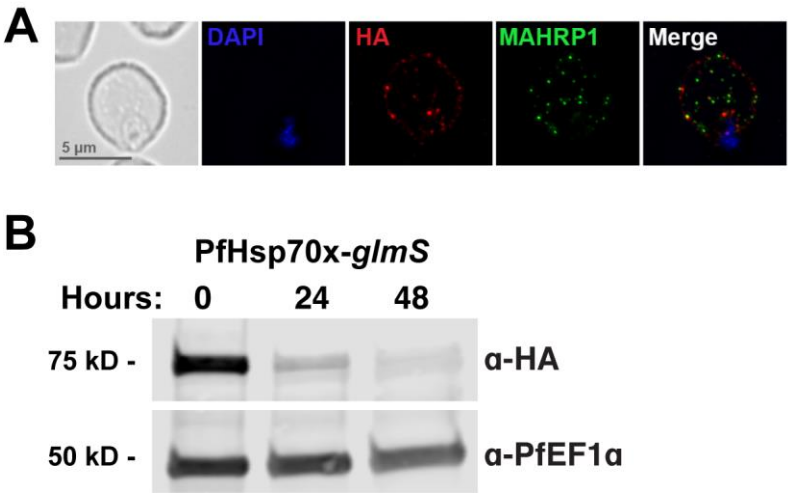

Figure 3.4: An immunofluorescence assay shows the correct HA-tagging of PfHsp70x and Western blotting shows reduction of PfHsp70x protein levels during treatment with glucosamine. A) PfHsp70x-*glmS* parasites were fixed and stained with DAPI (nucleus marker) and antibodies to HA and MAHRP1 (Membrane Associated Histidine Rich Protein 1, a marker of protein export to the host RBC)[13].B) PfHsp70x-*glmS* parasites were treated with 7.5 mM glucosamine and whole-parasite lysates were used for Western blotting analysis[13]. The membrane was probed with antibodies for HA and PfEF1α as a loading control[13]. As expected, glucosamine treatment results in a reduction of the protein.

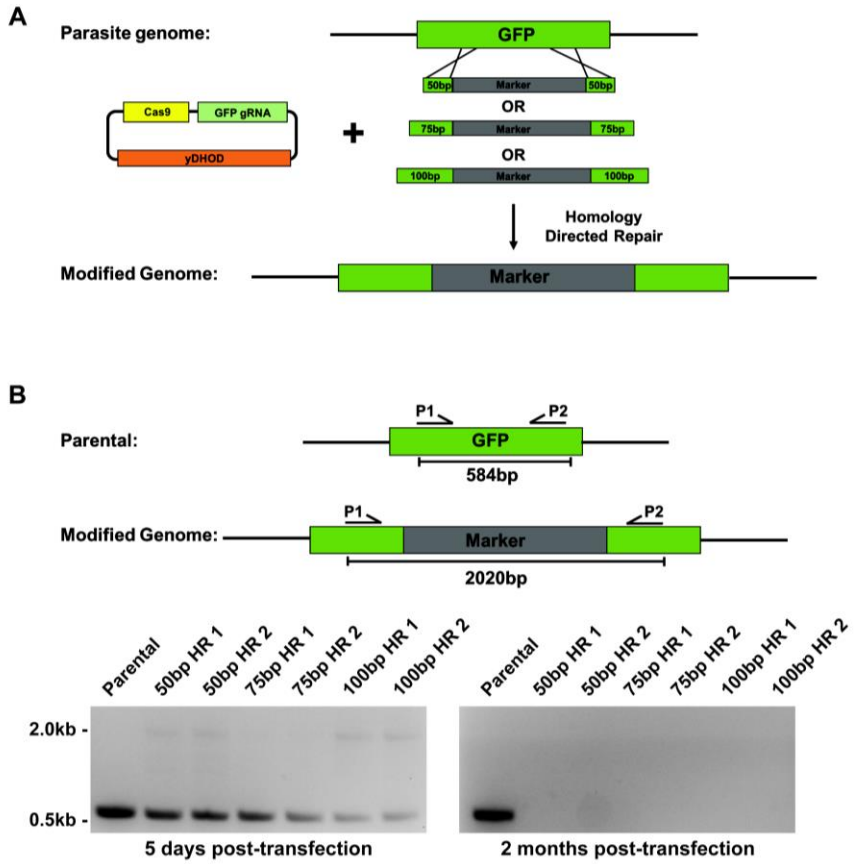

Figure 3.5: Using short homology sequences for repair. A) Schematic representation showing knockout of GFP in B7 parasites[21]. B7 parasites are a derivative of 3D7 where Plasmepsin II has been tagged with GFP. PCR products containing 50, 75, or 100 base pairs of GFP homology regions flanking a blasticidin S resistance cassette (labeled “marker”), along with pUF1-Cas9-eGFP-gRNA, a plasmid expressing Cas9 and a GFP gRNA, were transfected into B7 parasites. Each transfection was carried out twice. Drug pressure (DSM1) was applied 2-day post transfection. B) PCR test on DNA isolated from transfected parasites five days post-transfection and two months post-transfection. Primers used to test integration of the BSD resistance cassette will yield a 584 base pair product for B7 parental parasites and a 2020 base pair product for parasites that have integrated the marker.

CHAPTER 4

The ER chaperone PfGRP170 is essential for asexual development and is linked to stress response in malaria parasites.

Heather M. Kudyba, David W. Cobb, Manuel A. Fierro, Anat Florentin, Dragan Ljolje Balwan Singh, Naomi W. Lucchi, and Vasant Muralidharan. Submitted to *Cellular Microbiology*, November 20th, 2018.

ABSTRACT

The vast majority of malaria mortality is attributed to one parasite species: *Plasmodium falciparum*. Asexual replication of the parasite within the red blood cell is responsible for the pathology of the disease. In *Plasmodium,* the endoplasmic reticulum (ER) is a central hub for protein folding and trafficking as well as stress response pathways. In this study, we tested the role of an uncharacterized ER protein, PfGRP170, in regulating these key functions by generating conditional mutants. Our data show that PfGRP170 localizes to the ER and is essential for asexual growth, specifically required for proper development of schizonts. PfGRP170 is essential for surviving heat shock, suggesting a critical role in cellular stress response. The data demonstrate that PfGRP170 interacts with the *Plasmodium* orthologue of the ER chaperone, BiP. Finally, we found that loss of PfGRP170 function leads to the activation of the *Plasmodium* eIF2α kinase, PK4, suggesting a specific role for this protein in this parasite stress response pathway.

INTRODUCTION

Malaria is a deadly parasitic disease that causes over 212 million cases and nearly 430,000 deaths each year, primarily in children under the age of five[1]. The deadliest human malaria parasite, *P. falciparum*, infects individuals inhabiting subtropical and tropical regions. These are some of the most impoverished regions of the world, making diagnosis and treatment challenging. Moreover, the parasite has evolved resistance to all clinically available drugs, highlighting an important need for uncovering proteins that are essential to the biology of this parasite[2-6]. Malaria is associated with a wide array of clinical symptoms, such as fever, chills, nausea, renal failure, pulmonary distress, cerebral malaria, and cardiac complications. It is the asexual replication of the parasite within the red blood cell (RBC) that is responsible for the pathology of the disease[7].

In *P. falciparum,* the endoplasmic reticulum (ER) is a uniquely complex, poorly understood organelle. In fact, recent data suggest that ER proteins play a major role in resistance to the frontline antimalarial, artemisinin[8-10]. It is in this organelle that a variety of essential cellular functions occur, including protein trafficking, cellular signaling, and activation of stress response pathways[11-17]. Compared to other eukaryotes, the molecular mechanisms involved in these essential processes in *Plasmodium* remain poorly understood. Therefore, it is imperative to uncover proteins that regulate and maintain ER biology. One group of proteins likely governing many of these processes are ER chaperones[18-23].Very little is known about the roles that ER chaperones play in *Plasmodium*, many of them defined merely based on sequence homology to other organisms. The *Plasmodium* genome encodes a relatively reduced repertoire of

predicted ER chaperones, but it is predicted to contain two members of the conserved ER HSP70 chaperone complex, GRP78 (or BiP) and a putative HSP110 (PfGRP170 or PfHSP70-y)[24,25]. GRP170, in other eukaryotes, serves as nucleotide exchange factor for BiP[26,27]. Additionally, GRP170 has been reported to have holdase activity and can bind unfolded substrates independent of ATP or BiP[28-30].

In this study, we used a conditional auto-inhibition strategy to generate conditional mutants for the putative ER chaperone, PfGRP170 (PF3D7_1344200)[31-33]. Using these conditional mutants, we localized PfGRP170 to the parasite ER, and show that unlike its orthologs in other eukaryotes, it is essential for cell survival. Detailed life cycle analysis revealed that inhibition of PfGRP170 results in parasite death in early schizogony. The protein is required for surviving a brief heat shock, suggesting that PfGRP170 is essential during febrile episodes in the host. We show that despite a predicted transit peptide, PfGRP170 is not essential for protein trafficking to the apicoplast nor is it required for protein export into the host RBC. Using combined mass spectroscopy approaches we identified potential interactors. Moreover, we demonstrate here that PfGRP170 interacts with the *Plasmodium* homolog of BiP suggesting a conserved HSP70 ER chaperone complex. Finally, we show that conditional inhibition of PfGRP170 leads to the activation of the only known ER stress response pathway in Plasmodium, the PK4 pathway[10,16].

RESULTS

PF3D7_1344200 is a putative GRP170 in P. falciparum

A blast search to identify ER localized Hsp70 proteins in *P. falciparum* revealed two proteins, HSP70-2 (PfGRP78/BiP) and a putative HSP110 (PF3D7_1344200). HSP110 proteins are considered large HSP70 chaperones, having sequence homology to both the nucleotide and substrate binding domains of other HSP70 members[34]. The increased size of HSP110 family members is the result of an extended α-helical domain at the C-terminus as well as an unstructured loop inserted in the substrate-binding domain[28,34] (Figure 4.1A). In other eukaryotic organisms, the ER localized HSP110 (referred to as GRP170) is a chaperone with four primary protein domains: a signal peptide, a nucleotide binding domain, a substrate binding domain, and an extended C-terminus[26,34]. A protein sequence alignment using the yeast GRP170 (Lhs1) was used to predict the boundaries of these domains in PF3D7_1344200 (PfGRP170) (Figure 4.1A and Supplemental Figure 4.1). Most of the sequence conservation between Lhs1 and PfGRP170 was found to be in the nucleotide-binding domain (Supplemental Figure 4.1). PfGRP170 is well conserved across multiple *Plasmodium* species, including other human malaria-causing species (Supplemental Figure 4.2). This level of conservation decreases in another apicomplexan (*T. gondii*) and even more so in yeast and humans (Supplemental Figure 4.2).

Generating PfGRP170-GFP-DDD conditional mutants

Conditional mutants for PfGRP170 (termed PfGRP170-GFP-DDD) were generated by tagging the endogenous PfGRP170 locus at the 3’ end, using single homologous crossover, with a GFP reporter, the *E. coli* DHFR destabilization domain

(DDD), and an ER retention signal (SDEL) (Figure 4.1B). The endogenous PfGRP170 gene encodes a C-terminus SDEL sequence, a potential ER retention signal, and therefore we added an SDEL sequence after the DDD domain in order to avoid mislocalization of the tagged protein. In the presence of the small ligand Trimethoprim (TMP), the DDD is maintained in a folded state. However, if TMP is removed from the culture medium, the DDD unfolds and becomes unstable[31-33,35,36]. Intramolecular binding of the chaperone to the unfolded domain inhibits normal chaperone function (Figure 4.1B)[31-33]. Two independent transfections were carried out, and integrated parasites were selected via several rounds of drug cycling. PCR integration tests following drug selection indicated that the percentage of integrated parasites in both transfections were extremely low (Figure 4.1C). Consequently, standard limiting dilution could not be used to clone out integrated parasites. To circumvent this issue, flow cytometry was used to enrich and sort extremely rare GFP positive parasites. Despite low enrichments and sorting rates (GFP positive population =~1.13E-3), we successfully obtained two clones, termed 1B2 and 1B11, using flow sorting (Figure 4.1 C and D). Proper integration into the *pfgrp170* locus was confirmed by a Southern blot analysis (Figure 4.1E). Western blot analysis revealed that the PfGRP170-GFP-DDD protein was expressed at the expected size (Figure 4.1F). Immunofluorescence assays (IFA) and western blot analysis showed that the PfGRP170-GFP-DDD fusion protein was expressed and localized to the parasite ER during all stages of the asexual life cycle (Figure 4.1G and Supplemental Figure 4.3).

PfGRP170 is essential for asexual growth and surviving febrile episodes

To investigate the essentiality of PfGRP170, PfGRP170-GFP-DDD asynchronous parasites were cultured in the absence of TMP, and parasitemia was observed using flow cytometry. A growth defect was seen within 24 hours after the removal of TMP, resulting in parasite death (Figure 4.2A). Furthermore, the two clonal parasite lines exhibited a dose-dependent growth response to TMP (Figure 4.2B). Consistent with data from other chaperones tagged with the DDD[31-33], TMP removal did not result in degradation of PfGRP170-GFP-DDD (Figure 4.2C). Conditional inhibition of *Plasmodium* proteins that does not involve their degradation, has also been observed for other non-chaperone proteins [37,38]. Moreover, the removal of TMP did not affect the ER localization of PfGRP170 (Supplemental Figure 4.4).

Using a nucleic acid stain, acridine orange, we used flow cytometry to specifically observe each stage of the asexual life cycle (ring, trophozoite, and schizont) in PfGRP170-GFP-DDD parasites incubated with and without TMP (Figure 4.2D). The amounts of RNA and DNA increase over the asexual life cycle as the parasite transitions from a ring to trophozoite to a multi-nucleated schizont. We observed that upon TMP removal, mutant parasites arrested in a relatively late developmental stage (Figure 4.2D). To identify the stage in the asexual life cycle where the mutant parasites died, TMP was removed from tightly synchronized ring stage cultures and parasite growth and morphology was assessed over the 48-hour life cycle. We observed morphologically abnormal parasites late in the lifecycle, when control parasites had undergone schizogony (Figure 4.2E). The PfGRP170-GFP-DDD parasites grown

without TMP ultimately failed to progress through schizogony and did not reinvade new RBCs (Figure 4.2E).

The cytoplasmic ortholog of PfGRP170, PfHSP110, was previously shown to be essential for surviving heat stress[33]. Therefore, we tested whether PfGRP170 mutants were sensitive to a brief heat shock. Asynchronous parasites were incubated in the absence of TMP for 6 hours at either 37°C or 40°C. Following the 6-hour incubation, TMP was added back to all cultures, which were then grown at 37°C for two growth cycles, while measuring parasitemia every 24 hours. The growth of parasites at 37°C was not significantly affected by the brief removal of TMP (Figure 4.2F). In contrast, incubating parasites at 40°C without TMP resulted in reduced parasite viability compared to parasites grown at 40°C with TMP (Figure 4.2F).

PfGRP170 is not required for trafficking of apicoplast proteins

Protein trafficking to the apicoplast is essential for parasite survival. Proteins targeted to the apicoplast contain an N-terminal transit peptide that is revealed upon signal peptide cleavage in the ER[15,39]. It remains unclear whether apicoplast targeted proteins go through the Golgi before reaching their final destination. It has been shown that disruption of ER to Golgi trafficking, using Brefeldin A (BFA), does not reduce apicoplast transport[15,40]. One of these studies further demonstrated that the addition of an ER retention sequence (SDEL), to a GFP with a transit peptide, did not reduce apicoplast trafficking or transit peptide cleavage[40]. However, a separate but similar analysis came to the opposite conclusion[41]. Thus, the identification, packaging, and transport of apicoplast-targeted proteins from the ER remain unanswered questions.

Two software analysis tools (Prediction of Apicoplast-Targeted Sequences (PATS) and PlasmoAP) predicted a strong apicoplast transit peptide for PfGRP170, despite our observation of a definite ER localization (Figure 4.1G and Figure 4.3A). We were therefore interested to find out whether PfGRP170 plays a role in apicoplast trafficking. We tested whether the putative PfGRP170 transit peptide (amino acids: 1 to 150) could be trafficked to the apicoplast by episomally expressing the predicted PfGRP170-transit peptide fused to a GFP reporter without an ER retention signal (Figure 4.3B). We performed co-localization assays using ER, apicoplast, and Golgi markers and determined that the putative transit peptide localized to the ER due to colocalization with ER marker Plasmepsin V (Figure 4.3B).

To determine the role of PfGRP170 in trafficking proteins to the apicoplast, we removed TMP from PfGRP170-GFP-DDD parasites and examined the localization of the apicoplast-localized cpn60[32,42,43]. No defects in apicoplast localization of cpn60 were observed (Figure 4.3C). Additionally, incubation with the essential apicoplast metabolite IPP[44], failed to rescue or have any positive effect on TMP removal in PfGRP170-GFP-DDD parasites (Figure 4.3D).

Interactions of PfGRP170

Two independent approaches were taken to identify the interacting proteins of PfGRP170 (Figure 4.4A). The first was an anti-GFP Immunoprecipitation (IP) followed by mass spectroscopy. In the second approach we generated a parasite line episomally expressing PfGRP170 tagged with an HA, the promiscuous Biotin Ligase (BirA), and an ER retention signal (KDEL). When exogenous biotin is added to the PfGRP170-HA-BirA parasites, the BirA tagged protein will biotinylate interacting proteins or those that are in

close proximity[45]. These biotinylated proteins can be identified by performing pull down assays using streptavidin coated magnetic beads. A western blot analysis confirmed expression of the PfGRP170-HA-BirA fusion protein (Supplementary Figure 4.5A). Colocalization IFA's confirmed that the PfGRP170-HA-BirA protein localizes to the parasite ER (Supplementary Figure 4.5B). Additionally, western blot analysis demonstrates that proteins are biotinylated in the PfGRP170-HA-BirA parasite lines when biotin is added (Supplementary Figure 4.5C).

Mass spectroscopy data were obtained from two independent anti-GFP IP's of PfGRP170-GFP-DDD parasites and two biological replicates of streptavidin pulldowns from PfGRP170-HA-BirA parasites following an incubation with biotin (Table 4.2 and Table 4.4). In addition, mass spectroscopy data were obtained from two independent anti-GFP IP's of the PM1 parental control and one streptavidin pull down from 3D7 parasites incubated with biotin to filter out non-specific interactions (Table 4.1 and Table 4.3). Both BiP and PfGRP170 were found in the control IP's, albeit in lower peptide counts (Table 4.1 and table 4.3). This is not surprising as chaperones are common contaminants in mass spectroscopy. However, due to the documentation of PfGRP170 being an interactor and regulator of BiP function, we opted to keep BiP in our analysis[26]. In order to obtain a list of proteins specific to the ER and parasite secretory pathway, proteins identified by mass spectroscopy in each IP were filtered to include only those, which had a signal peptide or transmembrane domain. Thirty common proteins were found in both the 1B2 and 1B11 in the anti-GFP IP's and 37 common proteins were found in the two replicates of the PfGRP170-HA-BirA streptavidin pull down (Figure 4.4A). A high-confidence list of 11 proteins common between the two IP methods was

then generated (Figure 4.4B). Using recently published real-time transcriptional abundance data, we plotted the normalized transcriptional abundance values for all 11 proteins. We excluded 4 proteins which were expressed earlier in the life cycle, and kept proteins which were highly expressed in late stage development, the same time when the PfGRP170-GFP-DDD-KDEL parasites die (Figure 4.4C)[46].

PfGRP170 is not required for trafficking to the RBC

In order for the parasite to grow, develop, and divide, it must drastically remodel the host RBC[12]. These modifications are accomplished through the export of proteins from the ER to the RBC. In model eukaryotes, such as yeast and mammalian cells, molecular chaperones, and specifically those that are ER-localized, play central roles in protein trafficking[18,19]. Therefore, we tested whether conditional inhibition of PfGRP170 would prevent trafficking of several exported proteins (PfHSP70x, PfMAHRP1, and FIKK4.2). Our results demonstrate that loss of PfGRP170 function did not affect the localization of these proteins to the host RBC (Supplemental Figure 4.6A-C).

PfGRP170 and BiP interact

One of the most abundant proteins identified in our mass spectroscopy data was PfBiP (Figure 4.4B). Therefore, we were tested whether PfGRP170 and PfBiP interact in *P. falciparum*. We performed an anti-GFP Co-IP and probed the lysate for PfBiP. We observed that PfGRP170 and PfBiP interact and this interaction is not lost upon TMP removal (Figure 4.5A). As a control, we probed the GFP Co-IP lysates for a different ER protein, Plasmepsin V (PMV), and found that it did not pull down with PfGRP170 (Figure 4.5B).

To visualize the PfGRP170-PfBiP interaction within the cellular context of the infected RBC, we utilized a Proximity Ligation Assay (PLA)[47-49]. The PLA positive signal indicates that two proteins are within 40nm of each other, suggesting a close interaction within the cell. This approach has been used successfully in *Plasmodium* to demonstrate interaction of exported proteins[50]. We performed this assay using anti-GFP and anti-BiP antibodies and observed a positive signal at all life cycle stages (Figure 4.5C). As a negative control we also probed with an antibody against the ER localized protease PMV and despite the co-localization of these two proteins in the ER, we did not see a positive PLA signal, suggesting distinct sub-organellar localizations (Figure 4.5D). Together, these results demonstrate that PfGRP170 and PfBiP interact during all stages of the asexual life cycle of *P. falciparum.*

The function of BiP is critical for ER biology and in other eukaryotes, its function is regulated by GRP170[26,27], we tested whether the death phenotype observed in the PfGRP170-GFP-DDD mutants could be rescued by overexpression of PfBiP. We did this by episomally expressing PfBiP with a Ty1 tag and an ER retention signal (KDEL) in the PfGRP170-GFP-DDD mutants. Colocalization assays using IFA demonstrate that the PfBiP-Ty1 fusion protein is targeted to the ER and we observe that the protein is expressed at the correct size by western blot (Figure 4.5E and 4.5F). To determine if the overexpression of PfBiP could rescue parasite growth during TMP removal, the PfGRP170-GFP-DDD parasites expressing the PfBiP-Ty1 protein were incubated with and without TMP and the parasitemia was monitored using flow cytometry. We demonstrate that the overexpression of PfBiP in the PfGRP170-GFP-DDD parasites could not rescue parasite growth (Figure 4.5G).

Loss of PfGRP170 function activates the PK4 stress response pathway

In addition to their function in the secretory pathway, molecular chaperones perform a vital role in the management of cellular stress. *Plasmodium* lack much of the ER machinery used to activate stress response pathways[16,51,52]. The only identified ER stress response pathway in *Plasmodium* is the PERK/PK4 pathway[10,16]. Signaling through this pathway has been shown to occur in the parasite following artemisinin treatment[10]. Under normal conditions, PK4 exists as a transmembrane monomeric protein in the ER. When the ER is stressed, PK4 oligomerizes and becomes active, phosphorylating the cytoplasmic translation initiation factor EIF2-α to halt translation and flux through the ER[10,16]. To determine whether this pathway was activated during conditional inhibition of PfGRP170, PfGRP170-GFP-DDD parasites were tightly synchronized to the ring stage and grown without TMP for 24 hours, after which parasite lysate was collected and the phosphorylation state of EIF2-α determined by western blot. We observed that PfGRP170 auto-inhibition resulted in the phosphorylation of EIF2-α, indicating that this pathway was activated (Figure 4.6A).

Since conditional inhibition of PfGRP170 resulted in EIF2-α phosphorylation, which has been shown to be required for resistance to artemisinin resistance, we tested if PfGRP170 plays a role in drug resistance. For this purpose, we utilized PfGRP170-BirA parasites, which have an extra copy of PfGRP170. Using the ring-stage survival assay, we compared the growth of the parental parasite line (3D7) with that of PfGRP170-BirA parasites after brief exposure to artemisinin. Our data show that overexpression of PfGRP170 did not result in artemisinin resistance (Supplementary Figure 4.7A-B).

Several *Plasmodium* kinases have been shown to phosphorylate EIF2-α in late developmental stages or in response to other cellular stress or artemisinin treatment[16,53-55]. We were therefore interested in identifying the specific kinase that is responsible for the phosphorylation of EIF2-α during conditional inhibition of PfGRP170. The ER kinase, PK4, has been shown to be activated by ER stress in *Plasmodium*[52]. Therefore, we incubated synchronized PfGRP170-GFP-DDD parasites without TMP for 24 hours, in the presence or absence of a specific PK4 inhibitor GSK2606414[10]. Parasite lysates were used to determine the phosphorylation state of EIF2-α. We observed that in the presence of the PK4 inhibitor, EIF2-α phosphorylation was blocked, demonstrating that conditional inhibition of PfGRP170 specifically results in PK4 activation, which leads to phosphorylation of EF2-α (Figure 4.6B). As a control, we used the parental strain, PM1, and incubated these parasites with and without TMP or the PK4 inhibitor (Figure 4.6C). This experiment showed no changes in levels of EIF2-α regardless of the presence of TMP or the PK4 inhibitor.

DISCUSSION

We present in this work the first characterization of PfGRP170 in the asexual life cycle of *P. falciparum*. We have generated conditional mutants that allow us to probe the role of this protein using the DDD conditional auto-inhibition system[32,33,35-38]. Additionally, taking advantage of the GFP fused to PfGRP170, we were able to isolate an exceptionally rare clonal population using flow cytometry (Figure 4.1C-F). This technique achieved what a traditional limiting dilution method could not. Moreover, this type of flow sorting can be implemented not only for rare events but also to significantly cut down the time from transfection to a clonal cell population.

We demonstrate here that PfGRP170 is an ER resident protein that is essential for asexual growth in *P. falciparum* (Figure 4.1G and Figure 4.2A). Loss of PfGRP170 function leads to a growth arrest of parasites late in development and their subsequent death (Figure 4.2D and E). In yeast and mammals, GRP170 functions in a complex with the ER chaperone BiP, serving as the nucleotide exchange factor to regulate BiP activity[26,27]. Unlike *Plasmodium falciparum*, Yeast null for GRP170 are viable due to the upregulation of Sil1, another nucleotide exchange factor, that usually plays a role in the IRE1 stress response pathway[56]. The *Plasmodium* genome does not encode Sil1 and IRE1, which aligns with the observed essentiality of PfGRP170 during the blood stages. Additionally, research in mammalian systems suggests that GRP170 also has BiP-independent functions, such as binding unfolded substrates[28]. Our data show, via immunoprecipitation, mass spectroscopy, and proximity ligation assays (Figure 4.4 and Figure 4.5), that PfGRP170 interacts with BiP in *P. falciparum* suggesting that it regulates BiP function. Further, overexpression of PfBiP was unable to rescue loss of PfGRP170 function and the conditional inhibition of PfGRP170 does not reduce its interaction with PfBiP (Figure 4.5A and 4.5G). These data suggest that a PfBiP independent function of PfGRP170 is essential for parasite survival.

Previously it was shown that apicoplast transit peptides are predicted to bind the ER chaperone BiP, and when these predicted binding sites were mutated, targeting to the apicoplast was disrupted[57]. Moreover, an Hsp70 inhibitor with an antimalarial activity was shown to inhibit apicoplast targeting[58,59]. These data, combined with the predicted transit peptide of PfGRP170, led us to investigate the role of this chaperone in apicoplast trafficking (Figure 4.3A). Interestingly, when the putative transit peptide was

tagged with a GFP reporter and without an ER retention signal, the fusion protein was retained in the ER (Figure 4.3B). It was previously reported that proteins with a signal peptide and no ER retention signal are secreted to the parasitophorous vacuole[60-63]. However, it was also shown that some proteins with a signal peptide and GFP (lacking an ER retention or trafficking signals) remain in the parasite ER[61]. Regardless, this reporter was not sent to the apicoplast indicating that it is not a functional apicoplast transit peptide (Figure 4.3B). A manuscript published in 2012 demonstrated that appending the first 137 amino acids of PfGRP170 to a GFP reporter (without a retention signal) resulted in this chimeric protein localizing partially to the apicoplast and to the parasitophorous vacuole[64]. Our chimeric protein includes the first 150 amino acids of PfGRP170 which may account for some of the differences in the two studies. In addition, PfGRP170 auto-inhibition did not lead to any defects in trafficking to the apicoplast, nor could it be rescued with the essential apicoplast metabolite IPP (Figure 4.3C-D). This suggests that the primary function of PfGRP170 is not related to the apicoplast.

Protein trafficking to the host RBC originates in the parasite ER and is essential for parasite viability, and therefore could potentially account for the observed death phenotype during conditional inhibition of PfGRP170[11,12]. PfGRP170 was shown to associate with exported proteins in another study that identified proteins that bind to the antigenic variant surface protein, PfEMP1[65]. However, our data show that there is no significant difference in the trafficking of some exported proteins upon conditional inhibition of PfGRP170, suggesting that protein export is not blocked (Supplemental Figure 4.6).

ER chaperones are known in other eukaryotes to be vital to managing cellular stress[17,21]. However, several ER localized stress response pathways present in other eukaryotes are absent in *P. falciparum* and few molecular players in the parasite ER stress response pathway are known. Our data demonstrate that PfGRP170 is important for coping with a specific form of cellular stress, namely heat shock (Figure 4.2F). This finding highlights a potential critical role for PfGRP170 *in vivo*, as high febrile episodes are one of the main symptoms of clinical malaria and are considered a defense mechanism against parasites. GRP170 in mammalian systems has been shown to bind to the transmembrane proteins in the ER that are involved in the unfolded protein response (UPR), suggesting it may regulate these pathways[66,67]. The *Plasmodium* genome does not encode many of the UPR orthologues, but a single ER stress pathway (PK4 signaling) has been previously described and was shown to be activated following artemisinin treatment[10,16]. Here, we demonstrate that loss of PfGRP170 function results in the activation of PK4 stress pathway (Figure 4.6), providing the first link between an endogenous ER resident protein and the activation of the PK4 pathway in *P. falciparum*.

Our data suggest that unlike its homologs in other eukaryotes, the essential function of PfGRP170 is not entirely linked to its role in regulating BiP, since PfGRP170 binds to BiP upon removal of TMP and overexpression of PfBiP does not rescue the growth defect seen in the conditional mutants of PfGRP170 (Figure 4.5A and Figure 4.5G). Two separate IP/mass spectroscopy approaches generated a list of 11 high-confidence interacting partners of PfGRP170 (Figure 4.4B). Seven of the proteins (including PfBiP) have a peak expression pattern around the time PfGRP170-GFP-DDD parasites begin to die (Figure 4.2E and Figure 4.4C). SERA5 and SERA6 have been

shown to be required for egress from the RBC, which would be after the PfGRP170-GFP-DDD parasites die[68-70]. RON3 has been shown to been suggested to be a protein important for RBC invasion, which implies this protein interaction is also not why PfGRP170-GFP-DDD parasites are dying[71]. CLAG9, another identified protein, has been proposed to play a role in cytoadherence to CD36 and remodeling the host RBC after invasion by a merozoite[72,73]. PDI-11 was predicted to be non-essential in a *piggyBac* mutagenesis conducted in *Plasmodium*[74]*.* The remaining protein was parasite-infected erythrocyte surface protein 1 (PIESP1) (Figure 4.4B). This protein was published in the literature as an exported protein[75]. However, the last four amino acids of this protein are TDEL, which could potentially serve as an ER retention signal. These last four amino acids were left off of the GFP fusion protein that was expressed in the parasite as the authors predicted this protein was a transmembrane protein and thus leaving off these amino acids would have no effect on protein localization[75]. Further studies will be needed to determine its precise subcellular localization and its role if any with PfGRP170. Our data suggest that given the divergence between mammalian and parasite GRP170 and their divergent biological roles, PfGRP170 could be a viable antimalarial drug target.

ACKNOWLEDGMENTS

We thank Dan Goldberg for anti-EF1α and anti-PMV antibodies; Boris Striepen for anti-Cpn60 antibody; Hans-Peter Beck for anti-MAHRP antibody; Jude Przyborski for anti-PfHSP70x antibody; David Cavanagh and EMRR for anti-FIKK4.2 antibody; Drew Etheridge, Min Zhang, and Bill Sullivan for technical suggestions; Muthugapatti Kandasamy at the University of Georgia Biomedical Microscopy Core, Julie Nelson at

the CTEGD Cytometry Shared Resource Lab for technical assistance. We acknowledge assistance of the Emory University Integrated Proteomics Core for mass spectrometry. This work was supported by ARCS Foundation awards to H.M.K. and D.W.C., UGA Startup funds to V.M., CDC-UGA Seed Award to V.M. and N.W.L., and the US National Institutes of Health (R00AI099156 and R01AI130139) to V.M. and (T32AI060546) to H.M.K. and to M.A.F.

METHODS

Primers and Plasmid construction

All primer sequences used in this study can be found in Table 4.5. Generation of pGDB-SDEL plasmid was done using the QuikChange II Site-Directed Mutagenesis Kit (Agilent Technologies) on the pGDB plasmid with primers P1 and P2 per the manufacturer's protocol[36].

Genomic DNA was isolated using the QIAamp DNA blood kit (Qiagen). gDNA used in this study was isolated from either 3D7 or Plasmepsin I knockout parasites (PM1KO)[36]. The pPfGRP170-GFP-DDD plasmid used to generate the PfGRP170-GFP-DDD mutants was made by amplifying via PCR an approximately 1-kb region homologous to the 3'end of the PfGRP170 gene (stop codon not included) using primers P3 and P4. The amplified product was inserted into pGDB-SDEL plasmid using restriction sites Xho1 and AvrII (New England Biolabs) and transformed into bacteria. The construct was sequenced prior to transfection.

The pGRP170-HA-BirA-KDEL plasmid was prepared by amplifying PfGRP170 (without the stop codon) from 3D7 gDNA using primers P5 and P6 and 3xHA-BirA from the pTYEOE-3XHA-BirA plasmid (From D. Goldberg) using primers P7 and P8. Both

PCR products generated included homologous regions used for Sequence and Ligation Independent Cloning (SLIC)[76] .The primers to amplify the 3xHA-BirA included the sequence of an ER retention signal (KDEL). These PCR products were fused together using PCR sewing as described previously and subsequently PCR amplified using primers P5 and P8[35]. The resulting product was then inserted into pCEN-DHFR[77] that was digested with Nhe1 and BglII (New England Biolabs) using SLIC and transformed into bacteria as described previously[32,35].

The pPfGRP170TP-GFP plasmid was prepared by amplifying the first 450 bp (includes the signal peptide and putative transit peptide sequence) of PfGRP170 from PM1 gDNA using primers P5 and P9. The GFP sequence used was amplified from pGDB using primers P10 and P11. The PfGRP170 transit peptide PCR was digested with Nhe1 and AatII (New England Biolabs) and the GFP PCR was digested with AatII and BglII (New England Biolabs). The two fragments were then ligated together (via the AatII digest site) using a T4 ligase (kit from New England Biolabs) and subsequently PCR amplified using primers P5 and P11. The resulting product was then digested with Nhe1 and BglII and inserted into pCEN-DHFR[77] that was digested with Nhe1 and BglII (New England Biolabs) using a T4 ligase and transformed into bacteria as described previously[32,35].

The pPfBiP-Ty1overexpression plasmid was prepared first by generating cDNA using the SuperScript III reverse transcriptase kit (Invitrogen) using primer P14. PfBiP was then amplified from the cDNA using primers P14 and P15. The resultant PCR product included PfBiP, a single Ty1 tag, and an ER retention signal (KDEL). The pCEN vector was modified to contain the DHOD resistance gene instead of the DHFR for

parasite selection. The PfBiP-Ty1-KDEL-KDEL PCR was cloned into the pCEN-DHOD vector cut with Nhe1 and BglII (New England Biolabs) using the IN-Fusion HD EcoDry Cloning Kit (Clontech).

Cell Culture, transfections, and isolation of clonal cell lines

Parasites were grown in RPMI 1640 media supplemented with Albumax 1 (Gibco) and transfected as described previously[31-33,35,36].

To generate PfGRP170-GFP-DDD mutants, PM1KO parasites were transfected with the pPfGRP170-GFP-DDD plasmid in duplicate. PM1KO parasites contain the human dihydrofolate reductase (hDHFR) expression cassette which gives the parasites resistance to Trimethoprim (TMP)[36]. Drug selection and cycling were performed as described previously using 10μM TMP (Sigma) and 2.5μg/ml Blasticidin (Sigma)[32,33,36]. Following drug cycling, GFP positive cells were enriched using an S3 Cell Sorter (BioRad). Individual GFP positive cells from a single transfection were cloned into 96 well plates using a MoFlo XDP flow cytometer. After the EC_{50} of TMP was determined for clones 1B2 and 1B11, parasites were shifted into media containing 2.5μg/ml BSD and 20μM TMP to facilitate optimal growth.

The PfGRP170-BirA and PfGRP170TP-GFP parasites were generated by transfecting 3D7 parasites with plasmids pGRP170-HA-BirA-KDEL or pPfGRP170TP-GFP, respectively. Parasites expressing these episomal constructs were selected using 2.5nM WR99210.

To generate the PfGRP170-GFP-DDD parasites episomally expressing PfBiP-Ty1-KDEL-KDEL, PfGRP170-GFP-DDD clones 1B2 and 1B11 were each transfected

with pPfBiP-Ty1-KDEL. Parasites expressing this episomal construct were selected using 250nM of DSM1[78].

Integration tests for PfGRP170-GFP-DDD mutants

Genomic DNA was isolated from parasites using the QIAamp DNA blood kit (Qiagen). Control primers to amplify the genome were P4 and P12 and primers used to amplify integrated DNA were P12 and P13.

Southern blot analysis was performed on DNA isolated from PfGRP170-GFP-DDD parasites (1B2 and 1B11) as described previously[32,35]. The assay was also performed on PM1KO parental DNA and the pGRP170-DDD plasmid as a control. DNA was isolated from parasites using the QIAamp DNA blood kit (Qiagen). 10µg of precipitated PM1KO DNA, 1B2, and 1B11 DNA and 10ng of pGRP170-DDD plasmid was digested overnight with Mfe1 (New England Biolabs). The biotinylated probe used was generated by PCR using biotinylated-16-UTP (Sigma) and primers P3 and P4. The biotinylated probe on the southern blot was detected using IRDye 800CW streptavidin-conjugated dye (LICOR Biosciences) and imaged using the Odyssey infrared imaging system (LICOR Biosciences).

Growth assays using flow cytometry

TMP was removed from asynchronous PfGRP170-GFP-DDD cultures for growth assays by washing the culture in equal volume of complete RPMI three times. The culture was then resuspended in complete RMPI media containing either 2.5µg/ml Blasticidin (Sigma) for conditional inhibition (Sigma) or 2.5µg/ml Blasticidin (Sigma) and 20µM TMP (Sigma) for the control. Parasitemia was monitored using a flow cytometer, either a CyAn ADP (Beckman Coulter) or CytoFLEX (Beckman Coulter) instrument,

using either 1.5µg/ml acridine orange (Molecular Probes) as described previously[35] or similarly using 8µM Hoechst in filtered 1X phosphate-buffered saline (PBS). Flow cytometry data were analyzed using FlowJo software (Treestar Inc.). If the parasitemia was too high, parasites were subcultured during the experiment and the relative parasitemia was then calculated by multiplying the calculated parasitemia by the dilution factor. Parasitemia was normalized by using the highest parasitemia as one hundred percent. Using Prism software (GraphPad Software Inc), the parasitemia data were fit to an exponential growth curve equation.

To determine the EC_{50} of TMP for PfGRP170-GFP-DDD cell lines, parasites were washed as described above and seeded into a 96 well plate with 2.5µg/ml Blasticidin and varying TMP concentrations. Parasitemia was measured after 48 hours using flow cytometry as described above. The parasitemia data were fit to a dose-response equation using Prism.

For the IPP rescue experiment, asynchronous PfGRP170-GFP-DDD parasites were washed as described above and resuspended in media either with 2.5µg/ml Blasticidin or 2.5µg/ml Blasticidin and 20µM TMP with or without 200µM Isopentenyl pyrophosphate (Isoprenoids LC). Parasitemia were monitored using flow cytometry as described above and the data were fit to an exponential growth curve equation using Prism.

For the heat shock experiment, asynchronous PfGRP170-GFP-DDD parasites were washed as described above and resuspended in media either with 2.5µg/ml Blasticidin or 2.5µg/ml Blasticidin and 20µM TMP. Parasites were then incubated at either 37°C or 40°C for 6 hours. After 6 hours, 20µM TMP was added to cultures that

were incubated without it and all parasites were shifted back to 37ºC. Parasitemia was monitored using flow cytometry as described above and the data were fit to an exponential growth curve equation (GraphPad Software Inc).

For growth assays done with PfGRP170-GFP-DDD-GFP cell lines overexpressing PfBiP, asynchronous parasites were washed as described above and resuspended in media either with 2.5µg/ml Blasticidin and 250nM of DSM1 or 2.5µg/ml Blasticidin, 250nM of DSM1, and 20µM TMP. Parasitemia were monitored using flow cytometry as described above and the data were fit to an exponential growth curve equation using Prism.

Synchronized growth assay

PfGRP170-GFP-DDD Parasites were synchronized as described previously by sorbitol (VWR), followed by percoll (Genesee Scientific) the next day and then sorbitol four hours later to obtain 0-4 hour rings[32,36]. Parasites were washed as described above to remove TMP from the media and incubated in media either with 2.5µg/ml Blasticidin or 2.5µg/ml Blasticidin and 20µM TMP. Thin blood smears using the Hema 3 Staining Kit (PROTOCOL/Fisher) were prepared every few hours to monitor parasite growth and morphology. Slides were imaged using a Nikon Eclipse E400 microscope with a Nikon DS-L1-5M imaging camera.

Western blot

Western blotting was performed as described previously[32]. Parasite pellets were isolated using cold 0.04% Saponin (Sigma) in 1X PBS for 10 minutes as described previously[32,36]. Antibodies used for this study were: mouse anti-GFP JL-8 (Clontech, 1:3000), rabbit anti-PfEF1α (from D. Goldberg, 1:2,000), mouse anti-plasmepsin V (from

D. Goldberg, 1:400), rabbit anti-PfBiP MRA-1246 (BEI resources, 1:500), rabbit anti-GFP A-6455 (Invitrogen, 1:2,000), mouse anti-eIF2α L57A5 (Cell Signaling, 1:1,000), rabbit anti- Phospho-eIF2α 119A11 (Cell Signaling, 1:1,000), rat anti-HA (Roche 3F10, 1:3000), mouse anti-Ty1 (Sigma Clone BB2, 1:1000), and mouse anti-Ub P4D1 (Santa Cruz Biotechnology, 1:1,000). Secondary antibodies used were IRDye 680CW goat anti-rabbit IgG and IRDye 800CW goat anti-mouse IgG (LICOR Biosciences, 1:20,000). The western blots were imaged using the Odyssey infrared imaging system. Polyacrylamide gels used in this study were either prepared using 10% EZ-Run protein gel solution (Fisher) or precast gradient gels (4-20%, from Biorad).

PK4 Inhibitor Experiments

Synchronized ring stage PfGRP170-GFP-DDD parasites were incubated in media with either 2.5μg/ml Blasticidin or 2.5μg/ml Blasticidin and 20μM TMP in the presence or absence of a PK4 inhibitor GSK2606414 (Millipore Sigma) at 2μM for 24 hours. After 24 hours, the parasites were lysed for western blot analysis using 0.04% saponin in 1X PBS as described above. PM1 (parental control parasites) were incubated in media with either complete RPM1 (no drug) or media containing 20μM TMP in the presence or absence of PK4 inhibitor GSK2606414 (Millipore Sigma) at 2μM for 24 hours. After 24 hours, the parasites were lysed for western blot analysis using 0.04% saponin in 1X PBS as described above

Live Fluorescence Microscopy

To visualize PfGRP170-GFP-DDD live parasites, 100μL of parasite culture was pelleted. The supernatant was removed, and the parasites were resuspended in 100μL medium with 2.5μg/ml Blasticidin and 20μM TMP and 5μM Hoechst. The parasites were

incubated at 37°C for 20 minutes. The parasites were then pelleted again and 90% of the medium was removed. Parasites were resuspended in the remaining medium and 8µL of this culture was placed on a glass slide and covered with a coverslip. The edges were sealed with nail polish and the cells were imaged using a DeltaVision II Microscope.

Immunofluorescence trafficking assays and imaging processing

Immunofluorescence assays (IFA) were performed as described previously using a combination of 4% Paraformaldehyde and 0.015% glutaraldehyde for fixation and permeabilization using 0.1% Triton-X100[32,35] or by smearing cells on a slide and fixing them with acetone. For apicoplast and red blood cell trafficking assays, cells were synchronized and TMP was removed as described above. Cells were then fixed as described above, 24 hours after the removal of TMP.

Primary antibodies used for IFAs in this study were: rabbit anti-GFP A-6455 (Invitrogen, 1:200), rat anti-PfBiP MRA-1247 (BEI resources, 1:125), rabbit anti-PfBiP MRA-1246 (BEI resources (1:100), mouse anti-plasmepsin V (From D. Goldberg, 1:1), mouse anti-GFP clones 7.1 and 13.1 (Roche 11814460001, 1:500), rabbit anti-Cpn60 (From. B. Striepen, 1:1,000), rabbit anti-PfERD2 (MR4, 1:2,000), rabbit anti-HA 9110 (Abcam, 1:200), rabbit anti-PfMAHRP1C (From. Hans-Peter Beck, 1:500), mouse anti-PfFIKK4.2 (From David Cavanagh/EMRR, 1:1,000), mouse anti-Ty1 (Sigma Clone BB2, 1:200), and rabbit anti-PfHSP70X (From Jude Przyborski, 1:500). Secondary antibodies used in this study are Alexa Fluor goat anti-rabbit 488, Alexa Fluor goat anti-rabbit 546, Alexa Fluor goat anti-mouse 488, Alexa Fluor goat anti-mouse 546, and Alexa Fluor

goat anti-rat 546 (Life Technologies, 1:100). The mouse anti-PfFIKK4.2, rabbit anti-PfHSP70X, and anti-PfMAHRP1C require acetone fixation.

All fixed cells were mounted using ProLong Diamond with DAPI (Invitrogen) and imaged using the DeltaVision II microscope system or Zeiss ELYRA S1 (SR-SIM) Super Resolution Microscope using a 100X objective. Images taken using the DeltaVision II were collected as a Z-stack and were deconvolved using the DeltaVision II software (SoftWorx). The deconvolved Z-stacks were then displayed as a maximum intensity projection using SoftWorx. Images taken using the Super Resolution Microscope were taken as a Z-stack. The Z-stacks were analyzed using Zen Software (Zeiss, version from 2011) for SIM processing and obtaining the maximum intensity projection. Any adjustments made to the brightness and/or contrast of the images were made using either Softworx, Zen Software, or Adobe Photoshop and were done for display purposes only. Any quantification performed for microscopy images was done using ImageJ software as described previously[35]. The quantification data were analyzed using Prism (GraphPad Software, Inc.).

Co-immunoprecipitation assays and Mass Spectroscopy

Parasites pellets were isolated from 48 mL of asynchronous culture at high parasitemia (10% or higher) using cold 0.04% saponin in 1X PBS as described above. Parasite pellets were lysed by resuspending the pellet in 150µL of Extraction Buffer (40mM Tris HCL pH 7.6, 150mM KCL, and 1mM EDTA) with 0.5% NP-40 (VWR) and 1X HALT protease inhibitor (Thermo). The resuspended parasites were then incubated on ice for 15 minutes and then sonicated three times (10% amplitude, 5 second pulses). In between each sonication, the lysate was placed on ice for 1 minute. The lysate was

then centrifuged at 21,100g for 15 minutes at 4ºC. The supernatant was collected in a fresh tube and placed on ice. The remaining pellet was subjected to a second lysis step using 150µL of Extraction buffer as above without NP-40. The lysate was sonicated and centrifuged as above (no 15-minute incubation on ice). The supernatant was collected and combined with the lysate from the first lysis step (INPUT sample). 20µL of the input sample was collected into a fresh tube and stored in the -80ºC. The remaining input sample was combined with 2µL of rabbit anti-GFP monoclonal G10362 (Thermo) and incubated rocking for two hours at 4°C.

After the two-hour incubation, the lysate with antibody was added to 50µL of prepared protein G Dynabeads (Invitrogen). Dynabeads were prepared by washing 50µL of beads three times with 100µL of IgG binding buffer (20mM Tris HCL pH 7.6, 150mM KCL, 1mM EDTA, and 0.1% NP-40). The IgG binding buffer was removed from the beads each time using a magnetic rack (Life technologies). The beads, antibody, and lysate were incubated rocking for two hours at 4°C. After the two-hour incubation, the unbound fraction of protein was collected using the magnetic rack into a fresh tube and stored at -80°C until needed for western blot analysis. The beads were then washed two times in 300µL of IgG binding buffer with 1X HALT and one time in IgG binding buffer with 1X HALT without NP-40. Each wash was done for 10 minutes rocking at 4°C.

For Co-IP's to show PfGRP170-GFP-DDD/BiP interaction 0-4 hour ring stage parasites were obtained and TMP was removed as described under the synchronized growth assay section. Parasites were lysed and an anti-GFP IP was performed as described above, approximately 24 hours after the removal of TMP. Protein was eluted

off the beads for western blot using 1X Protein Loading Dye (LICOR) with 2.5% beta-Mercaptoethanol (Fisher) and boiled for 5 minutes. This was followed by a centrifugation at 16,200 g for 5 minutes. The eluted proteins are collected by placing the tube on a magnetic rack. The isolated proteins on magnetic beads were digested with trypsin and analyzed at the Emory University Integrated Proteomics Core using a Fusion Orbitrap Mass Spectrometer.

PfGRP170-BirA biotinylation and mass spectrometry

To confirm that proteins were biotinylated when biotin was added to the PfGRP170-BirA parasites, parasites were incubated 24 hours in media containing 2.5nM WR + 150µg of biotin (Sigma). Parasites were isolated using 0.04% saponin in 1X PBS and the lysates were analyzed via western blot as described above. Secondary antibodies used were IRDye 680CW goat anti-rabbit IgG and IRDye 800CW Streptavidin (LICOR). 3D7 parasites incubated with media containing 150µg of biotin for 24 hours was used as a control.

For PfGRP170-HA-BirA streptavidin IP's, cultures were incubated for 24 hours in media containing 2.5nM WR + 150µg of biotin (Sigma). 48 mL of asynchronous culture at high parasitemia (10% or higher) were harvested for IP as described above with the following modifications. Streptavidin MagneSphere Paramagnetic Particle beads (Promega) were used to isolated biotinylated proteins. To prepare the Streptavidin beads for IP, beads were washed three times in 1 mL of 1X PBS. Incubations of lysate with the magnetic beads were performed at room temperature for 30 minutes. After the unbound fraction was removed, beads were washed twice in 8M Urea (150mM NaCL, 50mM Tris HCL pH 7.4) and once in 1X PBS. The biotinylated proteins on magnetic

beads were digested with trypsin and analyzed at the Emory University Integrated Proteomics Core using a Fusion Orbitrap Mass Spectrometer. 3D7 control streptavidin IP's were conducted as above but without the addition of 2.5nM WR to the media.

Proximity Ligation Assays

Asynchronous PfGRP170-GFP-DDD parasites were fixed as described above, approximately 24 hours after the removal of TMP. The proximity ligation assay was performed using the Duolink PLA Fluorescence kit (Sigma) per the manufacturers protocol. For the BiP/PfGRP170 PLA assay, primary antibodies mouse anti-GFP (Roche 11814460001, 1:500) and rabbit anti-BiP MRA-1246 (BEI resources (1:100) were used. For the negative control primary antibodies mouse anti-plasmepsin V (From D. Goldberg, 1:1) and rabbit anti-GFP A-6455 (Invitrogen, 1:200) were used.

Ring Stage Survival Assay

The ring-stage survival assay method was performed on 3D7 (control) and PfGRP170-BirA parasites as described previously**,** with a slight adjustment[79]. Cultures were synchronized using 5% sorbitol (Sigma-Aldrich, St. Louis, MO, USA), pre-warmed to 37°C, to obtain the highest proportion of rings, $\geq$50%. The cultures were placed back under previously described conditions for 24 hours and followed-up the next morning. Thin blood smears were methanol fixed and stained with 10% Giemsa for 15 minutes and evaluated for mature schizonts with visible nuclei (10-12). The parasites were independently suspended in PRMI-1640 supplemented with 15U/ml of sodium heparin (Sigma-Aldrich, St. Louis, MO, USA) to disrupt spontaneous rosettes formation for 15 minutes at 37 °C. After incubation, each parasite culture was layered onto a 75/25% percoll (GE Healthcare Life Sciences, Pittsburgh, PA, USA) gradient, and centrifuged at

3000rpm for 15 minutes. The intermediate phases containing the mature schizonts of each culture, were independently collected, gently washed in RPMI and transferred into two new T25 flasks with fresh cRPMI and erythrocytes for 3-hour incubation at previously described conditions. Thin blood smears were prepared as previously described, to ensure >10% schizonts count.

At the 3-hour mark, the parasites were taken-out of incubation and treated with 5% sorbitol to remove the remaining mature schizonts, which had not invaded erythrocytes yet. Parasitemia was adjusted to 1% at 2% hematocrit by adding uninfected erythrocytes and cPRMI, after the evaluation of quick stained Giemsa smears. The parasites were exposed to 700nM DHA or 1% dimethyl sulfoxide (DMSO) for 6 hours. After the 6-hour incubation period, the parasites were washed to remove the drug or DMSO and re-suspended in 1ml of cRPMI. The parasites were then transferred into two new well in the 48-well culture plate, incubated at 37 °C under a 90 % N_2, 5 % CO_2, and 5 % O_2 gas mixture for 66 hours, after which thin blood smears were prepared, methanol fixed, stained with 10% Giemsa for 15 minutes and read by three operators. Growth rate and percent survival was calculated by counting the number of parasitized cells in an estimated 2000 erythrocytes**.**

REFERENCES

1 World Health Organization. World Malaria Report. (2017).

2 Amaratunga, C., Witkowski, B., Khim, N., Menard, D. & Fairhurst, R. M. Artemisinin resistance in Plasmodium falciparum. *The Lancet Infectious Disease* **14**, 449-450 (2014).

3 Dondorp, A. M. *et al.* Artemisinin resistance in Plasmodium falciparum malaria. *N Engl J Med* **361**, 455-467, doi:10.1056/NEJMoa0808859 (2009).

4 Roper, C. *et al.* Intercontinental spread of pyrimethamine-resistant malaria. *Science* **305**, 1124 (2004).

5 Wootton, J. C. *et al.* Genetic diversity and chloroquine selective sweeps in Plasmodium falciparum. *Nature* **418**, 320-323 (2002).

6 Mita, T. *et al.* Limited geographical origin and global spread of sulfadoxine-resistant dhps alleles in Plasmodium falciparum populations. *J Infect Dis* **204**, 1980-1988, doi:10.1093/infdis/jir664 (2011).

7 Miller, L. H., Baruch, D. I., Marsh, K. & Doumbo, O. K. The pathogenic basis of malaria. *Nature* **415**, 673-679 (2002).

8 Mok, S. *et al.* Drug resistance. Population transcriptomics of human malaria parasites reveals the mechanism of artemisinin resistance. *Science* **347**, 431-435, doi:10.1126/science.1260403 (2015).

9 Rocamora, F. *et al.* Oxidative stress and protein damage responses mediate artemisinin resistance in malaria parasites. *PLoS Pathog* **14**, e1006930, doi:10.1371/journal.ppat.1006930 (2018).

10 Zhang, M. *et al.* Inhibiting the Plasmodium eIF2alpha Kinase PK4 Prevents Artemisinin-Induced Latency. *Cell Host Microbe* **22**, 766-776 e764, doi:10.1016/j.chom.2017.11.005 (2017).

11 Deponte, M. *et al.* Wherever I may roam: protein and membrane trafficking in P. falciparum-infected red blood cells. *Mol Biochem Parasitol* **186**, 95-116, doi:10.1016/j.molbiopara.2012.09.007 (2012).

12 Boddey, J. A. & Cowman, A. F. Plasmodium nesting: remaking the erythrocyte from the inside out. *Annu Rev Microbiol* **67**, 243-269, doi:10.1146/annurev-micro-092412-155730 (2013).

13 Boddey, J. A. *et al.* Role of plasmepsin V in export of diverse protein families from the Plasmodium falciparum exportome. *Traffic* **14**, 532-550, doi:10.1111/tra.12053 (2013).

14 Russo, I. *et al.* Plasmepsin V licenses Plasmodium proteins for export into the host erythrocyte. *Nature* **463**, 632-636, doi:10.1038/nature08726 (2010).

15 Tonkin, C. J., Kalanon, M. & McFadden, G. I. Protein targeting to the malaria parasite plastid. *Traffic* **9**, 166-175, doi:10.1111/j.1600-0854.2007.00660.x (2008).

16 Zhang, M. *et al.* PK4, a eukaryotic initiation factor 2α(eIF2α) kinase, is essential for the development of the erythrocytic cycle of Plasmodium. *PNAS* **109**, 3956–3961 (2012).

17 Walter, P. & David, R. The unfolded protein response: from stress pathway to homeostatic regulation. *Science* **334**, 1081-1086 (2011).

18 Araki, K. & Nagata, K. Protein folding and quality control in the ER. *Cold Spring Harb Perspect Biol* **3**, a007526, doi:10.1101/cshperspect.a007526 (2011).

19 Gidalevitz, T., Stevens, F. & Argon, Y. Orchestration of secretory protein folding by ER chaperones. *Biochim Biophys Acta* **1833**, 2410-2424, doi:10.1016/j.bbamcr.2013.03.007 (2013).

20 Hotamisligil, G. S. Endoplasmic reticulum stress and atherosclerosis. *Nat Med* **16**, 396-399, doi:10.1038/nm0410-396 (2010).

21 Xu, C., Bailly-Maitre, B. & Reed, J. C. Endoplasmic reticulum stress: cell life and death decisions. *J Clin Invest* **115**, 2656-2664, doi:10.1172/JCI26373 (2005).

22 Rutkowski, D. T. & Hegde, R. S. Regulation of basal cellular physiology by the homeostatic unfolded protein response. *J Cell Biol* **189**, 783-794, doi:10.1083/jcb.201003138 (2010).

23 Wang, H. *et al.* The Endoplasmic Reticulum Chaperone GRP170: From Immunobiology to Cancer Therapeutics. *Front Oncol* **4**, 377, doi:10.3389/fonc.2014.00377 (2014).

24 Pavithra, S. R., Kumar, R. & Tatu, U. Systems analysis of chaperone networks in the malarial parasite Plasmodium falciparum. *PLoS Comput Biol* **3**, 1701-1715, doi:10.1371/journal.pcbi.0030168 (2007).

25 Shonhai, A., Boshoff, A. & Blatch, G. L. The structural and functional diversity of Hsp70 proteins from Plasmodium falciparum. *Protein Sci* **16**, 1803-1818, doi:10.1110/ps.072918107 (2007).

26 Andreasson, C., Rampelt, H., Fiaux, J., Druffel-Augustin, S. & Bukau, B. The endoplasmic reticulum Grp170 acts as a nucleotide exchange factor of Hsp70 via a mechanism similar to that of the cytosolic Hsp110. *J Biol Chem* **285**, 12445-12453, doi:10.1074/jbc.M109.096735 (2010).

27 de Keyzer, J., Steel, G. J., Hale, S. J., Humphries, D. & Stirling, C. J. Nucleotide binding by Lhs1p is essential for its nucleotide exchange activity and for function in vivo. *J Biol Chem* **284**, 31564-31571, doi:10.1074/jbc.M109.055160 (2009).

28 Behnke, J. & Hendershot, L. M. The large Hsp70 Grp170 binds to unfolded protein substrates in vivo with a regulation distinct from conventional Hsp70s. *J Biol Chem* **289**, 2899-2907, doi:10.1074/jbc.M113.507491 (2014).

29 Park, J. *et al.* The Chaperoning Properties of Mouse Grp170, a Member of the Third Family of Hsp70 Related Proteins. *Biochemistry* **42**, 14893-14902 (2003).

30 Buck, T. M. *et al.* The Lhs1/GRP170 chaperones facilitate the endoplasmic reticulum-associated degradation of the epithelial sodium channel. *J Biol Chem* **288**, 18366-18380, doi:10.1074/jbc.M113.469882 (2013).

31 Beck, J. R., Muralidharan, V., Oksman, A. & Goldberg, D. E. PTEX component HSP101 mediates export of diverse malaria effectors into host erythrocytes. *Nature* **511**, 592-595, doi:10.1038/nature13574 (2014).

32 Florentin, A. *et al.* PfClpC Is an Essential Clp Chaperone Required for Plastid Integrity and Clp Protease Stability in Plasmodium falciparum. *Cell Rep* **21**, 1746-1756, doi:10.1016/j.celrep.2017.10.081 (2017).

33 Muralidharan, V., Oksman, A., Pal, P., Lindquist, S. & Goldberg, D. E. Plasmodium falciparum heat shock protein 110 stabilizes the asparagine repeat-rich parasite proteome during malarial fevers. *Nat Commun* **3**, 1310-1310 (2012).

34 Easton, D. P., Kaneko, Y. & Subjeck, J. R. The hsp110 and Grp170 stress proteins: newly recognized relatives of the Hsp70s. *Cell Stress Chaperones* **5**, 276-290 (2000).

35 Cobb, D. W. *et al.* The Exported Chaperone PfHsp70x Is Dispensable for the Plasmodium falciparum Intraerythrocytic Life Cycle. *mSphere* **2**, doi:10.1128/mSphere.00363-17 (2017).

36 Muralidharan, V., Oksman, A., Iwamoto, M., Wandless, T. J. & Goldberg, D. E. Asparagine repeat function in a Plasmodium falciparum protein assessed via a regulatable fluorescent affinity tag. *Proc Natl Acad Sci U S A* **108**, 4411-4416, doi:10.1073/pnas.1018449108 (2011).

37 Ganter, M. *et al.* Plasmodium falciparum CRK4 directs continuous rounds of DNA replication during schizogony. *Nat Microbiol* **2**, 17017, doi:10.1038/nmicrobiol.2017.17 (2017).

38 Ito, D., Schureck, M. A. & Desai, S. A. An essential dual-function complex mediates erythrocyte invasion and channel-mediated nutrient uptake in malaria parasites. *Elife* **6**, doi:10.7554/eLife.23485 (2017).

39 Waller, R. F., Reed, M. B., Cowman, A. F. & McFadden, G. I. Protein trafficking to the plastid of Plasmodium falciparum is via the secretory pathway. *EMBO J* **19**, 1794-1802 (2000).

40 Tonkin, C. J., Struck, N. S., Mullin, K. A., Stimmler, L. M. & McFadden, G. I. Evidence for Golgi-independent transport from the early secretory pathway to the plastid in malaria parasites. *Mol Microbiol* **61**, 614-630, doi:10.1111/j.1365-2958.2006.05244.x (2006).

41 Heiny, S. R., Pautz, S., Recker, M. & Przyborski, J. M. Protein Traffic to the Plasmodium falciparum apicoplast: evidence for a sorting branch point at the Golgi. *Traffic* **15**, 1290-1304, doi:10.1111/tra.12226 (2014).

42 Fellows, J. D., Cipriano, M. J., Agrawal, S. & Striepen, B. A Plastid Protein That Evolved from Ubiquitin and Is Required for Apicoplast Protein Import in Toxoplasma gondii. *mBio* **8**, 1-18 (2017).

43 Sheiner, L. *et al.* A systematic screen to discover and analyze apicoplast proteins identifies a conserved and essential protein import factor. *PLoS Pathog* **7**, e1002392, doi:10.1371/journal.ppat.1002392 (2011).

44 Yeh, E. & DeRisi, J. L. Chemical rescue of malaria parasites lacking an apicoplast defines organelle function in blood-stage Plasmodium falciparum. *PLoS Biol* **9**, e1001138, doi:10.1371/journal.pbio.1001138 (2011).

45 Chen, A. L. *et al.* Novel components of the Toxoplasma inner membrane complex revealed by BioID. *MBio* **6**, e02357-02314, doi:10.1128/mBio.02357-14 (2015).

46 Painter, H. J. *et al.* Genome-wide real-time in vivo transcriptional dynamics during Plasmodium falciparum blood-stage development. *Nat Commun* **9**, 2656, doi:10.1038/s41467-018-04966-3 (2018).

47 Soderberg, O. *et al.* Direct observation of individual endogenous protein complexes in situ by proximity ligation. *Nat Methods* **3**, 995-1000, doi:10.1038/nmeth947 (2006).

48 Gullberg, M. *et al.* Cytokine detection by antibody-based proximity ligation. *Proc Natl Acad Sci U S A* **101**, 8420-8424, doi:10.1073/pnas.0400552101 (2004).

49 Fredriksson, S. *et al.* Protein detection using proximity-dependent DNA ligation assays. *Nature Biotechnology* **20**, 473-477 (2002).

50 Kulzer, S. *et al.* Plasmodium falciparum-encoded exported hsp70/hsp40 chaperone/co-chaperone complexes within the host erythrocyte. *Cell Microbiol* **14**, 1784-1795, doi:10.1111/j.1462-5822.2012.01840.x (2012).

51 Harbut, M. B. *et al.* Targeting the ERAD pathway via inhibition of signal peptide peptidase for antiparasitic therapeutic design. *Proc Natl Acad Sci U S A* **109**, 21486-21491 (2012).

52 Chaubey, S., Grover, M. & Tatu, U. Endoplasmic reticulum stress triggers gametocytogenesis in the malaria parasite. *J Biol Chem* **289**, 16662-16674, doi:10.1074/jbc.M114.551549 (2014).

53 Fennell, C. *et al.* PfeIK1, a eukaryotic initiation factor 2alpha kinase of the human malaria parasite Plasmodium falciparum, regulates stress-response to amino-acid starvation. *Malar J* **8**, 99, doi:10.1186/1475-2875-8-99 (2009).

54 Babbitt, S. E. *et al.* Plasmodium falciparum responds to amino acid starvation by entering into a hibernatory state. *Proc Natl Acad Sci U S A* **109**, E3278-3287 (2012).

55 Ward, P., Equinet, L., Packer, J. & Doerig, C. Protein kinases of the human malaria parasite Plasmodium falciparum: the kinome of a divergent eukaryote. *BMC Genomics* **5**, 79, doi:10.1186/1471-2164-5-79 (2004).

56 Tyson, J. R. & Stirling, C. J. LHS1 and SIL1 provide a lumenal function that is essential for protein translocation into the endoplasmic reticulum. *The EMBO Journal* **19**, 6440-6452 (2000).

57 Foth, B. J. *et al.* Dissecting Apicoplast Targeting in the Malaria Parasite Plasmodium falciparum. *Science* **299**, 705-708 (2003).

58 Ramya, T. N., Karmodiya, K., Surolia, A. & Surolia, N. 15-deoxyspergualin primarily targets the trafficking of apicoplast proteins in Plasmodium falciparum. *J Biol Chem* **282**, 6388-6397, doi:10.1074/jbc.M610251200 (2007).

59 Ramya, T. N., Surolia, N. & Surolia, A. 15-Deoxyspergualin modulates Plasmodium falciparum heat shock protein function. *Biochem Biophys Res Commun* **348**, 585-592, doi:10.1016/j.bbrc.2006.07.082 (2006).

60 Gruring, C. *et al.* Uncovering common principles in protein export of malaria parasites. *Cell Host Microbe* **12**, 717-729, doi:10.1016/j.chom.2012.09.010 (2012).

61 Boddey, J. A. *et al.* Export of malaria proteins requires co-translational processing of the PEXEL motif independent of phosphatidylinositol-3-phosphate binding. *Nat Commun* **7**, 10470, doi:10.1038/ncomms10470 (2016).

62 Marti, M., Good, R. T., Rug, M., Knuepfer, E. & Cowman, A. F. Targeting malaria virulence and remodeling proteins to the host erythrocyte. *Science* **306**, 1930-1933 (2004).

63 Hiller, N. L. *et al.* A Host-Targeting Signal in Virulence Proteins Reveals a Secretome in Malarial Infection. *Science* **306** (2015).

64 Heiny, S. R., Spork, S. & Przyborski, J. The apicoplast of the human malaria parasite P. falciparum. *Journal of Endocytobiosis and Cell Research* **23**, 91-95 (2012).

65 Batinovic, S. *et al.* An exported protein-interacting complex involved in the trafficking of virulence determinants in Plasmodium-infected erythrocytes. *Nat Commun* **8**, 16044, doi:10.1038/ncomms16044 (2017).

66 Wang, Y. *et al.* Involvement of oxygen-regulated protein 150 in AMP-activated protein kinase-mediated alleviation of lipid-induced endoplasmic reticulum stress. *J Biol Chem* **286**, 11119-11131, doi:10.1074/jbc.M110.203323 (2011).

67 Sanson, M. *et al.* Oxidized low-density lipoproteins trigger endoplasmic reticulum stress in vascular cells: prevention by oxygen-regulated protein 150 expression. *Circ Res* **104**, 328-336, doi:10.1161/CIRCRESAHA.108.183749 (2009).

68 Collins, C. R., Hackett, F., Atid, J., Tan, M. S. Y. & Blackman, M. J. The Plasmodium falciparum pseudoprotease SERA5 regulates the kinetics and efficiency of malaria parasite egress from host erythrocytes. *PLoS Pathog* **13**, e1006453, doi:10.1371/journal.ppat.1006453 (2017).

69 Ruecker, A. *et al.* Proteolytic activation of the essential parasitophorous vacuole cysteine protease SERA6 accompanies malaria parasite egress from its host erythrocyte. *J Biol Chem* **287**, 37949-37963, doi:10.1074/jbc.M112.400820 (2012).

70 Thomas, J. A. *et al.* A protease cascade regulates release of the human malaria parasite Plasmodium falciparum from host red blood cells. *Nat Microbiol* **3**, 447-455, doi:10.1038/s41564-018-0111-0 (2018).

71 Zhao, X. *et al.* PfRON3 is an erythrocyte-binding protein and a potential blood-stage vaccine candidate antigen. *Malaria Journal* **13**, 490, doi:10.1186/1475-2875-13-490 (2014).

72 Ling, I. T. *et al.* The Plasmodium falciparum clag9 gene encodes a rhoptry protein that is transferred to the host erythrocyte upon invasion. *Mol Microbiol* **52**, 107-118, doi:10.1111/j.1365-2958.2003.03969.x (2004).

73 Trenholme, K. R. *et al.* clag9: A cytoadherence gene in Plasmodium falciparum essential for binding of parasitized erythrocytes to CD36. *Proceedings of the National Academy of Sciences of the United States of America* **97**, 4029-4033, doi:10.1073/pnas.040561197 (2000).

74 Balu, B., Shoue, D. A., Fraser, M. J., Jr. & Adams, J. H. High-efficiency transformation of Plasmodium falciparum by the lepidopteran transposable element piggyBac. *Proc Natl Acad Sci U S A* **102**, 16391-16396, doi:10.1073/pnas.0504679102 (2005).

75 van Ooij, C. *et al.* The malaria secretome: from algorithms to essential function in blood stage infection. *PLoS Pathog* **4**, e1000084, doi:10.1371/journal.ppat.1000084 (2008).

76 Li, M. Z. & Elledge, S. J. Harnessing homologous recombination in vitro to generate recombinant DNA via SLIC. *Nat Methods* **4**, 251-256, doi:10.1038/nmeth1010 (2007).

77 Iwanaga, S., Kato, T., Kaneko, I. & Yuda, M. Centromere plasmid: a new genetic tool for the study of Plasmodium falciparum. *PLoS One* **7**, e33326, doi:10.1371/journal.pone.0033326 (2012).

78 Ganesan, S. M. *et al.* Yeast dihydroorotate dehydrogenase as a new selectable marker for Plasmodium falciparum transfection. *Mol Biochem Parasitol* **177**, 29-34, doi:10.1016/j.molbiopara.2011.01.004 (2011).

79 Witkowski, B. *et al.* Novel phenotypic assays for the detection of artemisinin-resistant Plasmodium falciparum malaria in Cambodia: in-vitro and ex-vivo drug-response studies. *The Lancet Infectious Diseases* **13**, 1043-1049, doi:10.1016/s1473-3099(13)70252-4 (2013).

Table 4.1: The gene ID, gene product, and unique peptides found in the PM1 anti-GFP IP/mass spectroscopy experiments. Data is shown only for proteins found in both replicates. The data has been filtered to remove proteins that do not contain a signal peptide or transmembrane domain.

Gene ID	Gene Product	Unique Peptides (replicate 1, replicate 2)
PF3D7_0930300	Merozoite surface protein 1	31, 69
PF3D7_0917900	Heat shock protein 70	23, 27
PF3D7_0707300	Rhoptry-associated membrane antigen	6, 7
PF3D7_1344200	Heat shock protein 110, putative	5, 3
PF3D7_1410400	Rhoptry-associated protein 1	5, 7
PF3D7_1364100	6-cysteine protein	2, 10
PF3D7_0508000	6-cysteine protein	2, 3
PF3D7_1335100	Merozoite surface protein 7	1, 10

Table 4.2: The gene ID, gene product, and unique peptides found for proteins identified in anti-GFP IP/Mass spectroscopy experiments for B2 and B11. Data is shown only for proteins found in both the B2 and B11 IP/mass spectroscopy experiments. The data has been filtered to remove proteins that do not contain a signal peptide or transmembrane domain.

Gene ID	Gene Product	Unique Peptides (B2, B11)
PF3D7_1344200	Heat shock protein 110, putative	132, 141
PF3D7_0917900	Heat shock protein 70	83, 80
PF3D7_0505700	Conserved Plasmodium membrane protein, unknown function	32, 31
PF3D7_1222300	Endoplasmin, putative	31, 26
PF3D7_0929400	High molecular weight rhoptry protein 2	28, 20
PF3D7_1252100	Rhoptry neck protein 3	22, 16
PF3D7_0827900	Protein disulfide isomerase	21, 16
PF3D7_1108700	Heat shock protein J2	14, 10
PF3D7_0207600	Serine repeat antigen 5	14, 7
PF3D7_0310400	Parasite-infected erythrocyte surface protein	13, 12
PF3D7_0905400	High molecular weight rhoptry protein 3	11, 4
PF3D7_0722200	Rhoptry-associated leucine zipper-like protein 1	11, 15
PF3D7_1116800	Heat shock protein 101	10, 14
PF3D7_0935800	Cytoadherence linked asexual protein 9	9, 8
PF3D7_1462300	GTP-binding protein, putative	9, 10
PF3D7_0629200	Dnaj protein, putative	8, 3
PF3D7_0501600	Rhoptry-associated protein 2	7, 5
PF3D7_0716300	Conserved Plasmodium protein, unknown function	6, 5
PF3D7_1129100	Parasitophorous vacuolar protein 1	5, 6

PF3D7_1134100	Protein disulfide isomerase	4, 3
PF3D7_1352500	Thioredoxin-related protein, putative	4, 4

Table 4.3: The gene ID, gene product, and number of unique peptides found using mass spectroscopy of 3D7 parasites incubated with biotin for 24 hours followed by IP with streptavidin coated magnetic beads. The data has been filtered to remove proteins that do not contain a signal peptide or transmembrane domain.

Gene ID	Gene product	Unique Peptides
PF3D7_0930300	Merozoite Surface Protein 1	56
PF3D7_1420700	Surface Protein P113	19
PF3D7_1364100	6-Cysteine Protein	14
PF3D7_0917900	Heat Shock Protein 70	11
PF3D7_1324900	L-Lactate Dehydrogenase	10
PF3D7_1222300	Endoplasmin, Putative	9
PF3D7_1121600	Exported Protein 1	8
PF3D7_1335100	Merozoite Surface Protein 7	8
PF3D7_1228600	Merozoite Surface Protein 9	8
PF3D7_0831400	Plasmodium Exported Protein, Unknown Function	7
PF3D7_1410400	Rhoptry-Associated Protein 1	7
PF3D7_1149400	Plasmodium Exported Protein, Unknown Function	6
PF3D7_1033200	Early Transcribed Membrane Protein 10.2	6
PF3D7_0707300	Rhoptry-Associated Membrane Antigen	5
PF3D7_0929400	High Molecular Weight Rhoptry Protein 2	5
PF3D7_1104400	Thioredoxin, Putative	5
PF3D7_1471100	Exported Protein 2	4
PF3D7_0606800	VFT Protein	4
PF3D7_1352500	Thioredoxin-Related Protein, Putative	4
PF3D7_0501600	Rhoptry-Associated Protein 2	4
PF3D7_1108700	Heat Shock Protein J2	4
PF3D7_1038000	Antigen UB05	3
PF3D7_1117300	Conserved Plasmodium Protein, Unknown Function	3
PF3D7_0501200	Parasite-Infected Erythrocyte Surface Protein	3
PF3D7_1464600	Serine/Threonine Protein Phosphatase UIS2, Putative	3

PF3D7_0725400	Conserved Plasmodium Protein, Unknown Function	2
PF3D7_0508000	6-cysteine protein	2
PF3D7_0905400	High Molecular Weight Rhoptry Protein 3	2
PF3D7_1306200	Conserved Plasmodium Protein, Unknown Function	2
PF3D7_1401200	Plasmodium Exported Protein, Unknown Function	2
PF3D7_1456800	V-Type H(+)-Translocating Pyrophosphatase, Putative	2
PF3D7_1344200	Heat Shock Protein 110, Putative	2
PF3D7_0913900	Arginine--Trna Ligase, Putative	1
PF3D7_1330200	Conserved Plasmodium Protein, Unknown Function	1
PF3D7_1411400	Plastid Replication-Repair Enzyme	1
PF3D7_0827900	Protein Disulfide Isomerase	1

Table 4.4: The gene ID, gene product, and number of unique peptides found using mass spectroscopy of PfGRP170-HA-BirA-KDEL parasites incubated with biotin for 24 hours followed by IP with streptavidin coated magnetic beads. Data is shown only for proteins found in both replicates. The data has been filtered to remove proteins that do not contain a signal peptide or transmembrane domain.

Gene ID	Gene Product	Unique Peptides (Replicate 1, Replicate 2)
PF3D7_1344200	Heat Shock Protein 110, Putative	55, 53
PF3D7_0917900	Heat Shock Protein 70	27, 30
PF3D7_0505700	Conserved Plasmodium Membrane Protein, Unknown Function	41, 39
PF3D7_1436300	Translocon Component PTEX150	34, 30
PF3D7_1462300	GTP-Binding Protein, Putative	26, 21
PF3D7_1024800	Exported Protein 3	23, 15
PF3D7_1252100	Rhoptry Neck Protein 3	23, 14
PF3D7_1108600	Endoplasmic Reticulum-Resident Calcium Binding Protein	18, 19
PF3D7_0310400	Parasite-Infected Erythrocyte Surface Protein	17, 13
PF3D7_1035300	Glutamate-Rich Protein GLURP	16, 14
PF3D7_1404900	Conserved Plasmodium Protein, Unknown Function	11, 13
PF3D7_0207600	Serine Repeat Antigen 5	11, 5
PF3D7_1123500	Conserved Plasmodium Protein, Unknown Function	10, 11
PF3D7_0302500	Cytoadherence Linked Asexual Protein 3.1	9, 5
PF3D7_0935800	Cytoadherence Linked Asexual Protein 9	8, 5
PF3D7_1226900	Parasitophorous Vacuolar Protein 2	8, 7
PF3D7_0918000	Glideosome-Associated Protein 50	6, 4
PF3D7_0103900	Parasite-Infected Erythrocyte Surface Protein	6, 6
PF3D7_1134100	Protein Disulfide Isomerase	6, 3
PF3D7_0314000	Hsp20-Like Chaperone, Putative	6, 3
PF3D7_1129100	Parasitophorous Vacuolar Protein 1	5, 3
PF3D7_1105600	Translocon Component PTEX88	5, 6
PF3D7_1116800	Heat Shock Protein 101	4, 9
PF3D7_1463900	EF-Hand Calcium-Binding Domain-Containing Protein, Putative	3, 2

PF3D7_1334800	Msp7-Like Protein	3, 2
PF3D7_1135400	Conserved Plasmodium Protein, Unknown Function	3, 3
PF3D7_1323500	Plasmepsin V	3, 4
PF3D7_0919100	Dnaj Protein, Putative	3, 3
PF3D7_0207500	Serine Repeat Antigen 6	2,1
PF3D7_1212000	Glutathione Peroxidase-Like Thioredoxin Peroxidase	2,2
PF3D7_0108700	Secreted Ookinete Protein, Putative	2,3
PF3D7_0625400	Conserved Plasmodium Protein, Unknown Function	2,1
PF3D7_0406200	Sexual Stage-Specific Protein Precursor	1,1
PF3D7_0103200	Nucleoside Transporter 4	1,2
PF3D7_0830400	CRA Domain-Containing Protein, Putative	1,2
PF3D7_1143200	Dnaj Protein, Putative	1,1
PF3D7_0811600	Conserved Plasmodium Protein, Unknown Function	1,1
PF3D7_1201000	Plasmodium Exported Protein (Phistb), Unknown Function	1,1

Table 4.5: Primers used in this study

Primer	Sequence
P1	cataaatatattatataactcgacgcggccgtcaaagttcatcactagcgtaatctggaacatcgtatggg
P2	cccatacgatgttccagattacgctagtgatgaactttgacggccgcgtcgagttatataatatatttatg
P3	CACTATAGAACTCGAGGATAAAGTTCTTGTTGTTTATGAAGAACAAAAAG ATGGAGCTGG
P4	CTGCACCTGGCCTAGGTTGATCTGATGCTCCATCATTTTTATTTTGCTCA TCGTTGG
P5	AAAAACTCACGCTAGCATGAGACCTCGTTTTTTTTTGTTCCTACTTTTTAT AATATATATATATAATAG
P6	GACGTCGTACGGGTACCTAGGTTGATCTGATGCTCCATCATTTTTATTTT GCTCATCGTTG
P7	GGAGCATCAGATCAACCTAGGTACCCGTACGACGTCCCGGACTACGCT GGCTATCCCTATG
P8	GAACAATAATAGATCTttataattcatctttCTTCTCTGCGCTTCTCAGGGAGATTT CTCCGCCCATCCAG
P9	TCTTCTCCTTTACTGACGTCACCTCTTTTATGATCTACTACATAATCATAT GAATAATAC
P10	TAAAAGAGGTGACGTCAGTAAAGGAGAAGAATTATTTACTGGAGTTGTC CCAATTCTTG
P11	GAACAATAATAGATCTTTATTTGTATAGTTCATCCATGCCATGTGTAATCC CAGCAGCTG
P12	ATGAGACCTCGTTTTTTTTTGTTCCTACTTTTTATAATATATATATATAATA

	GTTTAAG
P13	gtgcccattaacatcaccatctaattcaacaagaattggg

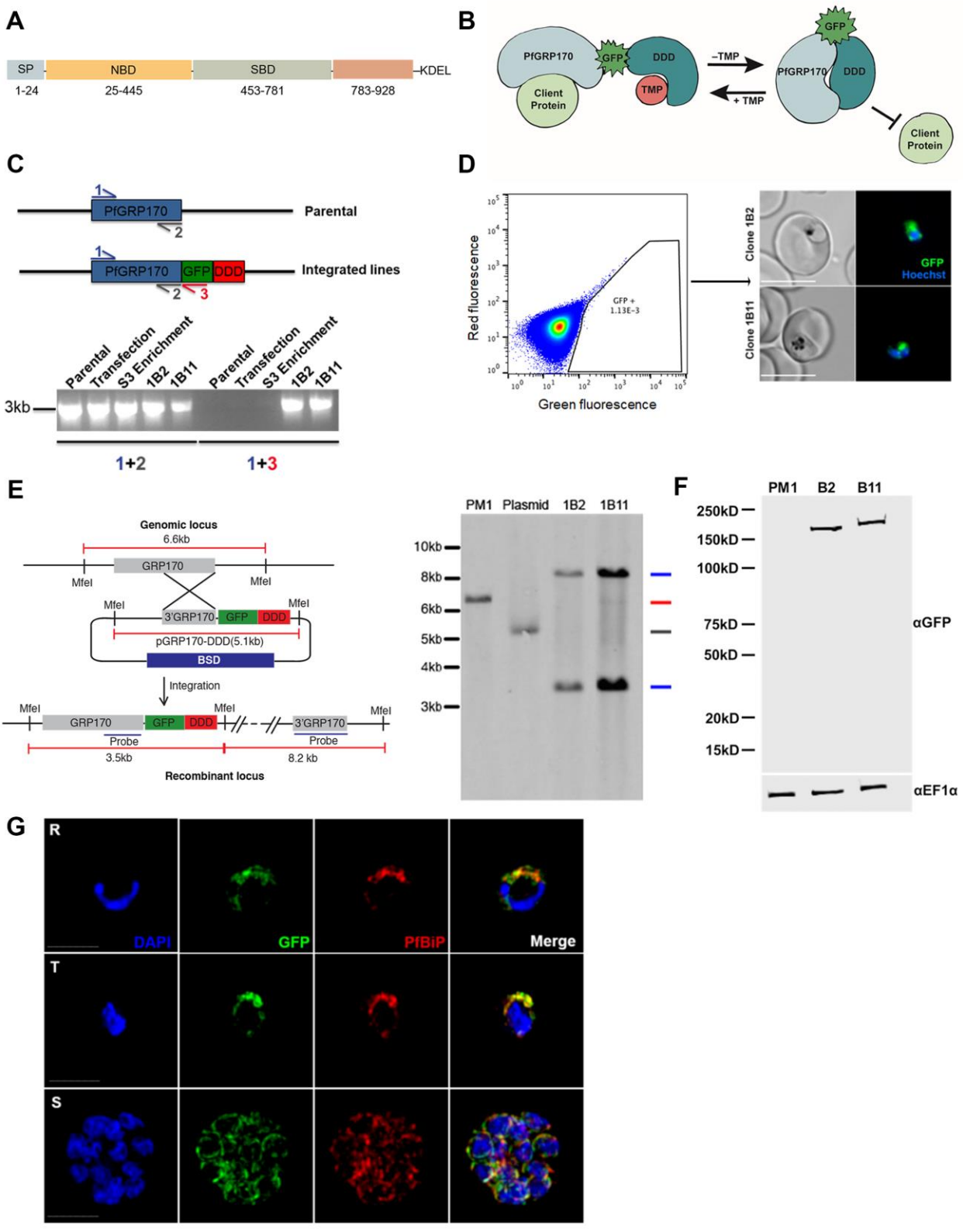
A
SP
NBD
SBD
KDEL
1-24
25-445
453-781
783-928
B
PfGRP170
GFP
DDD
Client Protein
TMP
–TMP
+ TMP
C
PfGRP170
Parental
Integrated lines
GFP
DDD
3kb
Parental
Transfection
S3 Enrichment
1B2
1B11
1+2
1+3
D
Red fluorescence
Green fluorescence
GFP +
1.13E-3
Clone 1B2
Clone 1B11
GFP
Hoechst
E
Genomic locus
6.6kb
GRP170
MfeI
3'GRP170
pGRP170-DDD(5.1kb)
BSD
Integration
Probe
3.5kb
8.2 kb
Recombinant locus
PM1
Plasmid
1B2
1B11
10kb
8kb
6kb
5kb
4kb
3kb
F
PM1
B2
B11
250kD
150kD
100kD
75kD
50kD
20kD
15kD
αGFP
αEF1α
G
R
T
S
DAPI
GFP
PfBiP
Merge

Figure 4.1: Generation of PfGRP170-GFP-DDD Parasites

(A). Schematic detailing the putative domain boundaries of PfGRP170 (PF3D7_1344200) based on the yeast homolog, Lhs1: Signal Peptide (SP), Nucleotide Binding Domain (NBD), Substrate Binding Domain (SBD), Extended C-terminus region (783-928), and an ER retention signal (KDEL).

(B). Schematic diagram demonstrating the conditional inhibition of PfGRP170. Conditional inhibition of PfGRP170 is achieved by the removal of Trimethoprim (TMP), which results in the unfolding of the destabilization (DDD). The chaperone recognizes and binds the unfolded DDD and is inhibited from interacting with client proteins.

(C). **(Top)** Schematic diagram of the PfGRP170 locus in the parental line (PM1KO) and the modified locus where PfGRP170 is endogenously tagged with GFP and DDD. Primers used for integration test and control PCR are indicated by arrows. The relative positions of Primer 1 (blue) and Primer 2 (Gray) on the PfGRP170 locus are shown. These two primers will amplify PfGRP170 in parental and transfected parasites. Primer 3 (Red) recognizes the GFP sequence. Primers 1 and 3 were used to screen for proper integration into the PfGRP170 locus. **(Bottom)** PCR integration test and control PCRs on gDNA isolated from the PM1KO (parental), the original transfection of the pPfGRP170-GFP-DDD plasmid after three rounds of Blasticidin (BSD) drug selection (Transfection), the PfGRP170-GFP-DDD transfected parasite lines after two rounds of enrichment for GFP positive cells (S3 enrichment), and PfGRP170-GFP-DDD clones 1B2 and 1B11 after MoFlo XDP flow sorting. The first 5 lanes are control PCRs using primers to amplify the PfGRP170 locus. The last 5 lanes are integration PCRs that only amplify if the GFP-DDD has been integrated into the genome.

(D). (Left) MoFlo XDP flow data demonstrating the percentage of GFP positive parasites in transfected PfGRP170-GFP-DDD parasites following three rounds of drug selection with Blasticidin (BSD) and two rounds of enrichment with an S3 cell sorter. Using the MoFlo, single GFP positive cells were cloned into a 96 well plate. Two clones, 1B2 and 1B11, were isolated using this method. **(Right)** 1B2 and 1B11 parasites, were observed using live fluorescence microscopy.

(E). Southern blot analysis of PfGRP170-GFP-DDD clones 1B2 and 1B11, PM1KO (parental control), and the PfGRP170-GDB plasmid is shown. Mfe1 restriction sites, the probe used to detect the DNA fragments, and the expected sizes are denoted in the schematic **(Left).** Expected sizes for PfGRP170-GFP-DDD clones (blue), parental DNA (red), and plasmid (gray) were observed **(Right).** Parental and plasmid bands were absent from the PfGRP170-GFP-DDD clonal cell lines.

(F). Western blot analysis of protein lysates from PM1KO (parental) and PfGRP170-GFP-DDD clonal cell lines 1B2 and 1B11 is shown. Lysates were probed with anti-GFP to visualize PfGRP170 and anti-PfEF1α as a loading control.

(G). Asynchronous PfGRP170-GFP-DDD parasites were paraformaldehyde fixed and stained with anti-GFP, anti-PfGRP78 (BiP), and DAPI to visualize the nucleus. Images were taken as a Z-stack using super resolution microscopy and SIM processing was performed on the Z-stacks. Images are displayed as a maximum intensity projection. The scale bar is 2μm.

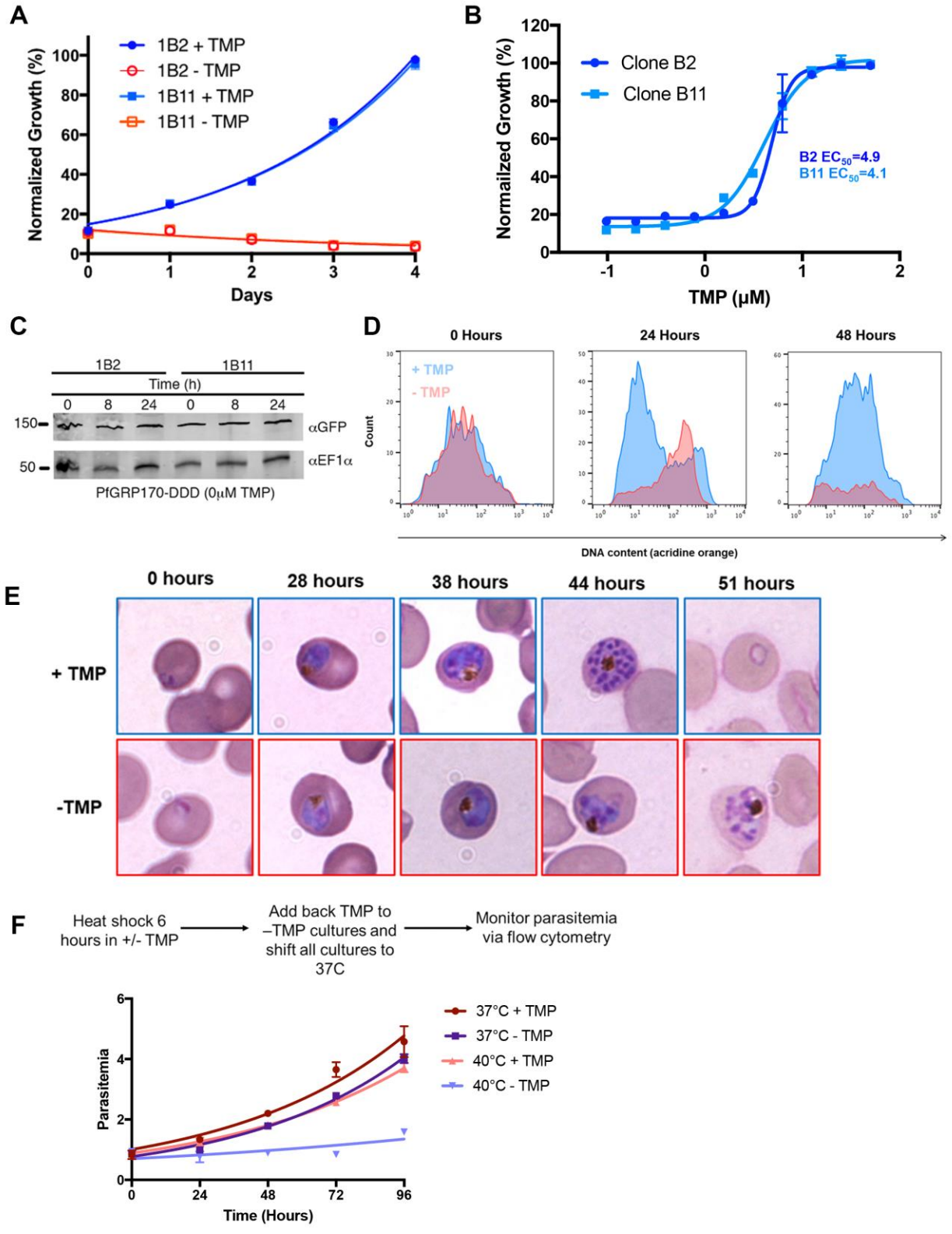
A
1B2 + TMP
1B2 - TMP
1B11 + TMP
1B11 - TMP
Normalized Growth (%)
Days
B
Clone B2
Clone B11
B2 EC50=4.9
B11 EC50=4.1
Normalized Growth (%)
TMP (μM)
C
1B2
1B11
Time (h)
0 8 24 0 8 24
150
50
αGFP
αEF1α
PfGRP170-DDD (0μM TMP)
D
0 Hours
24 Hours
48 Hours
+ TMP
- TMP
Count
DNA content (acridine orange)
E
0 hours
28 hours
38 hours
44 hours
51 hours
+ TMP
-TMP
F
Heat shock 6 hours in +/- TMP
Add back TMP to –TMP cultures and shift all cultures to 37C
Monitor parasitemia via flow cytometry
37°C + TMP
37°C - TMP
40°C + TMP
40°C - TMP
Parasitemia
Time (Hours)

Figure 4.2: PfGRP170 is Essential and Required for Surviving a Heat Shock

(A). Parasitemia of asynchronous PfGRP170-GFP-DDD clonal cell lines 1B2 and 1B11, in the presence or absence of 20μM TMP, was observed using flow cytometry over 4 days. One hundred percent growth is defined as the highest parasitemia on the final day of the experiment. Data was fit to an exponential growth curve equation. Each data point is representative of the mean of 3 replicates ± S.E.M.

(B). Asynchronous PfGRP170-GFP-DDD clonal cell lines 1B2 and 1B11 were grown in a range of TMP concentrations for 48 hours. After 48 hours, parasitemia was observed using flow cytometry. One hundred percent growth is defined as the highest parasitemia on the final day of the experiment. Data was fit to a dose-response equation. Each data point is representative of the mean of 3 replicates ± S.E.M.

(C). Western blot analysis of PfGRP170-GFP-DDD lysates at 0, 8, and 24 hours following the removal of TMP is shown. Lysates were probed with anti-GFP to visualize PfGRP170 and anti-PfEF1α as a loading control.

(D). Flow cytometric analysis of asynchronous PfGRP170-GFP-DDD parasites, incubated with (Blue) and without TMP (Red), and stained with acridine orange. Data at 0, 24, and 48 hours after the removal of TMP are shown.

(E). TMP was removed from tightly synchronized PfGRP170-GFP-DDD ring stage parasites and their growth and development through the life cycle was monitored by Hema 3 stained thin blood smears. Representative images are shown from the parasite culture at the designated times.

(F). PfGRP170-GFP-DDD clones 1B2 and 1B11 were incubated with and without TMP for 6 hours at either 37°C or 40°C. Following the incubation, TMP was added back to all

cultures and parasites were shifted back to 37°C. Parasitemia was then observed over 96 hours via flow cytometry. Data was fit to an exponential growth curve equation. Each data point shows the mean of 3 replicates ± S.E.M.

A

Protein	PATS Score	PlasmoAP Score
PfGRP170	Very Likely (0.943/1)	Very likely (5/5 tests positive)

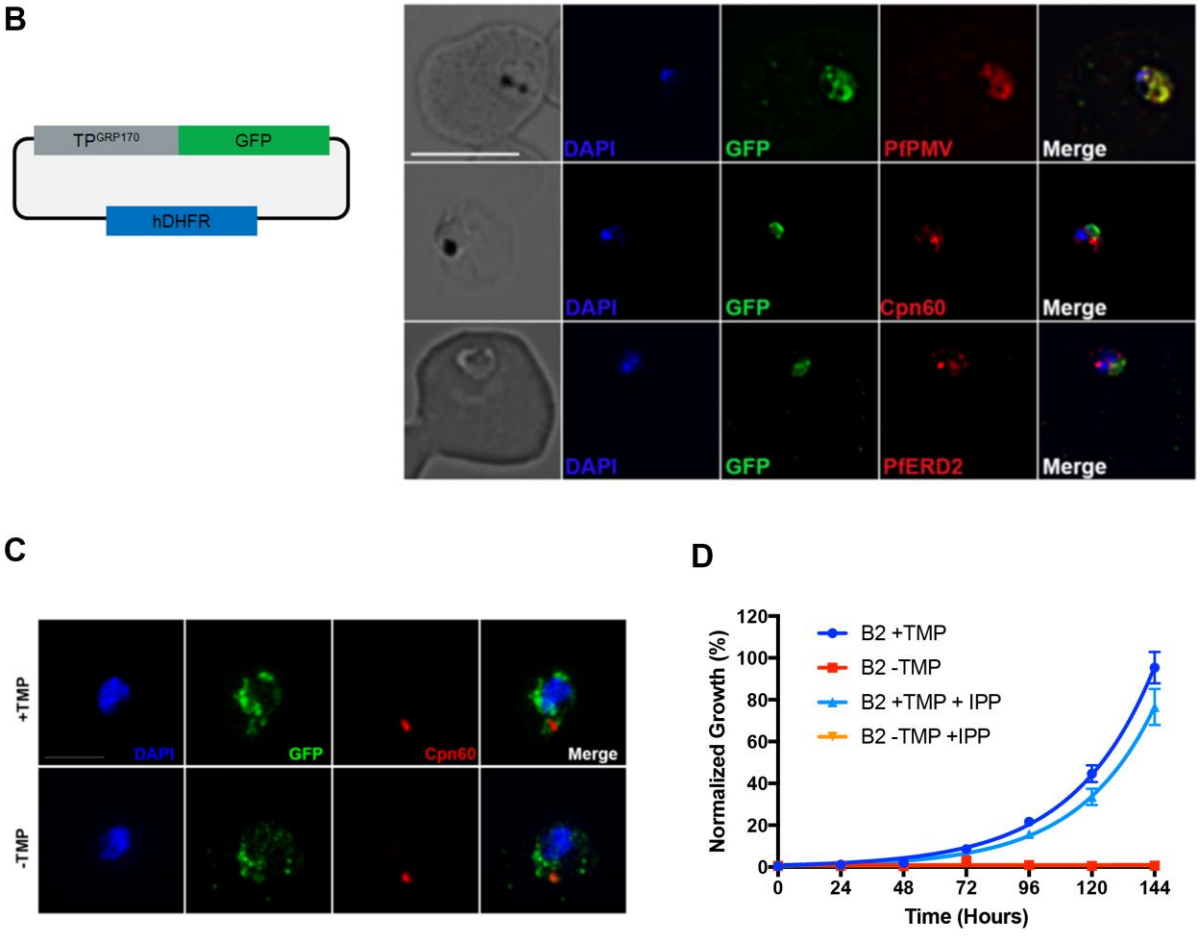

Figure 4.3: Putative PfGRP170 apicoplast transit peptide localizes to the ER and conditional inhibition of PfGRP170 does not affect trafficking of apicoplast proteins.

(A). Analysis of PfGRP170's protein sequence using two apicoplast transit peptide prediction programs: Prediction of Apicoplast-Targeted Sequences (PATS) and PlasmoAP.

(B). PfGRP170's putative apicoplast transit peptide was fused to GFP and transfected into 3D7 parasites. Parasites were fixed with acetone and stained with DAPI, anti-GFP (to label the PfGRP170 putative transit peptide) and either anti-PfPMV (ER), anti-PfERD2 (Golgi), or anti-Cpn60 (Apicoplast) to determine subcellular localization. The images were taken with Delta Vision II, deconvolved, and are displayed as a maximum intensity projection. The scale bar is 5µm.

(C). Synchronized ring stage PfGRP170 parasites were incubated for 24 hours with and without TMP. Following the incubation, the parasites were fixed with paraformaldehyde and stained with DAPI, anti-GFP (PfGRP170) and anti-Cpn60 (Apicoplast). Images were taken as a Z-stack using super resolution microscopy and SIM processing was performed on the Z-stacks. Images are displayed as a maximum intensity projection. The scale bar is 2µm.

(D). Asynchronous PfGRP170-GFP-DDD parasites were incubated with and without TMP and in the presence or absence of 200µM IPP. Parasitemia was monitored using flow cytometry for 144 hours. One hundred percent growth is defined as the highest parasitemia on the final day of the experiment. Data was fit to an exponential growth curve equation. Each data point is representative of the mean of 3 replicates ± S.E.M.

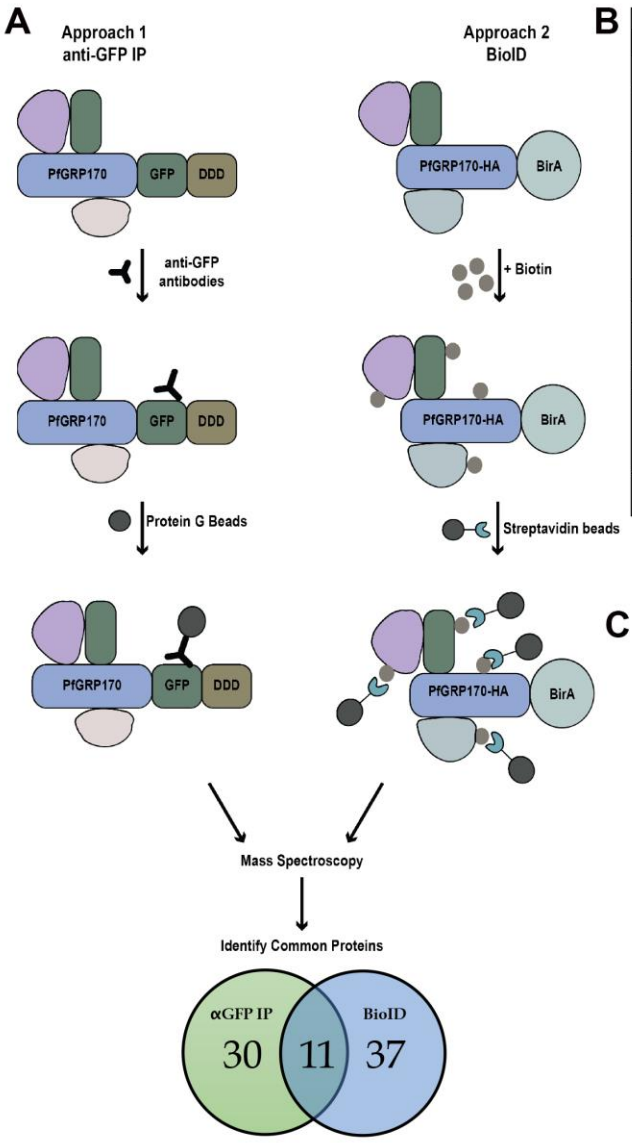

B

			Unique Peptides	
Gene ID	Gene Product	Localization	IP (B2, B11)	BioID (1, 2)
PF3D7_0917900	*Heat shock protein 70	ER	83, 80	27, 30
PF3D7_0310400	Parasite-infected erythrocyte surface protein	ER?	13, 12	17, 13
PF3D7_1134100	Protein disulfide isomerase	ER	4, 3	6, 3
PF3D7_1116800	Heat shock protein 101	Dense Granule	10, 14	4, 9
PF3D7_1129100	Parasitophorous vacuolar protein 1	Dense Granule	5, 6	5, 3
PF3D7_0207600	Serine repeat antigen 5	PV	14, 7	11, 5
PF3D7_0207500	Serine repeat antigen 6	PV	2, 3	2, 1
PF3D7_0935800	Cytoadherence linked asexual protein 9	Rhoptry	9, 8	8, 5
PF3D7_1252100	Rhoptry neck protein 3	Rhoptry	22, 16	23, 14
PF3D7_0505700	Conserved Plasmodium membrane protein, unknown function	Unknown	32, 31	41, 39
PF3D7_1462300	GTP-binding protein, putative	Unknown	9, 10	26, 21

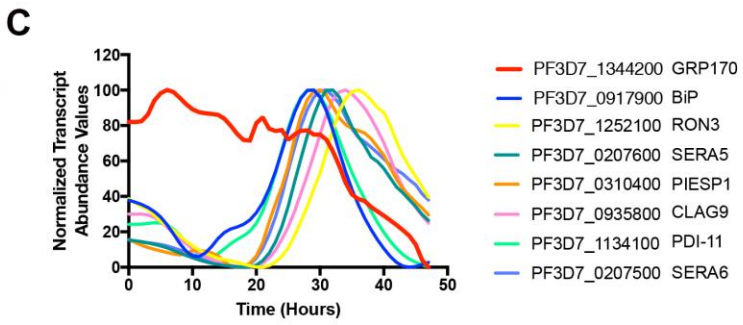

Figure 4.4: PfGRP170 interacting partners

(A). Schematic diagram illustrating the two independent methods were taken to identify potential interacting partners of PfGRP170: anti-GFP Immunoprecipitation (IP) using lysates from PfGRP170-GFP-DDD parasites and streptavidin IP of PfGRP170-BirA parasites incubated with biotin for 24 hours followed by mass spectroscopy. The proteins identified from each IP were filtered to include only proteins that had a signal

peptide and/or transmembrane domain using PlasmoDB. Proteins found in the respective control IP's (excluding PfBiP) were also removed from the analysis (data in Table 4.1 and 4.4).

(B). A table including the 11 proteins common proteins identified using two independent mass spectroscopy approaches (See Figure 4A). The PlasmoDB gene ID, gene product, and number of unique peptides identified for each protein in each independent experiment are listed.

(C). The relative transcript abundance of proteins, with peak expression around the time the PfGRP170-GFP-DDD parasites die, are plotted using genome-wide real-time transcript data previously published [46].

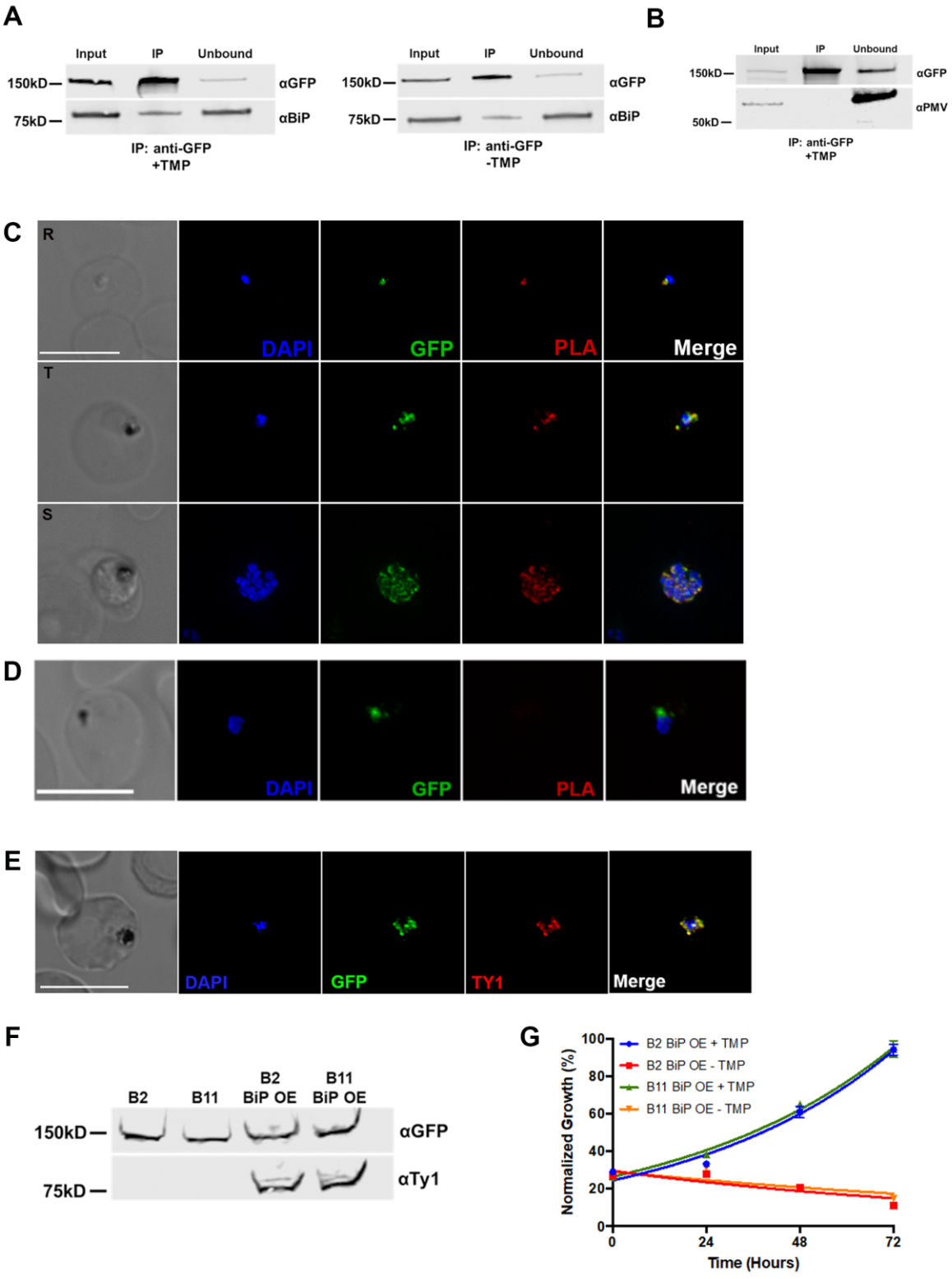
A
Input
IP
Unbound
150kD
75kD
αGFP
αBiP
IP: anti-GFP
+TMP
IP: anti-GFP
-TMP
B
αPMV
50kD
C
R
T
S
DAPI
GFP
PLA
Merge
D
E
TY1
F
B2
B11
B2
BiP OE
B11
BiP OE
αTy1
G
B2 BiP OE + TMP
B2 BiP OE - TMP
B11 BiP OE + TMP
B11 BiP OE - TMP
Normalized Growth (%)
Time (Hours)

Figure 4.5: PfGRP170 Interacts with BiP

(A) Synchronized ring stage PfGRP170-GFP-DDD parasites were incubated with and without TMP for 24 hours. Following this incubation, an anti-GFP IP was performed and input, IP, and unbound fractions were analyzed using a western blot. The blot was probed using anti-GFP and anti-BiP.

(B). Western blot analysis of an anti-GFP IP performed on asynchronous PfGRP170-GFP-DDD parasites. Input, IP, and unbound fractions are shown. The blot was probed using anti-GFP and anti-PfPMV.

(C). *In vivo* interaction of PfGRP170 and BiP. PfGRP170-GFP-DDD parasites were paraformaldehyde fixed and stained with anti-GFP and anti-BiP. A Proximity Ligation Assay (PLA) was then performed. The scale bar is 5µm. A negative control using anti-GFP and anti-PfPMV is shown in **(D).**

(E). Asynchronous PfGRP170-GFP-DDD parasites overexpressing PfBiP-Ty1were paraformaldehyde fixed and stained with anti-GFP (PfGRP170), anti-Ty1 (PfBiP-Ty1-KDEL), and DAPI to visualize the nucleus. The images were taken with Delta Vision II, deconvolved, and are displayed as a maximum intensity projection. The scale bar is 5µm.

(F). Western blot analysis of protein lysates from parental 1B2 and 1B11 parasites as well as 1B2 and 1B11 parasites overexpressing the PfBiP-Ty1fusion protein. Lysates were probed with anti-GFP to visualize PfGRP170 and anti-Ty1 to visualize PfBiP-Ty1-KDEL.

(G). Parasitemia of asynchronous PfGRP170-GFP-DDD parasites expressing PfBiP-Ty1-KDEL, in the presence or absence of 20µM TMP, was observed using flow

cytometry over 3 days. One hundred percent growth is defined as the highest parasitemia on the final day of the experiment. Data was fit to an exponential growth curve equation. Each data point is representative of the mean of 3 replicates ± S.E.M.

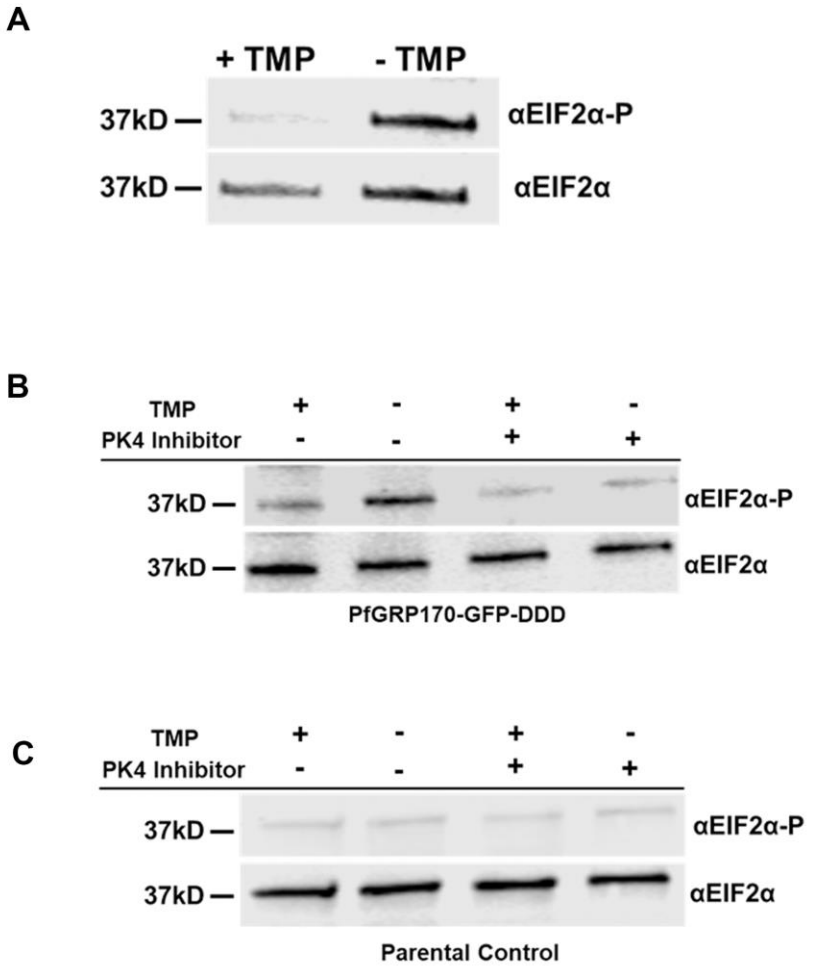

Figure 4.6: Loss of PfGRP170 function activates the PK4 stress pathway

(A). Synchronized ring stage PfGRP170-GFP-DDD parasites were incubated with and without TMP for 24 hours. Protein was isolated from these samples and analyzed via western blot, probing for anti-eIF2α and anti-Phospho-eIF2α.

(B). Synchronized ring stage PfGRP170-GFP-DDD parasites were incubated with and without TMP and in the presence and absence of 2μM PK4 inhibitor GSK2606414 for 24 hours. Protein was isolated from these samples and analyzed via western blot by

probing for anti-eIF2a and anti-Phospho-eIF2α. An identical experiment using PM1 (parental cell line) parasites was also conducted an is shown in Figure 6C.

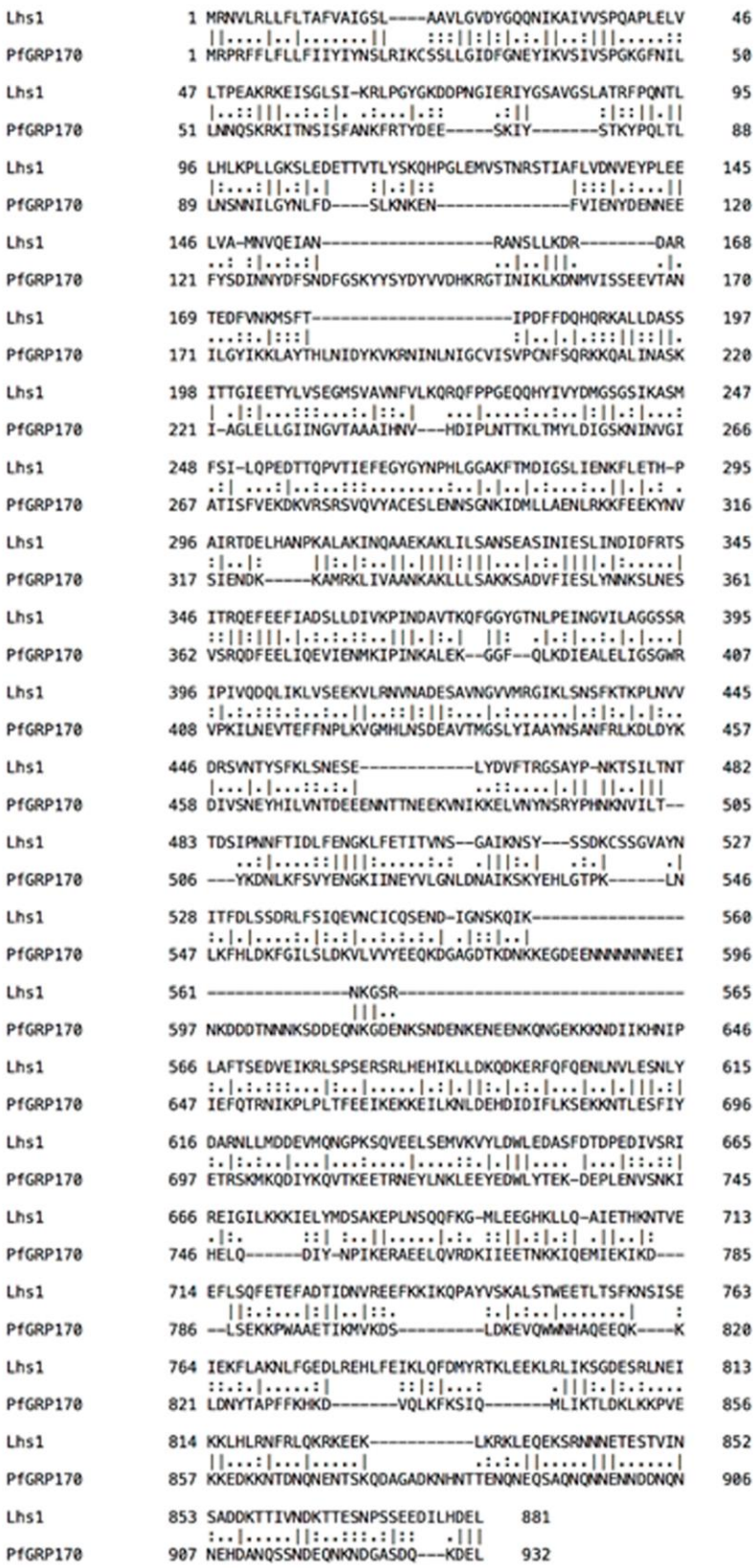
Lhs1 1 MRNVLRLLFLTAFVAIGSL----AAVLGVDYGQQNIKAIVVSPQAPLELV 46
PfGRP170 1 MRPRFFLFLLFIIYIYNSLRIKCSSLLGIDFGNEYIKVSIVSPGKGFNIL 50
Lhs1 47 LTPEAKRKEISGLSI-KRLPGYGKDDPNGIERIYGSAVGSLATRFPQNTL 95
PfGRP170 51 LNNQSKRKITNSISFANKFRTYDEE-----SKIY-------STKYPQLTL 88
Lhs1 96 LHLKPLLGKSLEDETTVTLYSKQHPGLEMVSTNRSTIAFLVDNVEYPLEE 145
PfGRP170 89 LNSNNILGYNLFD----SLKNKEN--------------FVIENYDENNEE 120
Lhs1 146 LVA-MNVQEIAN-----------------RANSLLKDR--------DAR 168
PfGRP170 121 FYSDINNYDFSNDFGSKYYSYDYVVDHKRGTINIKLKDNMVISSEEVTAN 170
Lhs1 169 TEDFVNKMSFT--------------------IPDFFDQHQRKALLDASS 197
PfGRP170 171 ILGYIKKLAYTHLNIDYKVKRNINLNIGCVISVPCNFSQRKKQALINASK 220
Lhs1 198 ITTGIEETYLVSEGMSVAVNFVLKQRQFPPGEQQHYIVYDMGSGSIKASM 247
PfGRP170 221 I-AGLELLGIINGVTAAAIHNV---HDIPLNTTKLTMYLDIGSKNINVGI 266
Lhs1 248 FSI-LQPEDTTQPVTIEFEGYGYNPHLGGAKFTMDIGSLIENKFLETH-P 295
PfGRP170 267 ATISFVEKDKVRSRSVQVYACESLENNSGNKIDMLLAENLRKKFEEKYNV 316
Lhs1 296 AIRTDELHANPKALAKINQAAEKAKLILSANSEASINIESLINDIDFRTS 345
PfGRP170 317 SIENDK-----KAMRKLIVAANKAKLLLSAKKSADVFIESLYNNKSLNES 361
Lhs1 346 ITRQEFEEFIADSLLDIVKPINDAVTKQFGGYGTNLPEINGVILAGGSSR 395
PfGRP170 362 VSRQDFEELIQEVIENMKIPINKALEK--GGF--QLKDIEALELIGSGWR 407
Lhs1 396 IPIVQDQLIKLVSEEKVLRNVNADESAVNGVVMRGIKLSNSFKTKPLNVV 445
PfGRP170 408 VPKILNEVTEFFNPLKVGMHLNSDEAVTMGSLYIAAYNSANFRLKDLDYK 457
Lhs1 446 DRSVNTYSFKLSNESE-----------LYDVFTRGSAYP-NKTSILTNT 482
PfGRP170 458 DIVSNEYHILVNTDEEENNTTNEEKVNIKKELVNYNSRYPHNKNVILT-- 505
Lhs1 483 TDSIPNNFTIDLFENGKLFETITVNS--GAIKNSY---SSDKCSSGVAYN 527
PfGRP170 506 ---YKDNLKFSVYENGKIINEYVLGNLDNAIKSKYEHLGTPK------LN 546
Lhs1 528 ITFDLSSDRLFSIQEVNCICQSEND-IGNSKQIK---------------- 560
PfGRP170 547 LKFHLDKFGILSLDKVLVVYEEQKDGAGDTKDNKKEGDEENNNNNNEEI 596
Lhs1 561 ---------------NKGSR---------------------------- 565
PfGRP170 597 NKDDDTNNNKSDDEQNKGDENKSNDENKENEENKQNGEKKKNDIIKHNIP 646
Lhs1 566 LAFTSEDVEIKRLSPSERSRLHEHIKLLDKQDKERFQFQENLNVLESNLY 615
PfGRP170 647 IEFQTRNIKPLPLTFEEIKEKKEILKNLDEHDIDIFLKSEKKNTLESFIY 696
Lhs1 616 DARNLLMDDEVMQNGPKSQVEELSEMVKVYLDWLEDASFDTDPEDIVSRI 665
PfGRP170 697 ETRSKMKQDIYKQVTKEETRNEYLNKLEEYEDWLYTEK-DEPLENVSNKI 745
Lhs1 666 REIGILKKKIELYMDSAKEPLNSQQFKG-MLEEGHKLLQ-AIETHKNTVE 713
PfGRP170 746 HELQ------DIY-NPIKERAEELQVRDKIIEETNKKIQEMIEKIKD--- 785
Lhs1 714 EFLSQFETEFADTIDNVREEFKKIKQPAYVSKALSTWEETLTSFKNSISE 763
PfGRP170 786 --LSEKKPWAAETIKMVKDS---------LDKEVQWWNHAQEEQK----K 820
Lhs1 764 IEKFLAKNLFGEDLREHLFEIKLQFDMYRTKLEEKLRLIKSGDESRLNEI 813
PfGRP170 821 LDNYTAPFFKHKD-------VQLKFKSIQ-------MLIKTLDKLKKPVE 856
Lhs1 814 KKLHLRNFRLQKRKEEK-----------LKRKLEQEKSRNNNETESTVIN 852
PfGRP170 857 KKEDKKNTDNQNENTSKQDAGADKNHNTTENQNEQSAQNQNNENNDDNQN 906
Lhs1 853 SADDKTTIVNDKTTESNPSSEEDILHDEL 881
PfGRP170 907 NEHDANQSSNDEQNKNDGASDQ---KDEL 932

Supplemental Figure 4.1: Sequence Alignment of Lhs1 and PfGRP170

Sequence alignment of *S. cerevisiae* GRP170 (Lhs1) and PfGRP170. The alignment was performed using EMBOSS Needle which creates a global alignment of two sequences using the Needleman-Wunsch algorithm. The software used to do this is provided by the European Bioinformatics Institute, which is a part of the European Molecular Biology Laboratory (EMBL). Identical residues are indicated by a “l”, strongly similar residues are indicated by a “:”, and weakly similar residues are indicated by a “.”.

Organism	% Identity	% Similarity
P. vivax	62.6	78.6
P. malariae	65.5	81.7
P. ovale	61.7	77.5
P. berghei	59.6	77.5
T. gondii	26.2	45.5
S. cerevisiae	22.4	40.1
H. sapiens	23.6	42.1

Supplemental Figure 4.2: Sequence homology of PfGRP170

Sequence identify and homology of *P. falciparum* GRP170 compared to GRP170 homologs from other *Plasmodium* Species (*P. vivax (*PVX_083105), *P. malariae (*PmUG01_12020700), *P. ovale (*PocGH01_12018900), and *P. berghei (*PBANKA_1357200)), *T. gondii* GRP170 (TGGT1_226830), yeast GRP170 (*S. cerevisiae*), and human GRP170 (*H. sapiens*). Alignments to determine sequence identify and homology were performed using EMBOSS Needle which creates a global alignment of two sequences using the Needleman-Wunsch algorithm. The software to do this is provided by the European Bioinformatics Institute, which is a part of the European Molecular Biology Laboratory (EMBL).

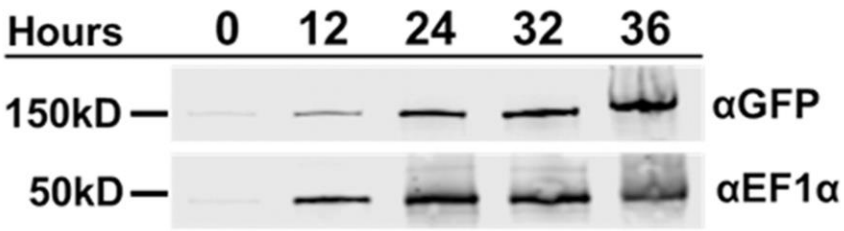

Supplemental Figure 4.3: PfGRP170 is Expressed Throughout the Asexual Life Cycle

TMP was removed from tightly synchronized ring stage PfGRP170-GFP-DDD parasites and protein was isolated throughout the asexual life cycle. Lysates were separated on a Western blot and probed with anti-GFP to visualize PfGRP170-GFP-DDD and anti-PfEF1α as a loading control.

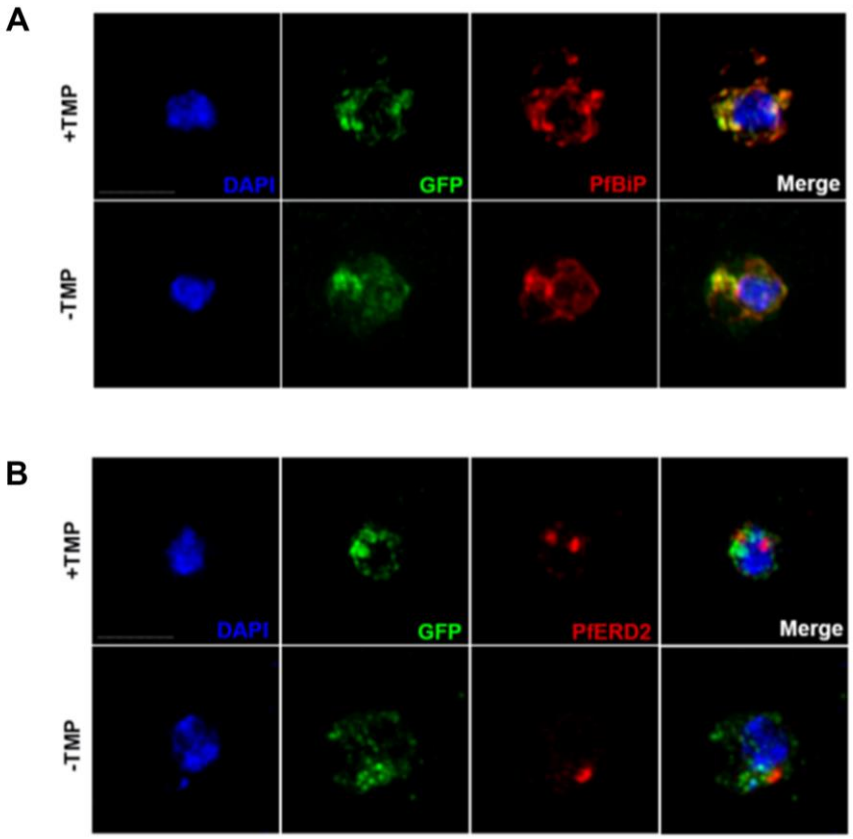

Supplemental Figure 4.4: Conditional mutants of PfGRP170 localize to the ER

Synchronized PfGRP170-GFP-DDD ring stage parasites were incubated with and without TMP for 24 hours. Parasites were then fixed with paraformaldehyde and stained with either DAPI, anti-GFP, and anti-BiP (ER) **(A)** or DAPI, anti-GFP, and anti-ERD2 (Golgi) **(B).** Images were taken as a Z-stack using super resolution microscopy and SIM processing was performed on the Z-stacks. Images are displayed as a maximum intensity projection. The scale bar is 2µm.

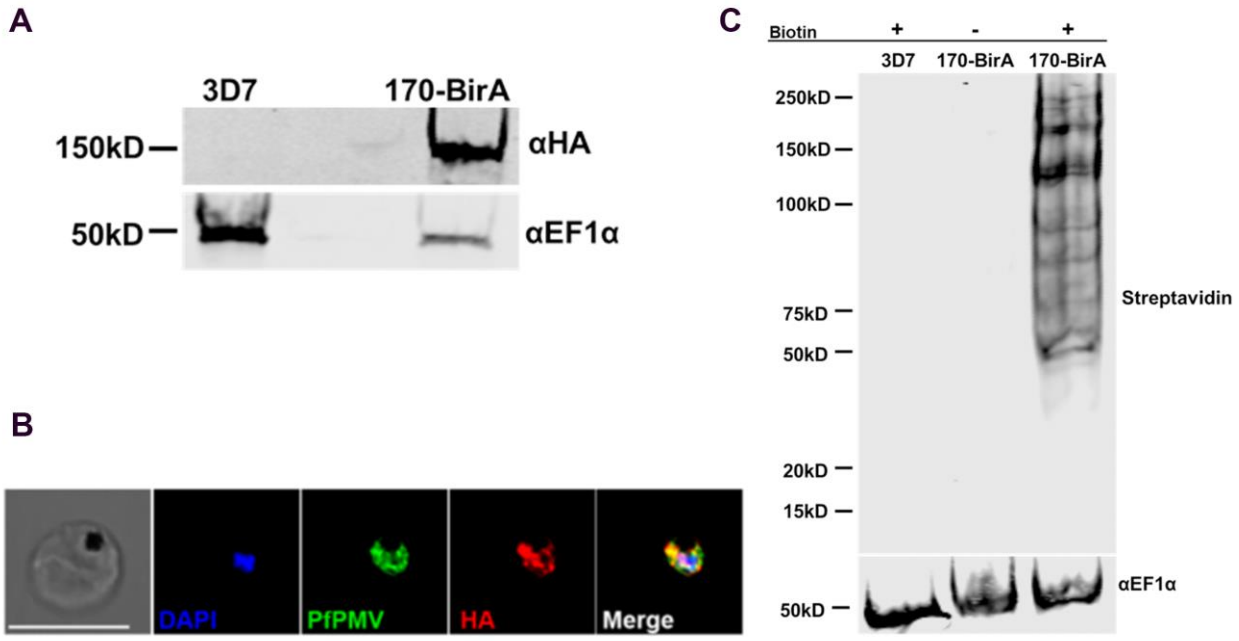

Supplemental Figure 4.5: PfGRP170-BirA localizes to the parasite ER and biotinylates proteins.

(A). Western blot of 3D7 (parental) and PfGRP170-BirA expressing parasites probed with anti-HA and anti-EF1α.

(B). Paraformaldehyde fixed PfGRP170-BirA parasites stained with anti-HA (PfGRP170-BirA), anti-PfPMV (ER), and DAPI. The images were taken with Delta Vision II, deconvolved and are displayed as a maximum intensity projection. The scale bar is 5μm.

(C). A western blot analysis of 3D7 (parental) and PfGRP170-BirA parasites following a 24-hour incubation with biotin is shown. A fluorophore-labeled streptavidin secondary antibody was used to visualize biotinylated proteins. A control with PfGRP170-BirA parasites incubated without biotin is also shown. Anti-EF1α is used as a loading control.

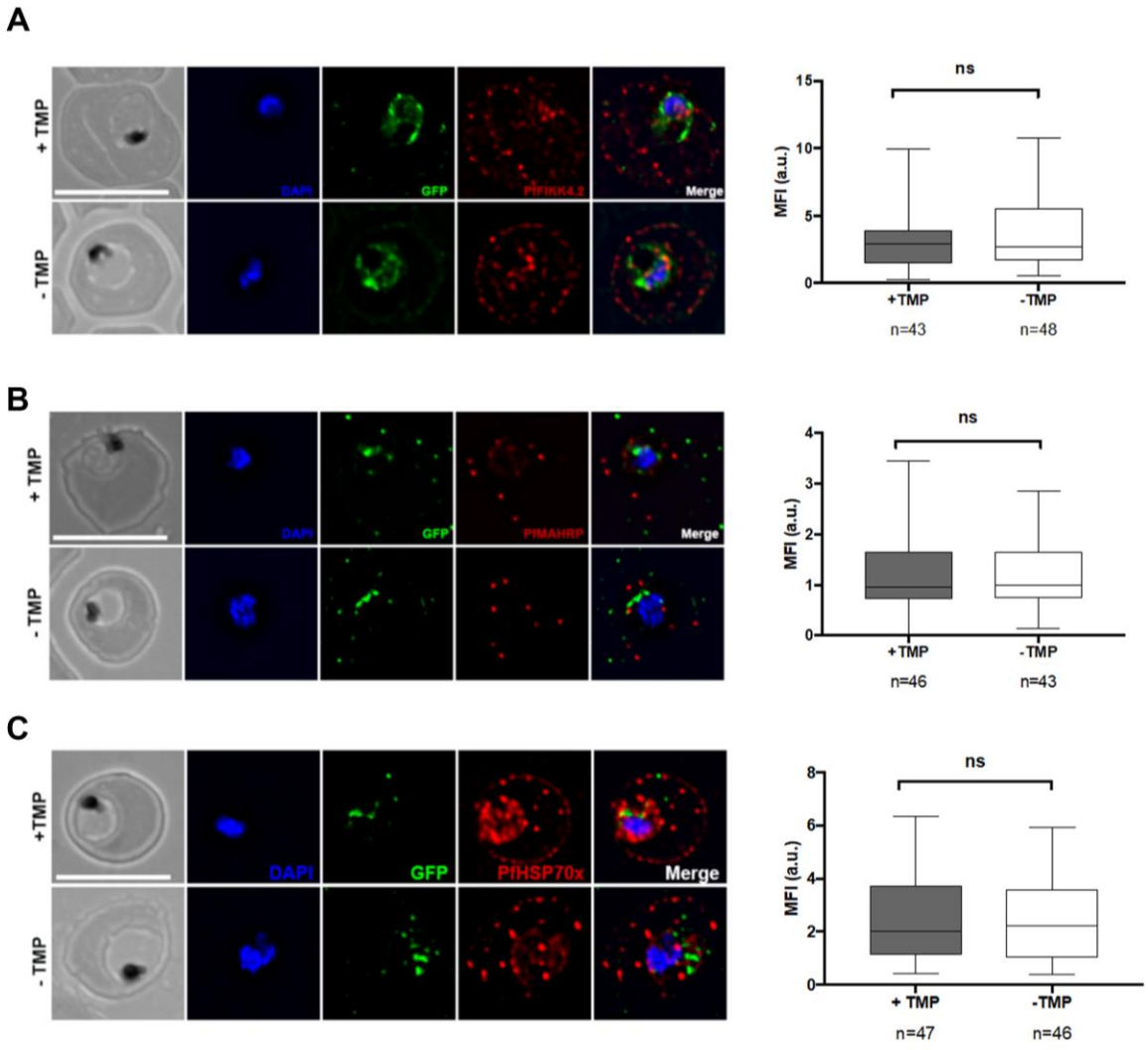

Supplemental Figure 4.6: PfGRP170 is not Required for Trafficking to the Host RBC.

Tightly synchronized ring stage PfGRP170-GFP-DDD parasites were incubated with and without TMP for 24 hours. Following this incubation, parasites were fixed with acetone and stained with DAPI, anti-GFP (PfGRP170) and either anti-PfFIKK4.2 **(A),** anti-PfMAHRP1C **(B),** or anti-PfHSP70X **(C).** The images were taken with Delta Vision II, deconvolved, and are displayed as a maximum intensity projection. The scale bar is 5µM. Mean Fluorescent Intensity (M.F.I) was calculated for the exported fraction

(PfFIKK4.2, PfMAHRP1C, and PfHSP70x) from individual cells. Data is from two independent experiments and is displayed as box-and-whiskers plots (whiskers represent the maximum and minimum M.F.I). The significance was calculated using an unpaired t test (NS= not significant).

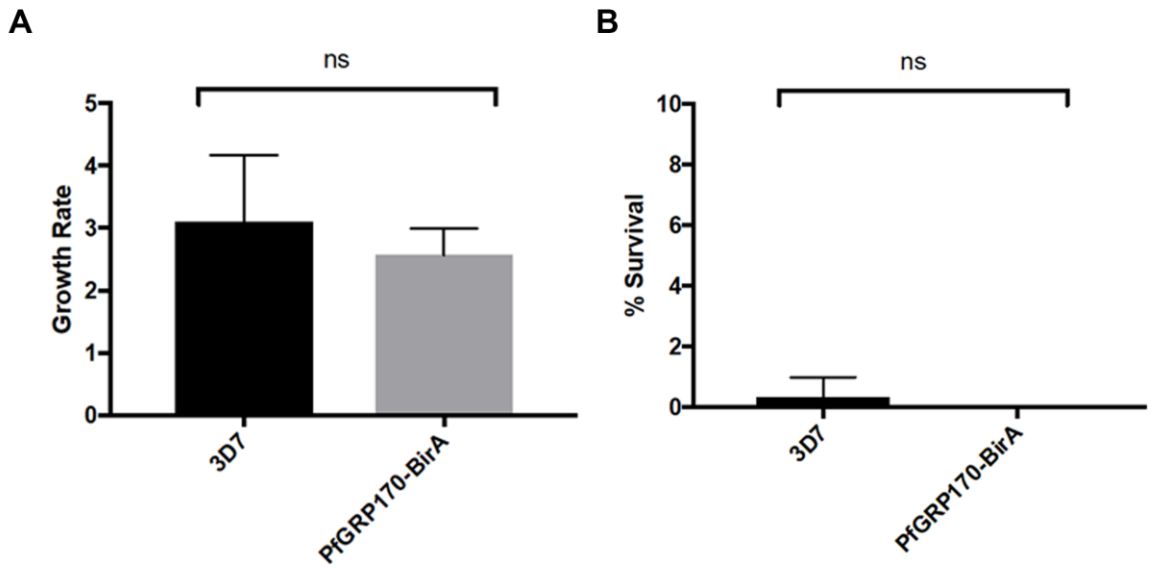

Supplemental Figure 4.7: Overexpression of PfGRP170 does not Confer Artemisinin Resistance

Tightly synchronized ring stage 3D7 and PfGRP170-BirA parasites were incubated with either 1% DMSO (Control) or Dihydroartemsinin (DHA) for 6 hours. After 6 hours the drug is removed by washing the culture with complete RPMI. Parasitemia was calculated using Giemsa stained thin blood smears at 0 hours (to calculate starting parasitemia) and 72 hours after either DMSO or DHA exposure. Four independent replicates of the experiment were completed for 3D7 and three for PfGRP170-BirA. The growth rate of the 3D7 and PfGRP170-BirA parasites, incubated only with DMSO, was calculated after 72 hours **(A).** The percent survival of parasites was calculated for 3D7 and PfGRP170-BirA after DHA exposure was calculated after 72 hours **(B).**

CHAPTER 5

Conclusions and Discussion

This dissertation presents three separate manuscripts on research pertaining to human malaria. The first focuses on the field evaluation of a malaria molecular diagnostic, the second demonstrates the use of CRISPR/Cas9 gene editing tools for rapid generation of mutant parasites, and the third utilizes molecular genetics to study the role of an ER protein in the asexual growth of *P. falciparum*. These three manuscripts show the development and use of novel molecular tools to answer key questions in malaria research.

Chapter 2 of this thesis demonstrated that the molecular assay, malachite green loop-mediated isothermal amplification (MG-LAMP), is a valuable method for the diagnosis of malaria patients with *P. falciparum* and *P. vivax*. The study was completed in outpatient clinics in Roraima, Brazil, and our data validated that MG-LAMP is a feasible diagnostic to perform in a resource-limited field setting. We also concluded that MG-LAMP is more sensitive in detecting low-density malaria infections in patients than standard light microscopy. Our data indicated that MG-LAMP was able to identify mixed species infections with *P. falciparum and P. vivax* that were missed during microscopic analysis. The ability to detect low-density and mixed infections is critical for both the elimination of malaria and the effective treatment of patients[1,2]. In addition, this study revealed several limitations of this diagnostic in a field setting. The DNA isolated from patients in Brazil was brought back to the Center for Disease Control (CDC) to undergo

an extremely sensitive malaria molecular test, Photo-induced Electron Transfer PCR (PET-PCR)[3]. The PET-PCR analysis revealed four positive samples and four mixed species infections that were missed by both microscopy and MG-LAMP. The missed infections that were revealed during PET-PCR were shown to have high Ct values (35 to 39). The PET-PCR method published by Lucchi et al. showed that a Ct value of 35 corresponds to approximately 16 parasites/μL[3]. The original MG-LAMP study completed by Lucchi et al. indicated that the range of detection was 1-8 parasites/μL[4]. However, this study was performed in a laboratory at the CDC not in a field setting. In addition, the WHO insists that new diagnostic tests have a sensitivity of 2 parasites/μL[5]. It is possible that the decreased sensitivity of MG-LAMP in the field could be improved by the development of more sensitive primers. Another limitation of the study was the use of DNA extraction kit, which decreases the adaptability of MG-LAMP in a field setting. The MG-LAMP study completed at CDC reported on the successful use of a boil and spin method using whole blood for DNA extraction[4]. This was not possible for this study as the DNA extracted needed to be stable for transport back to CDC for the PET-PCR reference test. In the future studies the specificity and sensitivity of MG-LAMP using the boil and spin method should be calculated in the field. Lastly, the polymerase and LAMP buffers used for MG-LAMP require a cold chain. This is not ideal for use in resource-limited areas. There are two commercially available LAMP assays that do not require a cold chain (EIKEN LAMP and illumigene) but they also have limitations in regards to the amount of samples that can be assessed and sensitivity of the assay[6]. In conclusion, we have shown in Chapter 2 that MG-LAMP is a portable, user-friendly,

timesaving diagnostic that is more sensitive than microscopy as well as proposed new ways to improve the MG-LAMP assay.

The introduction of CRISPR/Cas9 in malaria significantly improved the efficiency and time required to edit the parasite genome. Chapter 3 focuses on the advancements of genetic tools to study *P. falciparum* and a specific protocol that our lab currently utilizes to generate HA-*glmS* mutants. The strategy that we have presented here can be adapted for use with other knockdown systems, the tagging of genes, gene knockouts, and insertion of point mutations. While the length of the homology regions our lab utilizes for homology directed repair is between 500-800 base pairs, in this study we evaluated the use of smaller homology regions (50, 75, and 100bp). This method was found to be unsuccessful but we have suggested in Chapter 3 ways to optimize the use of smaller homology arms such as the use of drug pressure to select for integrated parasites. The procedure to generate mutants in Chapter 3 utilizes a three-plasmid approach where the gRNA, Cas9, and repair template are on three separate plasmids. However, our lab and others have published using a two-plasmid approach where the gRNA and Cas9 are on a single plasmid and the repair template on a second[7-11]. Having Cas9 and the gRNA on a single plasmid is advantageous as both components are segregated into dividing cells together. In summary, CRISPR/Cas9 is an extremely effective tool to study *P. falciparum* biology in our field and we presented a comprehensive and adaptable protocol for conditional mutagenesis of malaria parasites[7,10,12-15].

Chapter 4 of this thesis constitutes a study of an ER chaperone, PfGRP170, during asexual development of *P. falciparum* parasites. Conditional mutants for

PfGRP170, using the destabilization domain system, were generated using single homologous crossover[7,16,17]. The use of single homologous crossover, a technique used prior to the establishment of CRISPR/Cas9 in *Plasmodium,* yields very few integrated parasites after three rounds of drug selection. Taking advantage of the GFP reporter appended to PfGRP170, I created a flow sorting protocol to isolate rare fluorescent parasites, thus establishing a PfGRP170-GFP-DDD parasite line. Using these mutants we have shown that this protein localizes to the parasite ER and is essential for asexual growth of *P. falciparum*, specifically required for late stage development. Since ER chaperones have been shown to be involved in the trafficking of proteins, we originally hypothesized that PfGRP170 played a role in protein transport in *Plasmodium*. However, I detected no observable defects in protein trafficking to the apicoplast or the red blood cell during PfGRP170 knockdown. However, I have revealed that PfGRP170 is linked to parasite stress response as a brief heat shock during knockdown decreases parasite viability. Additionally, I have concluded that PfGRP170 knockdown activates the ER stress response pathway, PK4, indicating that the ER is in distress without this essential chaperone[18,19]. Using several methods, including immunoprecipitation and proximity ligation assays, I have confirmed an interaction of PfGRP170 and PfBiP in *P. falciparum*. This suggests that these two proteins may work in a complex as they do in higher eukaryotes. Interestingly, knockdown of PfGRP170 does not inhibit this interaction with PfBiP and overexpression of BiP fails to rescue the PfGRP170 death phenotype. This leads us to believe that death observed during PfGRP170 knockdown is not entirely attributable to a loss of functional PfBiP.

In order to elucidate the molecular mechanism behind why parasites die without functional PfGRP170, we utilized two independent mass spectroscopy methods to generate a list of 11 candidate proteins to study further. Using published transcriptomics data to only look at proteins expressed late in the life cycle when the PfGRP170-GFP-DDD mutants die, essentiality data generated using a recent piggyBac screen in *P. falciparum*, and elimination of proteins with known functions in egress and invasion we further narrowed down this list to one candidate protein: parasite-infected erythrocyte surface protein 1 (PIESP). PIESP, using the published piggyBac screen[20], is predicted to be essential in the asexual stages of *P. falciparum*. It has been suggested that PIESP is exported to the RBC through the overexpression of the protein tagged with a GFP reporter[21] However, the last four amino acids of this protein are TDEL, which is quite possibly an ER retention signal, and were left off of the expressed construct. Furthermore, a blast search we conducted suggested that this protein is involved in glycosylation in the ER lumen in *Plasmodium*[22]*.* This mammalian PIESP homolog we identified, B3GLCT, is an ER enzyme that catalyzes the attachment of glucose to O-linked fucose residues on thromospondin type 1 repeats (TSRs)[22-24]. The O-linked fucose is added to TSR domains via another enzyme, POFUT2, an enzyme that was previously shown to be nonessential for *P. falciparum* asexual growth[22]. In mammalian cells, POFUT2 and B3GLCT work together in a non-canonical ER quality control pathway that recognizes TSR domain containing proteins and stabilizes their folding via glycosylation[23]. It is intriguing that POFUT2 is nonessential for asexual growth and that most TSR domain containing proteins in *Plasmodium* can be found on mosquito stage proteins, yet PIESP is predicted to be essential for asexual growth[20,22].

It is possible that PIESP has been falsely predicted to be an essential protein or that the protein may be functioning in a different mechanism than the eukaryotic homolog. We are currently in the process of developing conditional knockdown parasites using the TetR-DOZI system for PIESP to study its localization and essentiality in the asexual blood stages[25]. In summary, we have identified and characterized a protein essential for asexual growth in *P. falciparum* that is involved in stress response. Furthermore, we have pinpointed future protein candidates to investigate, which will expand our knowledge of malaria ER biology.

References

1 World Health Organization. World Malaria Report. (2018).

2 WHO. Global Technical Strategy for Malaria 2016-2030. (2015).

3 Lucchi, N. W. *et al.* Molecular diagnosis of malaria by photo-induced electron transfer fluorogenic primers: PET-PCR. *PLoS One* **8**, e56677, doi:10.1371/journal.pone.0056677 (2013).

4 Lucchi, N. W., Ljolje, D., Silva-Flannery, L. & Udhayakumar, V. Use of Malachite Green-Loop Mediated Isothermal Amplification for Detection of Plasmodium spp. Parasites. *PLoS One* **11**, e0151437, doi:10.1371/journal.pone.0151437 (2016).

5 World Health Organization. WHO Evidence Review Group on Malaria Diagnosis in Low Transmission Settings. (2014).

6 Lucchi, N. W., Ndiaye, D., Britton, S. & Udhayakumar, V. Expanding the malaria molecular diagnostic options: opportunities and challenges for loop-mediated isothermal amplification tests for malaria control and elimination. *Expert Review or Molecular Diagnostics* **18**, 195-203 (2018).

7 Florentin, A. *et al.* PfClpC Is an Essential Clp Chaperone Required for Plastid Integrity and Clp Protease Stability in Plasmodium falciparum. *Cell Rep* **21**, 1746-1756, doi:10.1016/j.celrep.2017.10.081 (2017).

8 Spillman, N. J., Beck, J. R., Ganesan, S. M., Niles, J. C. & Goldberg, D. E. The chaperonin TRiC forms an oligomeric complex in the malaria parasite cytosol. *Cell Microbiol* **19**, doi:10.1111/cmi.12719 (2017).

9 Brancucci, N. M. B. *et al.* Lysophosphatidylcholine Regulates Sexual Stage Differentiation in the Human Malaria Parasite Plasmodium falciparum. *Cell*, doi:10.1016/j.cell.2017.10.020 (2017).

10 Ng, C. L. *et al.* CRISPR-Cas9-modified pfmdr1 protects Plasmodium falciparum asexual blood stages and gametocytes against a class of piperazine-containing compounds but potentiates artemisinin-based combination therapy partner drugs. *Mol Microbiol* **101**, 381-393, doi:10.1111/mmi.13397 (2016).

11 Lim, M. Y. *et al.* UDP-galactose and acetyl-CoA transporters as Plasmodium multidrug resistance genes. *Nat Microbiol*, 16166, doi:10.1038/nmicrobiol.2016.166 (2016).

12 Ghorbal, M. *et al.* Genome editing in the human malaria parasite Plasmodium falciparum using the CRISPR-Cas9 system. *Nat Biotechnol* **32**, 819-821, doi:10.1038/nbt.2925 (2014).

13 Wagner, J. C., Platt, R. J., Goldfless, S. J., Zhang, F. & Niles, J. C. Efficient CRISPR-Cas9-mediated genome editing in Plasmodium falciparum. *Nat Methods* **11**, 915-918, doi:10.1038/nmeth.3063 (2014).

14 Cobb, D. W. *et al.* The Exported Chaperone PfHsp70x Is Dispensable for the Plasmodium falciparum Intraerythrocytic Life Cycle. *mSphere* **2**, doi:10.1128/mSphere.00363-17 (2017).

15 Counihan, N. A. *et al.* Plasmodium falciparum parasites deploy RhopH2 into the host erythrocyte to obtain nutrients, grow and replicate. *Elife* **6**, doi:10.7554/eLife.23217 (2017).

16 Beck, J. R., Muralidharan, V., Oksman, A. & Goldberg, D. E. PTEX component HSP101 mediates export of diverse malaria effectors into host erythrocytes. *Nature* **511**, 592-595, doi:10.1038/nature13574 (2014).

17 Muralidharan, V., Oksman, A., Iwamoto, M., Wandless, T. J. & Goldberg, D. E. Asparagine repeat function in a Plasmodium falciparum protein assessed via a regulatable fluorescent affinity tag. *Proc Natl Acad Sci U S A* **108**, 4411-4416, doi:10.1073/pnas.1018449108 (2011).

18 Zhang, M. *et al.* PK4, a eukaryotic initiation factor 2α(eIF2α) kinase, is essential for the development of the erythrocytic cycle of Plasmodium. *PNAS* **109**, 3956–3961 (2012).

19 Zhang, M. *et al.* Inhibiting the Plasmodium eIF2alpha Kinase PK4 Prevents Artemisinin-Induced Latency. *Cell Host Microbe* **22**, 766-776 e764, doi:10.1016/j.chom.2017.11.005 (2017).

20 Zhang, M. *et al.* Uncovering the essential genes of the human malaria parasite Plasmodium falciparum by saturation mutagenesis. *Science* **360**, doi:10.1126/science.aap7847 (2018).

21 van Ooij, C. *et al.* The malaria secretome: from algorithms to essential function in blood stage infection. *PLoS Pathog* **4**, e1000084, doi:10.1371/journal.ppat.1000084 (2008).

22 Lopaticki, S. *et al.* Protein O-fucosylation in Plasmodium falciparum ensures efficient infection of mosquito and vertebrate hosts. *Nature communications* **8**, 561-561, doi:10.1038/s41467-017-00571-y (2017).

23 Vasudevan, D., Takeuchi, H., Johar, S. S., Majerus, E. & Haltiwanger, R. S. Peters plus syndrome mutations disrupt a noncanonical ER quality-control mechanism. *Current biology : CB* **25**, 286-295, doi:10.1016/j.cub.2014.11.049 (2015).

24 Weh, E., Takeuchi, H., Muheisen, S., Haltiwanger, R. S. & Semina, E. V. Functional characterization of zebrafish orthologs of the human Beta 3-Glucosyltransferase B3GLCT gene mutated in Peters Plus Syndrome. *PloS one* **12**, e0184903-e0184903, doi:10.1371/journal.pone.0184903 (2017).

25 Ganesan, S. M., Falla, A., Goldfless, S. J., Nasamu, A. S. & Niles, J. C. Synthetic RNA-protein modules integrated with native translation mechanisms to control gene expression in malaria parasites. *Nat Commun* **7**, 10727, doi:10.1038/ncomms10727 (2016).